Università degli Studi di Cagliari

DOTTORATO DI RICERCA

Scienze della Vita dell'Ambiente e del Farmaco

Ciclo XXX

DEVELOPMENT OF INTERFERING STRATEGIES AGAINST THE INNATE IMMUNE INHIBITION BY THE VP35 EBOLA VIRUS PROTEIN, A KEY VIRAL TARGET

Settore scientifico disciplinare di afferenza

Microbiologia BIO/19

Presentata da: **ALDO FRAU**

Coordinatore Dottorato **Prof. Enzo Tramontano**

Tutor **Prof. Enzo Tramontano**

Esame finale anno accademico 2016 – 2017

Tesi discussa nella sessione d'esame Febbraio-Marzo 2018

CONTENTS

1. OVERVIEW ON EBOLA VIRUS DISEASE

A date to remember

It was September 1976 when a package containing a shiny, blue thermos flask arrived at the Institute of Tropical Medicine in Antwerp, Belgium. From that key date, humankind started to talk, discuss, study, know and fear the dreadful *Ebola virus*.

1.1. A short history about Ebola virus discovery

Nearly 40 years ago, a team of brave scientists travelled to a remote part of the Congolese rainforest, directed to the rural village of Yambuku. They were to help finding out why so many people were dying from an unknown and terrifying disease spread across human communities in northern Zaire, affected by an acute, and still unclassified, severe viral hemorrhagic fever. Two weeks before a package containing a blue thermos flask was delivered to the Institute of Tropical Medicine in Antwerp, Belgium. This unusual delivery had travelled all the way from Zaire's capital city Kinshasa, on a commercial flight, in one of the passengers' hand luggage. That day, working in the lab run by Dr. Stefaan Pattyn was Peter Piot, a 27-year-old scientist and medical school graduate, who was training as a clinical microbiologist junior researcher. "*It was just a normal flask like any other you would use to keep coffee warm.*" recalled Piot, now Director of the London School of Hygiene and Tropical Medicine. However, that thermos was not carrying coffee, inside was an altogether different cargo; nestled amongst a few melting ice cubes were vials of blood along with a note. Sent by a Belgian doctor based in what was then Zaire, a handwritten message explained that the blood was that of a nun who had fallen ill with a mysterious illness, which he could not identify. Still unknowingly, Piot and his colleagues were handling one of the deadliest, frightening and most virulent pathogen ever known to humankind, the *Ebola virus*.

The samples were treated like numerous others the lab had tested before, but when Dr. Pattyn and his team of scientists placed some of the cells under an electron microscope,

they saw something they didn't expect. *"…a gigantic worm-like structure – gigantic by viral standards – a very unusual shape for a virus, …only one other virus looked like that and that was the Marburg virus*". However, Pattyn and his colleagues did not know what they were looking at, it was something never seen before. Under the lens of their microscope they saw a lasso-shaped virus that resembled Marburg virus – that was discovered nine years earlier and caused a similar type of hemorrhagic fever – but did not have the ability to determine for sure whether what they observed was something new. The Antwerp laboratory was not equipped to work on deadly viruses like Marburg, so the World Health Organization instructed Pattyn to send the samples to the British military laboratories at Porton Down. Scientists started studying it, and also sent a sample to the Centers for Disease Control and Prevention (CDC) based in Atlanta (United States of America). The Atlanta team was able to show that the outbreak was caused by a previously unknown virus, that was not Marburg (Fig. 1).

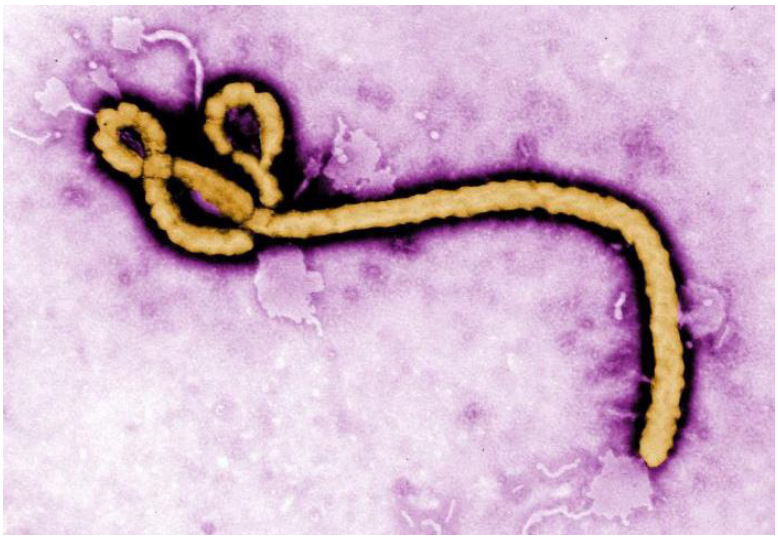

Fig. 1. The first microscopic image of *Ebola virus*. Created by CDC microbiologist, Frederick A. Murphy, this colorized transmission electron microscopic (TEM) image revealed for the first time some of the ultrastructural morphology displayed by an Ebola virus virion.

In the meanwhile, alarming news had reached Antwerp; the nun under the care of the doctor in Zaire had died and many others were falling ill with this mysterious illness in a remote area in the north of the country, with symptoms including fever, diarrhoea and vomiting followed by bleeding and eventually death.

Two weeks later, a team of researchers composed by the Belgian scientists and CDC members, directed by Dr. Joel Breman, a CDC epidemiologist who was in charge of the field investigation of the outbreak, were on a night flight directed to Kinshasa, heading to the center of the outbreak, the town of Yambuku. The area was in complete panic and chaos, and it was thanks to the intercedence of Dr. Bill Close (who was the personal physician to Zaire's president at the time, Mobutu Sese Seko, and ran the biggest hospital in the capital Kinshasa) that Breman, Piot, and three others had secured a plane that would take them to a town within driving distance of Yambuku, a remote village in the equatorial rainforest about 1,000 km (620 miles) further north from Kinshasa, which was under a quarantine order and martial law (Fig. 2).

Fig. 2. The first group of scientist and missionaries involved with *Ebola*. From the second row, dressing a flowered shirt, stands Dr. Piot.

The outbreak was centered in the Bumba zone of the Equateur Region and most of the cases were recorded within a radius of 70 km of Yambuku causing 280 deaths and 38 serologically confirmed survivors (WHO 1978). When the research team arrived to the zone, it needed firstly to find out how this virus was moving from person to person: by air, in food, by direct contact or even by insects. By visiting all the surrounding villages and mapping out the number of infections (Fig. 3), it was clear that the outbreak was related to areas served by the local hospital.

Furthermore, the team found that more women than men caught the disease and particularly women between 18 and 30 years old, discovering also that many of them in this age group were pregnant. Each morning, many of them received a routine injection at the antenatal clinic at the hospital. Sadly, just five syringes were distributed and the needles reused, usually rinsed in a pan of warm water and, at the end of the day, sometimes boiled, so the virus could spread between the patients.

During three months spent in Yambuku the team of researchers learned a lot about the virus, but it was still lacking a name. "*In the early days of the outbreak, people were calling the disease Yambuku fever, but we didn't want to name it thus because it would forever stigmatize the settlement.*" declared Dr. Karl Johnson, at that time head of special pathogen of CDC and the scientific director of the International Commission in charge with the study and management of the disease. Therefore, the team decided to name the virus with the closest river they could see on their map, the Ebola river, headwater of the Mongala river, a tributary of Congo river (former Zaire), that flows past Yumbuku (Fig. 4).

From that point on, the virus arrived in an anonymous flask in Antwerp months earlier would have been known to the world as the *Ebola virus*.

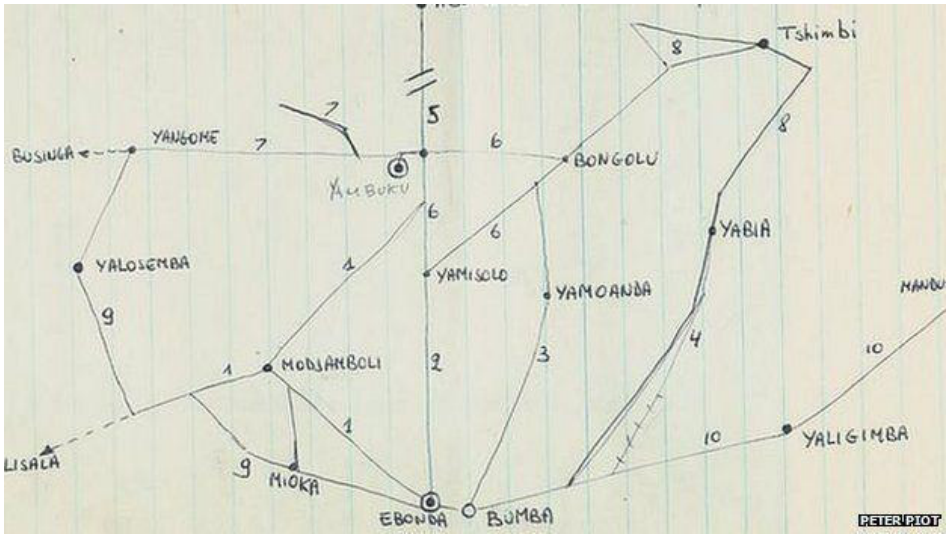

Fig. 3. **The map of villages involved in the first Ebola outbreak.** To investigate the spread of the virus the research team drew maps and plotted each village they visited (credit: Dr. Peter Piot).

Fig. 4. **The Ebola river.** A snapshot of the Ebola River in 1976 (credit: Dr. Peter Piot).

1.2. Classification and taxonomy of filoviruses

Since its establishment in 1991, the viral order *Mononegavirales* gathered together related viruses with non-segmented, linear, single-stranded and negative-sense RNA genomes (ssRNA-). Members belonging to this order possess other peculiar characteristics: the genomic RNA is uncapped, not polyadenylated and not covalently linked to any protein; the replication process occurs through the synthesis of a complete antigenome; the gene order within the genome is 3'-UTR-core protein genes-envelope protein gene-polymerase gene-5'-UTR; the formation of helical nucleocapsids (NCs) (Kuhn et al., 2010).

As a member of the family *Filoviridae*, the *Ebola virus* belongs to the order *Mononegavirales*. The classification and taxonomy of filoviruses continuously changed from the discovery, in 1967, of Marburg virus as the first member of the group (Kuhn et al. 2010). Recently updated in 2017 with the inclusion of 69 more novel species (Amarasinghe et al. 2017), the taxonomy of the order *Mononegavirales* proposed by the International Committee on Taxonomy of Viruses (ICTV) accounts today 8 families (Fig. 5) together with five non-assigned viruses. The *Mononegavirales* order currently includes together the *Paramyxoviridae*, *Rhabdoviridae*, *Bornaviridae*, *Pneumoviridae*, *Mymonaviridae, Nyamiviridae*, *Sunviridae* and *Filoviridae* viral families and five new species of unassigned viral family (*Anphevirus*, *Arlivirus*, *Chengtivirus*, *Crustavirus*, *Wastrivirus*), which all share a similar organization in their ssRNA- genome to the other order members.

The genus *Ebolavirus*, along with *Marburgvirus* and *Cuevavirus* genera, is located into the family *Filoviridae*. As mentioned before, after the identification of Marburg virus almost 50 years ago, *Ebolavirus* was the second genus of the *Filoviridae* family to be discovered (M. A. de La Vega, Stein, and Kobinger 2015). The family name, from the Latin word "filum", which is for thread, was designated for reflecting the agents peculiar filamentous morphology (Kuhn et al. 2010) (Fig. 1).

The genus *Marburgvirus* includes two clades: *Marburg virus* (MARV) and *Ravn virus* (RAVV) in a single species *Marburg marburgvirus*, formerly known as "*Lake Victoria marburgvirus*", a species name not completely accepted and barely used by the virology community and thus renamed in 2010 (Kuhn et al. 2010). The Marburg virus was the first recognized member of filoviruses, in 1967, when 31 people became ill with haemorrhagic fever in the cities of Marburg and Frankfurt in Germany and in Belgrade, the capital of former Yugoslavia, during an outbreak of laboratory staff exposed to African green monkeys' tissues (*Cercopithecus aethiops*) imported from Uganda.

The genus *Cuevavirus* includes only one species *Lloviu cuevavirus*, because of the recent discovery of *Lloviu virus* (LLOV), detected from carcasses of Schreiber's bats (*Miniopterus schreibersii*) from Europe (Negredo et al. 2011).

Into the genus *Ebolavirus* five distinct species are embraced: *Bundibugyo ebolavirus*, *Reston ebolavirus* (the only species that owns the unique feature of an airborne propagation), *Sudan ebolavirus*, *Taï Forest ebolavirus* (formerly *Cote d'Ivoire ebolavirus*), and the type species *Zaire ebolavirus*. In Table 1, a summary of the current, ICTV-accepted taxonomy and correspondent abbreviations of the family *Filoviridae* is presented.

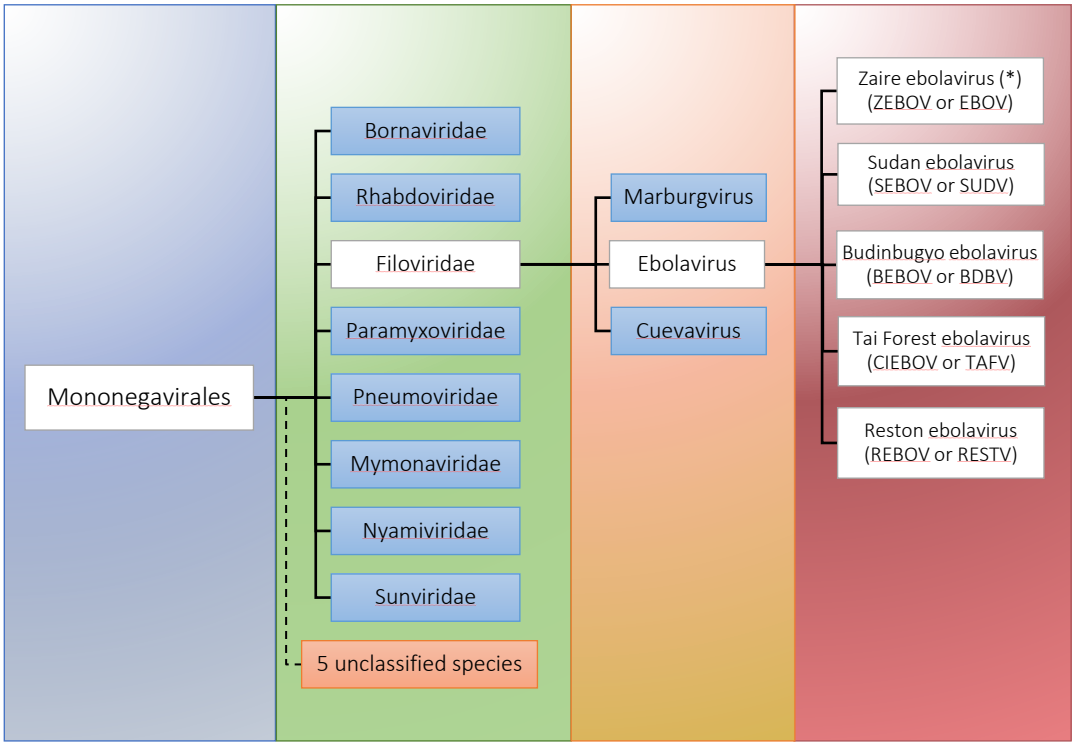

Fig. 5. Taxonomy of the order *Mononegavirales*. (*) Asterisk denote type species.

Table 1. ICTV-accepted taxonomy of the family *Filoviridae* as of 2017.

Genus	Species	Abbreviation
Cuevavirus	*Lloviu cuevavirus**	Lloviu virus (LLOV)
Ebola virus	*Bundibugyo ebolavirus*	Bundibugyo virus (BDBV)
	Reston ebolavirus	Reston virus (RESTV)
	Sudan ebolavirus	Sudan virus (SUDV)
	Taï Forest ebolavirus	Taï Forest virus (TAFV)
	*Zaire ebolavirus**	Ebola virus (EBOV)
Marburgvirus	*Marburg marburgvirus**	Marburg virus (MARV) Ravn virus (RAVV)

* Asterisks denote type species.

1.3 Epidemiology of Ebola virus disease: origin and chronology of the epidemics.

From the first reported case in 1976 of the Ebola virus disease (EVD) occurred in Zaire, actually known as the Democratic Republic of Congo (DRC), with 318 cases reported and 88% of case fatality rate (CFR), numerous outbreaks took place in multiples African countries (Table 2).

The first known case in 1976 was a 44-year-old male instructor at the Yambuku Catholic Mission (established by Belgian missionaries in 1935), who presented himself to the outpatient clinic at Yambuku Mission Hospital (YMH) on 26 August 1976 with a febrile illness thought to be malaria (WHO 1978). Immediately treated with an antimalarial drug chloroquine by parenteral injection, his fever resolved rapidly and he was afebrile until 1 September when he had fever to 39.2° C. On 5 September, he was admitted again to YMH with gastrointestinal bleeding and died on 8 September. Between 1 September and 24 October, 318 probable and confirmed cases/infections of haemorrhagic fever were registered and the epidemic reached a peak during the fourth week, causing a total of 280 deaths.

Simultaneously in the same year, between June and November, another outbreak of EVD took place in Sudan (now South Sudan), causing 284 infections and 150 deaths (CFR of 53%); it occurred in the source towns of Nzara, Maridi and the surrounding areas located in the remote savanna of southern Sudan (Fig. 6), near to the border with Zaire (Deng, Duku, and Gillo 1978). Originated in a cotton factory and then amplified by transmission in a large hospital, the disease spread mainly through close personal contact within hospitals, with many medical care personnel infected. Although the outbreaks occurred at a similar time and in the same geographical area of central Africa (Yambuku is ~500 km from Nzara), no definite link between the two was established. In fact, later virological studies demonstrated differences between the two strains, subsequently described as the Sudan and Zaire strains (Baron, McCormick, and Zubeir 1983).

Since 1976, the *Zaire ebolavirus* species, known as the most lethal species of *Ebolavirus*, has caused 15 subsequent outbreaks with an average CFR of 79%, whereas the *Sudan ebolavirus* ended up causing 6 additional outbreaks with an average CFR of 63% (M. A. de La Vega, Stein, and Kobinger 2015).

Fig. 6. **Main centers involved in the first EVD outbreak.** First depicted map of Sudan and Zaire showing main centers of infection during firsts EVD outbreaks (source: Bulletin of the World Health Organization, 1978).

Following the 1976 Sudan and Zaire outbreaks, the occurring of EVD outbreaks showed a fluctuating trend during time, with other consistent and remarkable outbreaks distributed in different areas of Africa (Fig. 7).

Three years after the 1976 Sudan epidemic, a recurrent outbreak occurred in the same site of Nzara and Maridi between 31 July and 6 October 1979, causing 34 cases of EVD, 22 of which were fatal (CFR of 65%). The occurrence of this event was important for two aspects: i) it confirmed that to allow the virus to spread was necessary a direct physical contact with an infected person and the body fluids of infectious persons, ii) it also confirmed previous impressions that there was no risk of airborne transmission.

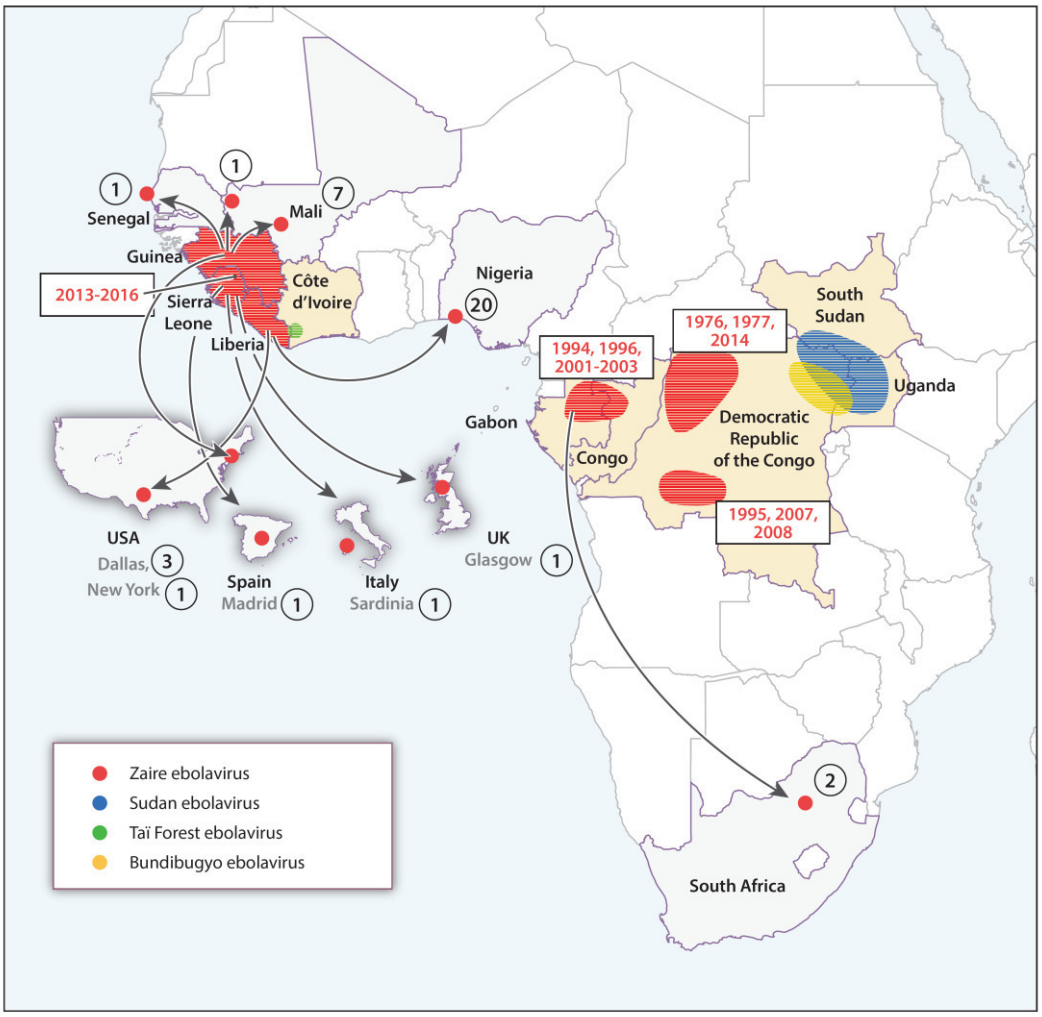

Fig. 7. Geographical distribution of EBOV infections and outbreaks. The map shows the occurrence of all known human outbreaks associated with four different ebolavirus species across the equatorial belt within the African continent (from 1976 to August 2016). The circled numbers indicate EVD cases resulting from introductions of EBOV-infected persons from Guinea, Sierra Leone, Liberia, or, in one instance, from an individual infected in Gabon during the 2013–2015 West African epidemic (source: Baseler et al. 2017).

In fact, the illness occurred only among those who had direct physical contact with an infected person and, furthermore, among family members who did have physical contact with cases (the risk of acquiring illness was much greater if they provided nursing care with an estimated 5.1-fold increased risk of infection). The absence of illness among not-exposed persons to cases in confined spaces, but without physical contact, confirmed previous impressions that there was no risk of airborne

transmission. Moreover, the presence of anti-Ebola antibodies in the sera of 18% of persons who were unassociated with the outbreak supported the notion that Ebola virus was an endemic focus in that region (Baron, McCormick, and Zubeir 1983).

Less than twenty years later, in 1994, new remarkable outbreaks took place in Africa. In northeastern Gabon an outbreak of Zaire virus, originated in gold-panning encampments deep in the rain forest and then spread to human communities, caused 52 cases and 31 deaths (CFR of 60%). Initially thought to be yellow fever, it was subsequently identified as Ebola hemorrhagic fever in 1995 (Georges et al. 1999). Concurrently, at a considerable geographic distance from previous outbreaks a new Ebola species, the new species of *Taï Forest ebolavirus* was identified in West Africa. A scientist practicing an autopsy on a chimpanzee contracted the virus; after receiving treatments in Switzerland, the patient fully recovered and this is the only known case of TAFV disease in humans to date (Le Guenno et al. 1995; M. A. de La Vega, Stein, and Kobinger 2015).

The following year, an important outbreak of Zaire virus occurred in Kikwit (DRC), spreading across human community from a case-patient who worked in the forest adjoining the city and causing 315 human cases and 250 deaths (CFR of 81%) (Khan et al. 1995). Zaire virus species continued to claim victims between 1996 and 1997 causing further 99 cases and 67 deaths in Gabon and South Africa (the latter case was of a medical professional who traveled from Gabon to Johannesburg; once hospitalized, also a nurse who took care of him became infected and died). Several EVD epidemics occurred in the following mid-2000s: i. Zaire virus affected African countries in further 6 different occasions for a total of 596 human cases, causing 455 deceases overall for a CFR of 74.5%, ii. Sudan virus outbreaks occurred in other 4 outbreaks, involving southern Sudan and Uganda, for a total of 35 cases and 15 deaths (CFR of 43%). Across the years 2000 and 2001, Sudan virus caused another large epidemic spread in Gulu, Masindi, and Mbarara districts of Uganda, causing 425 cases and 224 deaths, with a CFR of 53%. It is worth to note that the diffusion of the disease into human community

was facilitated by lack of compliance with the adequate personal protective measures against three of the most important risks associated with Ebola virus infection: i. attending to funerals, ii. providing medical care, iii. having direct contacts with Ebola hemorrhagic fever case-patients.

Thirteen years after the identification of the third species of Ebolavirus, in the Bundibugyo District in western Uganda, another episode of a viral hemorrhagic fever occurred. This time, the causative agent was a genetically distinct species of Ebolavirus, called *Bundibugyo ebolavirus*, and determined 37 reported deaths over a total of 149 cases, for a CFR of 25% (MacNeil et al. 2011). Only one other outbreak caused by this species occurred in 2012 in the DRC (Albariño et al. 2013), settling BDBV as the least lethal species of Ebolavirus in humans as of now, with an average CFR of 38%.

The last species of the genus, *Reston ebolavirus*, has surfaced on seven different occasions infecting non-human primates (NHPs), pigs, and humans. Due to its lack of pathogenicity in humans to date, with the only exception represented by 6 cases registered in Valenzuela City – a neighborhood within Metro Manila (Philippines), it lies in a different category from the four species previously mentioned. In fact in 2008, six workers from a pig farm and slaughterhouse developed antibodies but did not become sick, demonstrating that RESTV could be transmitted to humans without resulting in illness (Barrette et al. 2009; M. A. de La Vega, Stein, and Kobinger 2015; WHO 2009).

The EVD outbreaks have occurred with a sporadic frequency from 1976, being characterized by a small size and generally well contained. This until December 2013, when the largest outbreak of EVD ever recorded emerged in the west African country of Guinea and quickly spread to surrounding countries, also exporting cases outside the African continent (in Europe and the USA). This biggest and most devastating outbreak of EVD occurred over the years 2014 and 2016 and affected primarily Guinea, Liberia and Sierra Leone. In addition to these countries, other 36 confirmed cases were reported from Italy, Mali, Nigeria, Senegal, Spain, the United Kingdom, and the United

States, and further 24 Ebola-confirmed patients were medically evacuated from West Africa (in France, Germany, Italy, the Netherlands, the United Kingdom, the United States, Norway, Spain, and Switzerland). Noteworthy, the 81.5% of these patients who received a close monitoring and an aggressive supportive care survived to the disease (Uyeki et al. 2016). Altogether, the epidemic of 2014-2016 caused 28.616 human cases, with 11.310 deaths (World Health Organization 2016).

Contemporary to West Africa outbreaks, an EVD epidemic involved once again the DRC, where 66 cases of Ebola virus disease and 49 deaths occurred. This outbreak, with clinical and epidemiologic characteristics similar to those of previous EVD outbreaks in equatorial Africa, had a zoonotic origin different from that in the 2014 epidemic in West Africa and spread from a pregnant woman who butchered a monkey (of an unknown arboreal species) found dead by her husband (Maganga et al. 2014).

On 1 and 9 June 2016, World Health Organization (WHO) declared the end of the most recent outbreak of EVD in Guinea and Liberia, since 42 days (two 21-day incubation cycles of the virus) passed since the last person confirmed to have EVD was tested negative for the second time. However, the performance indicators suggested that Guinea, Liberia and Sierra Leone still had a variable capacity to prevent, detect and respond to new outbreaks, thus, the risk of additional outbreaks remained sustained (World Health Organization 2016).

More recently, on May 11, 2017, the Ebola Zaire subtype provoked an outbreak of EVD in the Democratic Republic of Congo, in the Likati health zone of the province of Bas Uélé. Due to the remoteness of the area and the limited services, only mobile diagnostic laboratories were able to provide testing of samples, confirming 8 total human cases and 4 deaths (CFR of 50%). Teams from international agencies, including CDC, WHO, MSF (Doctors without Borders), and others, supported the Ministry of Public Health's epidemiologic, diagnostic, clinical, and communications efforts to respond to the outbreak. Following a period of 42 days since the second negative laboratory diagnostic

test of the last confirmed patient, WHO declared an end to the outbreak on July 2, 2017 (Fig. 8, Table 2).

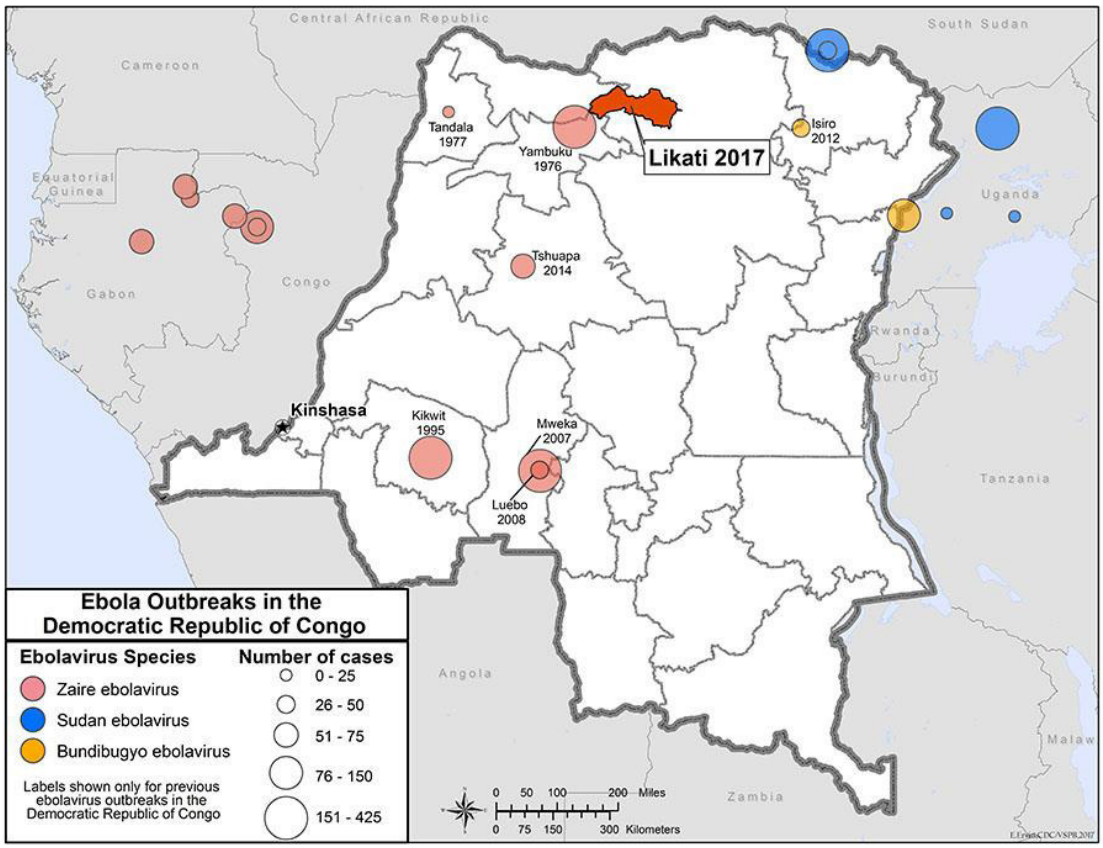

Fig. 8. Outbreaks in the Democratic Republic of Congo. The map shows the DRC country and indicates the outbreaks of EVD in Yambuku in 1976, Tandala in 1977, Kikwit in 1995, Mweka in 2007, Luebo in 2008, Isiro in 2012, Tshuapa in 2014, and, presently, in Likati in 2017. All outbreaks were of the Ebola Zaire subtype, except for the Isiro outbreak (Ebola Bundibugyo).

Table 2. EVD: Outbreaks Chronology. Known human cases and outbreaks of Ebola Virus Disease, showed in reverse chronological order (source: CDC - July 28, 2017).

YEAR	Country	Ebola subtype	Cases	Deaths
May-Jul 2017	Democratic Republic of Congo	Ebola virus	8	4
Aug-Nov 2014	Democratic Republic of Congo	Ebola virus	66	49
Mar 2014-2016	Multiple countries	Ebola virus	28,616	11,310
Nov 2012-Jan 2013	Uganda	Sudan virus	6	3
Jun-Nov 2012	Democratic Republic of Congo	Bundibugyo virus	36	13
Jun-Oct 2012	Uganda	Sudan virus	11	4
May 2011	Uganda	Sudan virus	1	1
Dec 2008-Feb 2009	Democratic Republic of Congo	Zaire virus	32	15
Nov 2008	Philippines	Reston virus	6	0
Dec 2007-Jan 2008	Uganda	Bundibugyo virus	149	37
2007	Democratic Republic of Congo	Zaire virus	264	187
2004	Russia	Zaire virus	1	1
2004	Sudan (South Sudan)	Sudan virus	17	7
2003 (Nov-Dec)	Republic of Congo	Zaire virus	35	29
2003 (Jan-Apr)	Republic of Congo	Zaire virus	143	128
Oct 2001-Mar 2002	Republic of Congo	Zaire virus	57	43
Oct 2001-Mar 2002	Gabon	Zaire virus	65	53
2000-2001	Uganda	Sudan virus	425	224
1996	Russia	Zaire virus	1	1
1996	Philippines and USA	Reston virus	0	0
1996	South Africa	Zaire virus	2	1
1996-1997 (Jul-Jan)	Gabon	Zaire virus	60	45
1996 (Jan-Apr)	Gabon	Zaire virus	37	21
1995	Democratic Republic of Congo (formerly Zaire)	Zaire virus	315	250
1994	Cote d'Ivoire (Ivory Coast)	Taï Forest	1	0
1994	Gabon	Zaire virus	52	31
1992	Italy	Reston virus	0	0
1989-1990	Philippines and USA	Reston virus	7	0
1979	Sudan (South Sudan)	Sudan virus	34	22
1977	Zaire	Zaire virus	1	1
1976	Sudan (South Sudan)	Sudan virus	284	151
1976	Zaire (Democratic Republic of the Congo – DRC)	Zaire virus	318	280

1.4 The phylogenetics of filoviruses

The ages of filoviruses have been estimated through phylogenetic techniques. It is worth noting that ancestor age estimates have ranged from thousands to millions of years, suggesting that a better understanding of filovirus evolution has still to be gained before reliable dates can be defined (M. A. de La Vega, Stein, and Kobinger 2015; Negredo et al. 2011; Olival and Hayman 2014; D. J. Taylor et al. 2011). The analysis of ZEBOV L protein sequences proposed that the type specie *Zaire ebolavirus* diverged in recent times from a common ancestor as a result of mutations accumulated within the last 30 years (Biek et al. 2006). Recently, Carroll et al. performed phylogenetic analyses on 97 whole-genome sequences within the family *Filoviridae* being able to estimate recent common ancestry (50 years ago) for *Reston ebolavirus* and *Zaire ebolavirus* species as a result of a recent genetic bottleneck. Moreover, *Marburg marburgvirus* and *Sudan ebolavirus* species were estimated to have common ancestors less than 1000 years ago (approximately 700 and 850 years ago, respectively). The examination of the whole *Filoviridae*, including the recently described *Lloviu virus*, suggested that members of the family shared a most recent common ancestor approximately 10,000 years ago (Carroll et al. 2013).

1.5 Evidence of bats as Ebola reservoirs in nature

Ebola virus is considered a zoonotic pathogen capable to affect humans and several animal species but, to date, the natural reservoir of the virus is not known with certainty and still remains a complicated and discussed case.

From the first EVD outbreak in 1976, thousands of animals and insects have been collected and studied, although it is believed that fruit bats (*Chiroptera*: *Pteropodidae*) play an important role in preserving the presence of the virus in nature (Dutto et al. 2016; Leroy et al. 2009; Pourrut et al. 2005).

Ecological niche models were used to provide the geographic and ecological distributions of Ebolavirus, suggesting that various bats, mouse, rat, dormice, and

shrew species may be sources of the infection (Pigott et al. 2014). Other virological studies suggested small mammals, comprising rodents and shrews, might be reservoirs. Also arthropods vectors were also considered, but viral replication in arthropod cell lines was unsuccessful (Feldmann and Geisbert 2011; Morvan et al. 1999; Swanepoel et al. 1996).

Primates have been considered as EVD reservoirs, since they are known to have a role in EVD dissemination, as the first known human cases were linked to exposure to lab primates in Europe in 1967 (the *Lake Victoria marburgvirus*). However, it is uncertain whether there is a primate-to-primate transmission, or if primates are "dead-end" hosts. It is worth of note that primates, especially great apes, appear to have been severely affected by ZEBOV and populations of western lowland gorillas (*Gorilla gorilla gorilla*) and common chimpanzees (*Pan troglodytes*) have declined by approximately 80% in parts Central Africa and these declines were linked to *Ebolavirus*. This susceptibility of African apes, together with the fact that many years are required for these ape populations to recover following mass mortality events, suggests that African apes are unlikely to be able to act as sole reservoirs for infection (Olival and Hayman 2014).

The natural reservoir for *Marburg-* and *Ebolavirus* remained elusive for decades and diverse taxa have been suggested as potential reservoirs (Olival and Hayman 2014). In 1995, a massive study on 78 mammal species, 51 bird species, and 22 reptiles and amphibian's species, with bats that were approximately 1/5 of all the animals collected, was conducted in DRC. Samples were collected from 3066 vertebrates and tested for the presence of antibodies to Ebola (subtype Zaire) virus, but all tests were negative, and attempts to isolate Ebola virus were unsuccessful (Leirs et al. 1999). Swanepoel et al. demonstrated that plants, reptiles, invertebrates and some vertebrates were unlikely reservoirs, because experimentally they were refractory to infections. However, the bats they tested were able to survive infection, to support replication, and to mount an

adaptive immune response (Swanepoel et al. 1996). This result was a first data at support to the hypothesis of bats as natural reservoirs of the virus.

It is interesting to note that the geographic ranges of many animal species took in consideration, such as bats, squirrels, mice and rats, dormice, and shrews, matched or overlapped with known outbreak sites of African filoviruses; nonetheless, none of these mammals have yet been universally accepted as an EBOV reservoir (Baseler et al. 2017).

Indeed, insectivorous and fruit-eating bats (particularly *Pteropodidae*) are considered among the prime reservoir suspects because they apparently do not develop the filoviral disease, but their implication as EBOV natural reservoirs is a complicated case. Despite EBOV epidemics have been temporally associated with bat migrations, infections, and die-offs, the attempts to implicate bats as EBOV reservoirs have been problematic (Baseler et al. 2017). However, the association of a new Cuevavirus with European bats (Negredo et al. 2011) and a stronger case for bats, in particular *Rousettus aegyptiacus*, serving as reservoirs of Marburg viruses (Paweska et al. 2016) added greatly to the plausibility of bats serving as EBOV reservoirs.

1.6 Pathogenesis of the viral disease

1.6.1 Viral haemorragic fevers and EVD

Previously known as Ebola hemorrhagic fever (EHF), the clinical syndrome caused by Ebola virus is today called Ebola virus disease (EVD). In fact, the uncontrolled viral replication, coupled with the systemic importance of the disease symptoms and clinical manifestations, has prompted the international scientific community to redefine the disease as EVD, replacing the old characterization. Further, it is important noting that this new definition reflects the fact that Ebola virus does not uniformly cause overt signs of hemorrhage. In fact, when referring to a viral haemorragic fever (VHF) we typically mention a viral syndrome characterized by malaise, fever, vascular permeability, decrease plasma volume, coagulation abnormalities, and varying degrees of hemorrhage. Several RNA virus families, such as arenaviruses (e.g., Lassa, Junin, and Lujo virus), nairoviruses (Crimean-Congo hemorrhagic fever and hemorrhagic fever with renal syndrome virus), filoviruses (Ebola and Marburg virus), and flaviviruses (yellow fever virus and dengue virus) induce a VHF. Moreover, among those viruses that cause VHF, the frequency of hemorrhagic manifestations can vary and generally represents the most severe form of disease caused by these pathogens; therefore, because of the possibility that these diseases progress to VHF of high fatality rates, the viruses associated with this syndrome are of particular concern from a public health perspective (Basler 2017; Feldmann and Geisbert 2011).

1.6.2 Routes of infection and mechanisms of viral transmission

Even if the scientific community currently possesses a robust knowledge on the Ebola virus and its mechanisms of diffusion¸ the route of primary transmission from the unknown reservoir to an end host species, such as humans, remains unknown.

EVD is a zoonotic disease and as such can infect both human and animals (Fig. 9). Animals carrying the virus can infect other animals, as well as humans, and after a "spill over event", occurring when an animal or human become infected with EBOV

through contact with the reservoir host, the disease can spread among human communities. Once introduced among humans, various are the possibilities of EBOV transmission from human-to-human: the virus can be inoculated by injection into the bloodstream, or via exposure of mucous membranes, or non-intact skin to infectious body fluids or tissues. In humans, EBOV has been found in variety of bodily fluids, including saliva, blood, breast milk, stool, and semen. Laboratory exposure through needlesticks and blood has been reported. This route of transmission was observed during the first EVD outbreaks, when the reuse of contaminated needles played an important part in the 1976 outbreaks of Ebola virus in Sudan and Zaire (Baseler et al. 2017; Feldmann and Geisbert 2011; Judson, Prescott, and Munster 2015).

Besides direct contact, multiple potential routes of transmission are documented, such as droplets, aerosols and fomites (Fig. 10). In fact, a direct (versus indirect) contact with infectious material is associated with a significantly increased risk of infection. The presence of infectious viral particles into proteinaceous material give the possibility to the virus to persist on inanimate surfaces for days or weeks (and even longer in conditions as the climate-controlled hospital settings), allowing previously contaminated fomites (such as bed sheets or gurneys that have been in contact with EBOV patients or other surfaces contaminated with EBOV-containing bodily fluids upon which dried blood persists) to serve as viable sources of infection (Baseler et al. 2017). Also, it must be considered the panorama of public health infrastructures in the countries afflicted by EVD outbreaks; in fact, it is common to find in those areas open sewage canals or waste-containing buckets and, because EBOV is shed in feces and other bodily secretions that come into contact with water, contaminated waters could come into contact with the eyes, nose, or mouth of individuals, leading to possible infection through contact with mucous membranes (Judson, Prescott, and Munster 2015).

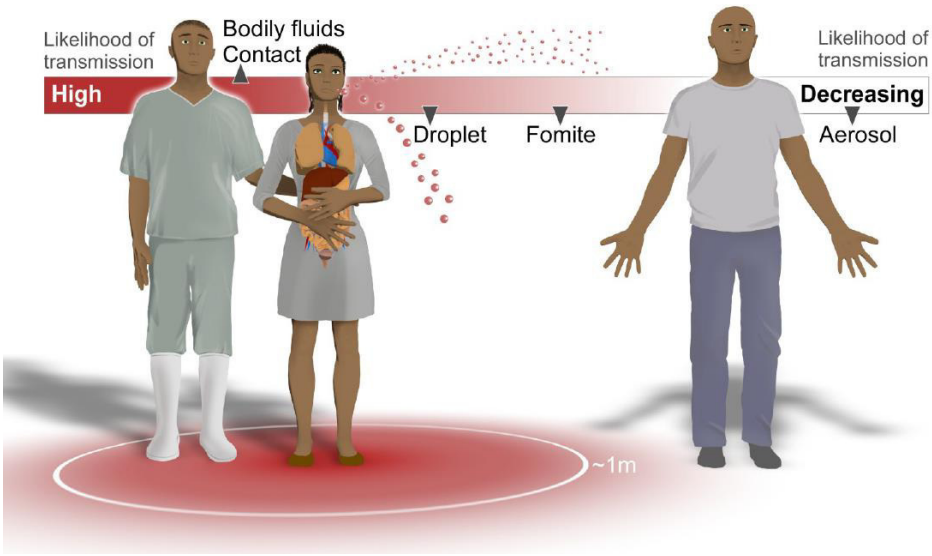

Fig. 9. The transmission mechanisms of Ebola virus. The image illustrates and describes the various routes of transmission of EVD and the chain of events that leads to the spread of the disease among humans (source: Judson, Prescott, and Munster 2015).

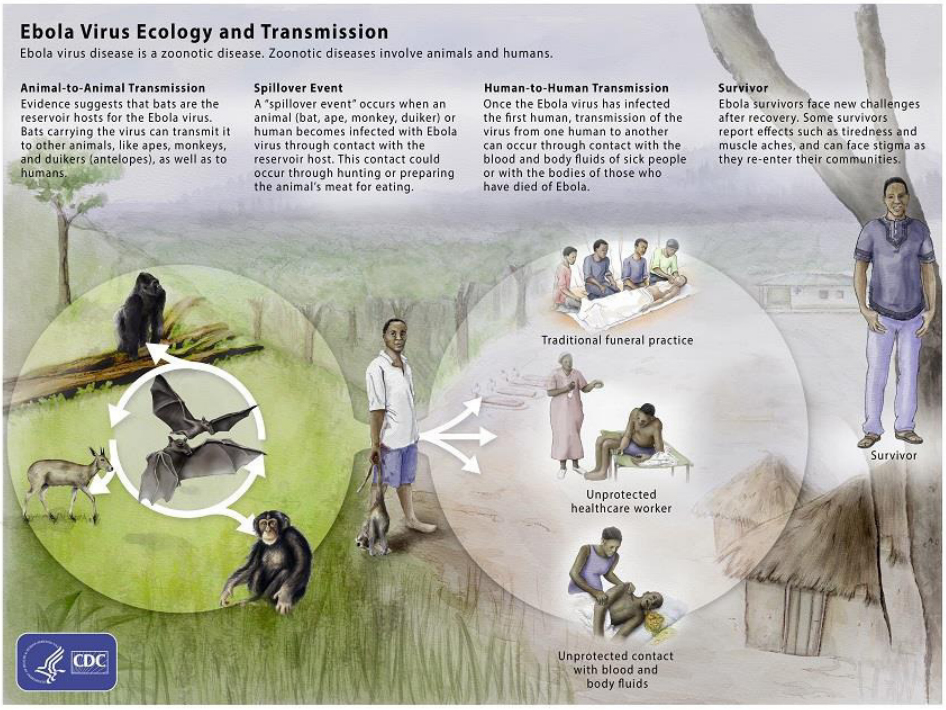

Fig. 10. Potential routes of Ebola virus transmission and infection between people. Ebola virus has been isolated from a number of bodily fluids including blood, stool, semen, saliva, and breast milk and contact with these fluids from infected individuals creates a high risk of transmission. These infectious fluids can also be formed into droplets which travel in the air (range unknown, possibly 1 meter) and potentially infect others. EBOV has been detected in dried blood and persists on surfaces, so the possibility of fomite transmission exists. Airborne transmission via small aerosol droplets is unlikely from current EBOV epidemiology (source: cdc.gov/vhf/ebola/resources/virus-ecology).

The recent West African epidemic showed long chains of intensive person-to-person transmission into human communities that was associated with both intimate and unappreciated exposures; the risk of secondary transmission was calculated to be 47.9% for those providing direct care and, in a different study, to 83% for persons touching corpses (Bower et al. 2016; Dean et al. 2016). Currently, one of the most dangerous mechanisms of EBOV spread seems to be body washing and other burial practices (Nielsen et al. 2015).

The role of aerosol transmission in outbreaks is unknown, is thought to be rare, but the possibility of an aerosol/airborne diffusion was also estimated. It occurs when small, virus-laden droplets evaporate before settling on surfaces, leaving behind infectious droplet nuclei that can travel long distances. Currently no data exist on the formation of EBOV droplet nuclei. However, since in one outbreak 5 out of 19 patients reported not having had direct contact with an infected individual and, because these patients were in close proximity with infected individuals, it was speculated that a droplet transmission could have occurred (Roels et al. 1999). While there is no evidence of airborne transmission of EBOV in humans, experiments in NHPs have shed light on this mode of infection; however, it is important to note that in these experiments the virus was aerosolized mechanically and at temperate conditions, 24 °C and <40% relative humidity (to simulate an outbreak in the United States), and therefore do not reflected the environment of African outbreaks (Feldmann and Geisbert 2011). Other ways that EBOV-containing droplets and aerosols could be created are through aerosol-generating procedures (AGPs), which refer to: i. the procedures in clinical settings aimed to stimulate coughing or manipulate the patient's airway (including activities such as intubation, manual ventilation, and bronchoscopy); ii. spraying and pressure washing procedures of infected materials (for example, indirect EBOV infections from NHPs that are believed to have occurred during pressure washing cages, or from activities by the NHPs themselves that could have formed EBOV-containing droplets that infected other animals) (Judson, Prescott, and Munster 2015).

Further, pregnant women have an increased risk of miscarriage, and clinical findings suggest a high death rate for children of infected mothers that may be due to transmission from the infected mother to the child in utero (during delivery), or during breastfeeding, either through milk or close contact. EVD is almost universally fatal to the developing fetus, but limited fetal autopsy data prevent interpretations on risk of birth defects. The vast majority of pregnancies affected by EVD end in fetal loss (78% stillbirths or miscarriages) and newborns die within 19 days of life. In the academic literature, there is one report of a neonatal survivor born to a mother with EVD surviving beyond 19 days of life (Bebell, Oduyebo, and Riley 2017; Dornemann et al. 2017).

Finally, it is notable that EVD spread among population settled in remote and rural central Africa regions, where it is common the use of bushmeat as an alimentary source. In fact, butchering of a chimpanzee for food was linked to outbreaks of Zaire Ebola virus in Gabon, and contact exposure was the probable route of transmission. Although proper cooking of foods should inactivate infectious Ebola virus, ingestion of contaminated food cannot wholly be ruled out as a possible route of exposure in natural infections. Notably, handling and consumption of freshly killed bats was associated with an outbreak of Zaire Ebola virus in DRC (Feldmann and Geisbert 2011).

1.6.3 Clinical manifestations

Ebola viruses are the causative agents of a severe form of VHF, endemic in regions of central Africa. The only exception is the species Reston Ebola virus, which has not been associated with human disease.

Signs and symptoms. The problem with the diagnosis of Ebola infection is that the early stages of the infection include an asymptomatic incubation followed by the onset of nonspecific signs and symptoms consisting of onset of fever, myalgia, and general malaise and sometimes accompanied by chills that can be easily (and often) confused with malaria or dengue in tropical climates. During incubation, patients are able to

carry on routinely activities, including work and travel, so facilitating the spread of the disease, but become quickly incapacitated upon illness onset (Baseler et al. 2017).

Typical cases of EVD occur as follows: after an incubation period of generally 2–21 days (mean 3–13) characterized by the onset of non-specific symptoms (often referable to flu-like symptoms) such as fever, chills, fatigue, headache, myalgia, nausea, vomiting, and diarrhea, the disease makes its sudden appearance (Fig. 11). Fever is usually a presenting sign (>37.5°C) and should raise concern in any patient with suspected epidemiological risks. However, normal temperature or even hypothermia may occur, especially in late stages. Also, in the initial stages of the disease bradycardia is usually present, in contrast to tachycardia which occurs later in the fatal infections (Basler 2017; Khalafallah et al. 2017).

Subsequent signs and symptoms indicate a multisystem involvement and include systemic (prostration), gastrointestinal (anorexia, nausea, vomiting, abdominal pain, diarrhoea), respiratory (chest pain, shortness of breath, cough, nasal discharge), vascular (conjunctival injection, postural hypotension, oedema), and neurological (headache, confusion, coma) manifestations. During the peak of the illness the haemorrhagic manifestations arise and include petechiae, ecchymoses, uncontrolled oozing from venepuncture sites, mucosal haemorrhages, and (post-mortem) evidence of visceral haemorrhagic effusions. A nonpruritic, erythematous, macropapular rash associated with varying severity of erythema and desquamate can often be noted by day 5–7 of the illness, usually developing early in 25%–52% of patients and involving neck, trunk, and arms; this symptom is a valuable differential diagnostic feature and is usually followed by desquamation in survivors (Feldmann and Geisbert 2011; Khalafallah et al. 2017). In later stages, shock, convulsions, severe metabolic disturbances, and, in more than half of the cases, diffuse coagulopathy supervene. Tachypnea occurs in the severe infections, and it is explained by the respiratory compensation of the metabolic acidosis rather than the infection itself. Patients with fatal disease develop clinical signs early during infection and die typically between day

6 and 16 with hypovolaemic shock and multiorgan failure. Haemorrhages can be severe but are only present in fewer than half of patients (Fig. 11).

In non-fatal cases, patients have fever for several days and improve typically around day 6–11, about the time that the humoral antibody response is noted, and mount specific IgM and IgG responses that seem to be associated with a temporary early and strong inflammatory response, including the production of interleukin β (IL-β), interleukin 6 (IL-6), and tumor necrosis factor α (TNFα). However, whether this is the sole mechanism for protection from fatal disease remains to be proven (Feldmann and Geisbert 2011).

Laboratory findings. The laboratory variables are less characteristic respect to the visible clinical manifestations of the disease, but the following laboratory findings are often associated with EVD (Table 3): an early leucopenia (as low as 1000 cells/μL) with loss of lymphocytes (lymphopenia) and subsequent neutrophilia, followed by a left shift with the presence of atypical lymphocytes, thrombocytopenia (50000–100000 cells/μL), highly raised by serum aminotransferase concentrations (aspartate aminotransferase typically exceeding alanine aminotransferase), hyperproteinaemia, and proteinuria (Feldmann and Geisbert 2011).

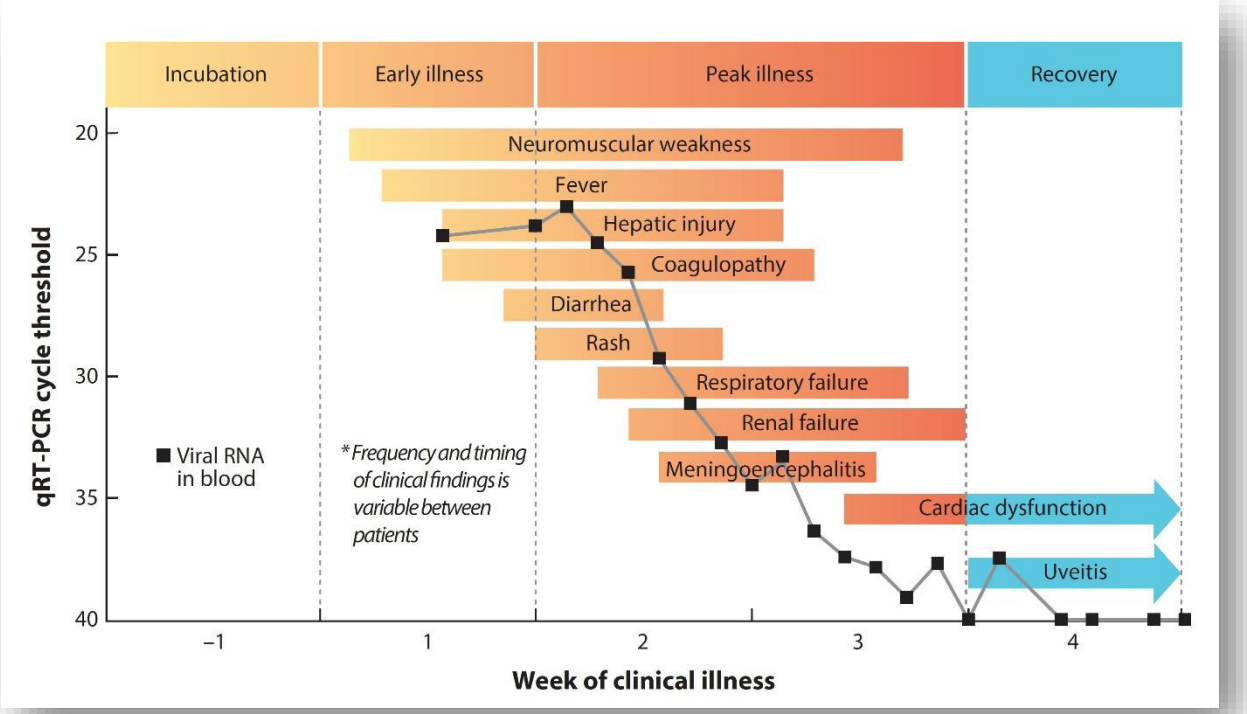

Fig. 11. The clinical course of EVD. After the detection, through quantitative reverse transcription polymerase chain reaction (qRT-PCR) of viral RNA in blood (line graph), the clinical illness has its onset and progress. A sequential organ failure, despite declining viral RNA in blood, takes place. New or persistent clinical findings occur during recovery, following clearance of viral RNA in the blood (source: Baseler et al. 2017).

Table 3. Common laboratory findings in EVD.

Timing	Laboratory finding
Early illness	• Leukopenia, lymphopenia, and thrombocytopenia • Elevated hemoglobin and hematocrit • Elevated aspartate aminotransferase and alanine aminotransferase (ratio ≥3:1) • Elevated prothrombin time, activated partial thromboplastin time, and d-dimer
Peak illness	• Leukocytosis, neutrophilia, and anemia • Hyponatremia, hypo- or hyperkalemia, hypomagnesemia, hypocalcemia, hypoalbuminemia, hypoglycemia • Elevated creatinine phosphokinase and amylase • Elevated blood urea nitrogen and creatinine • Elevated serum lactate and low serum bicarbonate
Recovery	• Thrombocytosis

Long term consequences of EVD. Finally, it is worth to mention the clinical picture of EVD survivors. The recent ZEBOV outbreak in West Africa highlighted the complexity of EVD sequelae in clinically recovered patients (Fig. 12). In fact, a series of studies on the long-term health outcomes in EBOV survivors pointed out the attention on a number of clinical consequences affecting those patients, such as a greater risk for ocular problems (retro-orbital pain and blurred vision), loss of hearing, swallowing difficulties, arthralgia, abdominal and back pain, fatigue, impotence, severe headaches, memory problems, sleeping difficulties and confusion (Clark et al. 2015). Further investigation of recovering survivors revealed that EBOV persists in a number of bodily fluids (semen, ocular fluid, cerebrospinal fluid, placenta and amniotic fluid) and that is still capable of being transmitted, thus increasing the risk of sexual transmission from male survivors to their partners as recently demonstrated by Mate et al. in 2015 (Deen et al. 2015; Mate et al. 2015; Rodriguez et al. 1999).

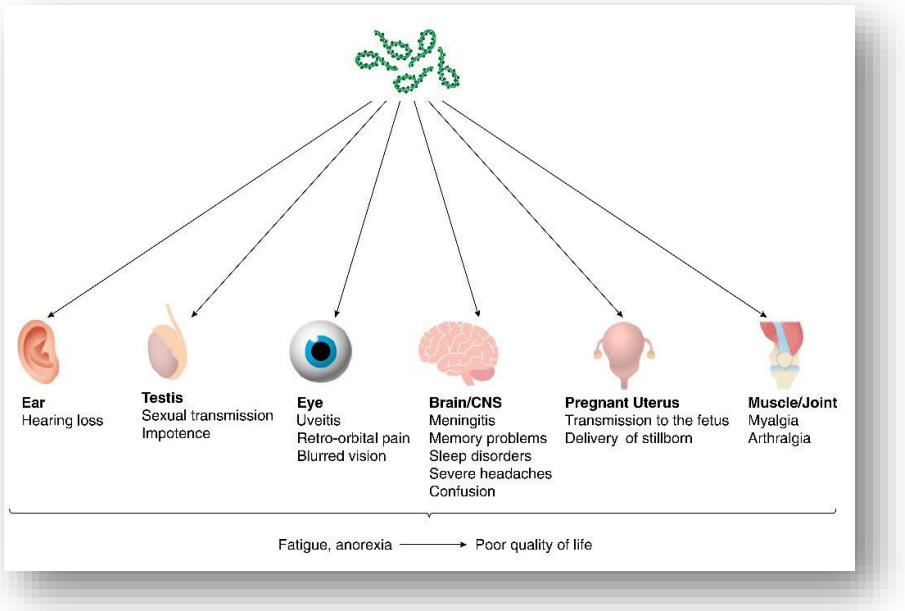

Fig. 12. Long-term post-EBOV consequences. The image shows EBOV persistence into organs that are immune privileged for infection (including the ear, testis, eye, CNS, pregnant uterus, and muscle tissue), observed in clinically recovered patients and resulting in Ebola disease sequelae (source: Rivera and Messaoudi 2016).

1.6.4 Target cells and tissues

Following viral inoculation onto mucous membranes or nonintact skin, EBOV targets dendritic cells and other cells of the monocyte/macrophage lineage. Importantly, this virus infection first disables the immune system. Subsequently, it disables the vascular system that leads to blood leakage (hemorrhage), hypotension, drop in blood pressure, followed by shock and death (Ansari 2015; Baseler et al. 2017).

Ebola virus shows a broad cell tropism, and it is capable to infect a wide range of cell types. In-situ hybridization and electron microscopic analyses of tissues from patients with fatal disease or from experimentally infected NHPs showed that monocytes, macrophages, dendritic cells, endothelial cells, fibroblasts, hepatocytes, adrenal cortical cells, and several types of epithelial cells all lend support to replication of these viruses. Notably, temporal studies in NHPs experimentally infected with Zaire Ebola virus suggested that monocytes, macrophages, and dendritic cells are early and, most importantly, a preferred replication site for Ebola viruses.

EBOV appears to sequentially infect DCs disabling the interferon system (one of the major host anti-viral immune systems) then macrophages (that trigger the formation of blood clots, release of inflammatory proteins and nitric oxide, damaging the lining of blood vessels leading to blood leakage) and finally endothelial cells that contribute to blood leakage. Moreover, in an integrated manner, the virus also affects organs such as the liver (that dysregulates the formation of coagulation proteins), the adrenal gland (that destroys the ability of the patient to synthesize steroids and leads to circulation failure and disabling of regulators of blood pressure) and the gastro-intestinal tract (leading to diarrhea). By efficiently disabling such major mechanisms in the body defenses facilitates the ability of the virus to replicate in an uncontrolled manner, leading to the rapidity by which the virus can cause lethality (Fig. 13) (Ansari 2015).

EBOV infection of humans and NHPs has been shown to trigger the activation and the intervention of a cytokine storm and chemokines that leads to the recruitment of leukocytes to infected tissues, in order to limit virus dissemination and kill virus-

infected host cells, thus contributing to tissue damage. NO release is a trigger for the activation of macrophages that, in turn, may trigger parenchymal cell apoptosis or necrosis (Baseler et al. 2017).

Likewise, the infection of various primary human cells *in vitro* showed that EBOV infection can trigger the production of many of these same inflammatory mediators. To date, most current models suggest that excessive proinflammatory cytokine production and absence of an adaptive immune response are major factors in Ebola virus pathogenesis. However, the most important *in vivo* sources of the cytokine storm, the relevant signaling pathways that trigger these responses, the mechanisms by which these signals are activated, and the specific contribution of cytokine production to dysregulation of antiviral immunity, disseminated intravascular coagulation and circulatory shock all remain to be defined (Basler 2017).

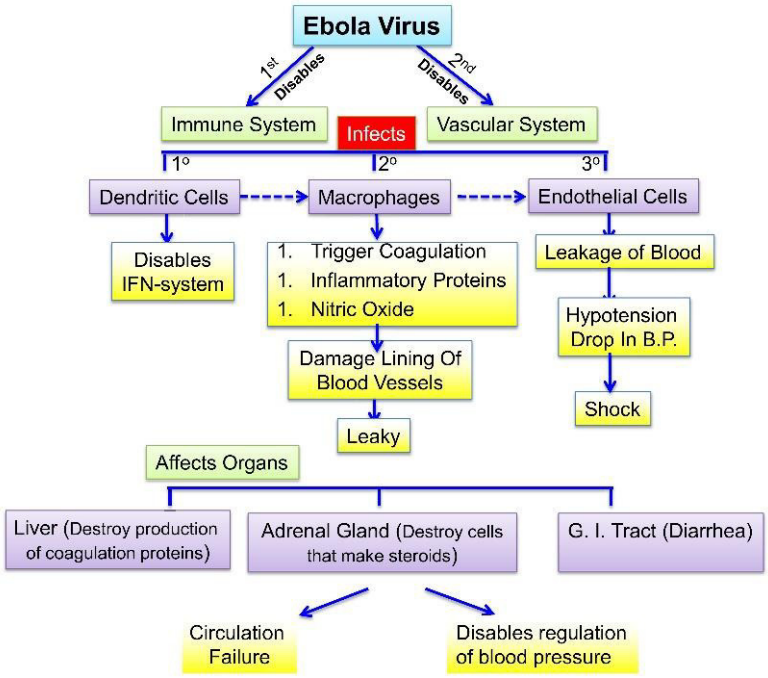

Fig. 13. Pathological events in EVD. The scheme describes the cascade of pathological events during EVD. EBOV first disables the immune system acting on dendritic cells maturation, thereby inhibiting macrophages in triggering the formation of blood clots, release of inflammatory proteins and nitric oxide, so damaging the lining of blood vessels (leading to blood leakage) and finally endothelial cells that contribute to blood leakage (source: Ansari 2015).

1.6.5 Countermeasures against EVD

Within the last 40 years of research multiple antiviral compounds have shown therapeutic promise in *in vitro* and animal studies. Several of these were administered to EVD patients or to persons undergoing prospective clinical trial evaluation, in particular during the West African epidemic.

Vaccine and drug development for EBOV has been in progress for several decades, primarily fueled by concerns about the potential use of the Category A agent as a bioweapon; in fact, EBOV is classified by the Centers of Diseases Control and Prevention as Category A biowarfare agent, because of the high virulence and the consequent ability to induce panic. The unprecedented magnitude and scale of the 2014–2016 outbreak in West Africa, combined with the potential spread to other corners of the world, led to a renewed focus on medical countermeasures for EVD (Bixler, Duplantier, and Bavari 2017). Only a small number of cases were treated with putative therapeutics in the U.S and Europe before formalized clinical trials were established late in the outbreak (Mohammadi 2014). Potentially, an effective therapeutic available in large quantities could not only treat individual cases but halt outbreaks. To date, however, no EBOV-specific therapy has been proven efficacious, nor has any therapy achieved regulatory approval for use in humans. Consequently, supportive care remains the mainstay of treatment (Baseler et al. 2017).

Drugs and small molecules

One of the most popular strategies for EBOV therapeutics is antivirals that directly target critical stages in the viral life cycle such as binding and/or entry of the virus into host cells, viral replication, packaging, or release of viral progeny from target cells. Small molecules, antisense therapies, and immunotherapeutics comprise the diverse list of EBOV antiviral compounds. A disproportionate number of the most advanced therapeutics currently under evaluation are small molecules directed against the RNA-

dependent RNA polymerase L required for viral replication (Bixler, Duplantier, and Bavari 2017).

Nucleic-acid based inhibitors, antisense phosphorodiamidate morpholino oligomers (PMOs) and small-interfering RNAs (siRNAs), had shown promise as EBOV therapeutics in non-clinical studies prior to the West Africa EBOV Outbreak. However, a key concern with these products is that they are sequence specific and may be ineffective for new outbreak variants (Cardile et al. 2016a). PMOs and siRNAs have shown efficacy in reducing mortality when administered to NHPs. Among them AVI 6002, a combination of positively charged PMOs designed to target mRNA sequences of VP24 and VP35 in EBOV, which is undergoing Phase I safety trials for EBOV post exposure treatment, shown to be well tolerated in healthy adult subjects. TKM-Ebola (formerly Tekmira), is a combination of small interfering RNAs (siRNAs) formulated in stable nucleic acid lipid particles. When administered to 7 NHPs, the combination of siRNAs targeting the EBOV L polymerase, VP24 and VP35, protected from EBOV infection six out of the 7 NHPs, with good tolerance of the drug. Furthermore, it is also being designed to target the Guinea variant of EBOV and was planned to enter human clinical evaluation in Guinea in emergency situations (Trad et al. 2017).

Nucleoside and nucleotide antivirals have thus far been the most successful class of antivirals given their success in treating HIV and herpes viruses. Four are the nucleoside/nucleotide analogues mentionable as anti-EBOV therapeutics: favipiravir, brincidofovir, BCX4430 and GS-5734.

The pyrazinecarboxamide derivative T-705 (favipiravir) is licensed in Japan for the treatment of influenza not responding to conventional therapies. It has antiviral activity against other negative stranded RNA viruses, and has been used in the European centers that treated EVD in the last outbreak. In a rodent model, favipiravir induced rapid Ebola viral clearance when administered as late as day 6 following inoculation with EBOV. However, in a non-randomized study conducted in Guinea during 2013–2015, no reduction in viral load or mortality was observed among 99 EVD

patients, adults and adolescents, treated with favipiravir when compared to untreated historical control subjects (91%mortality rate in those treated with favipiravir vs 85% in historic controls) (Cardile et al. 2016b; Sissoko et al. 2016).

Brincidofovir (CMX001) is a prodrug of cidofovir originally studied as a treatment for double-stranded DNA viruses. It is an effective anti-DNA antiviral medication that acts by inhibiting viral replication secondary to selectively inhibiting viral DNA polymerases. Even though the mechanism of action is not well characterized for RNA viruses, *in vitro* studies with EBOV demonstrated a relationship between the antiviral properties and the lipid nucleotide conjugate, and its efficacy against EBOV (McMullan et al. 2016). Consequently, Brincidofovir has been used in emergency situations in patients infected with EBOV (was experimentally used to treat one of the first patients to be transferred to the U.S.) and was undergoing Phase II clinical trials, which were unfortunately halted due to lack of new cases (Warren et al. 2014).

BCX4430 is an adenosine nucleoside analogue currently under investigation as a treatment for a number of viral infections including EBOV (R. Taylor et al. 2017). This compound inhibits the viral RNA polymerase activity by adding a highly selective monophosphate nucleotide to the nascent RNA chain, interrupting elongation. When administered 48 hours after infection via IM injection, BCX4430 demonstrated a 100% protection from Marburg virus in a NHP model, and could potentially be used for EVD. Also, it has shown efficacy in pre-exposure treatment of EBOV *in vitro* and in small animal models. BCX4430 is planned for further animal studies (Cardile et al. 2016b).

As BCX4430, GS-5734 is another but newest polymerase inhibitor being evaluated as a therapeutic for EBOV. It is a small-molecule monophosphoramidate prodrug of an adenosine analogue that is rapidly converted to its pharmacologically active triphosphate form. In NHP model of EBOV infection resulted in 100% survival and, significantly, the drug has been found to distribute into the testes, epididymis, eyes, and brain within 4 hours of administration. As a consequence, GS- 5734 may also be of efficacy in post-Ebola syndrome and eradication of persistent viral replication in the

genital tract. Another advantage of GS-5734 is the rapid distribution to cells of the mononuclear line with maintenance of levels as sufficient for viral inhibition for approximately 24 hours. Given that the initial target cells for EBOV infection are properly the cells of the mononuclear line, GS-5734 may also be valuable for post-exposure prophylaxis of high-risk exposures. For this reason, the drug was used in the case of a nurse who suffered an EBOV relapse causing meningoencephalitis and in an infant in Guinea, and both individuals survived infection (Jacobs et al. 2016). Intravenous GS-5734 is currently undergoing human phase 1 studies (Warren et al. 2016).

Multiple other compounds have been evaluated in preclinical studies for the treatment of EVD, such as the antisense oligonucleotides (Iversen et al. 2012) or the therapies targeting the disordered coagulation induced by EBOV infection using recombinant nematode anticoagulant protein C2 or recombinant activated protein C, but has not yet advanced to human trials and not been studied for safety and efficacy in humans (Baseler et al. 2017).

Vaccines

Vaccines are a potential cornerstone for limiting or fully preventing an EVD outbreak. Their development for protection against infection with rare or exotic pathogens typically falls into the spheres of public health and/or biodefense and such development does not, however, often attract the interest from the pharmaceutical industry, so candidate vaccines for rare diseases often languish at the research bench stage. The 2013–2016 EVD outbreak in Western Africa however, was a shock to the system and was a strong incentive in this sense. To date, numerous are the vaccine trials, including the two leading candidates in Phase III trials rVSV-ZEBOV (recombinant vesicular stomatitis virus vector) and ChAd3-ZEBOV (adenovirus vector) vaccines (Trad et al. 2017).

The “rVSV-ZEBOV” vaccine (also known under a number of different names such as VSVG-ZEBOV-GP, rVSVdeltaG-ZEBOV-GP, BPSC1001, and, most recently, V920) is the only EVD candidate vaccine for which human efficacy data exist. It was developed on the base of Vesicular stomatitis Indiana virus (VSIV), which is a single-stranded, negative-sense RNA mononegavirus (*Mononegavirales*: *Rhabdoviridae*: *Vesiculovirus*) that typically infects livestock and rarely infects humans. Recombinant VSIV-based vaccines induce strong cellular and humoral immunity, are easily propagated *in vitro*, and undergo little, if any, genetic recombination or genetic reassortment. The distinguishing feature of rVSV-ZEBOV is that EBOV GP1,2 replaces the VSIV glycoprotein (G), resulting in an exclusive expression of EBOV GP1,2 on virions produced from the recombinant VSIV. The vaccine has been used in ten clinical vaccination ring trials, including trials in Liberia, Kenya, and Sierra Leone (according to the registry of clinical trials maintained by NIH: https://clinicaltrials.gov), but the most impactful trials were the ones performed in the Guinea (in Conakry and eight surrounding prefectures in the Basse-Guinée region), and in Tomkolili and Bombali in Sierra Leone 2015 (Henao-Restrepo et al. 2015). Instead, the DRC has not made a formal request for the vaccine but it has been in discussions with WHO and other partners so far. On December 2016 the GRT was concluded, and the evidence from all 117 clusters showed an estimated vaccine efficacy of 100% (95% CI 79.3 – 100.0, p = 0.0033). A total of 5837 individuals received the vaccine (5643 adults and 194 children), and all vaccines were followed up for 84 days. Adversely, while the efficacy associated with rVSV-ZEBOV is highly encouraging, the duration of vaccine-induced protective immunity remains unknown and, importantly, the vaccine has been marred by safety concerns. The 53.9% (3149) of 5837 individuals reported at least one adverse event in the 14 days after vaccination, with these that were typically mild (87.5% of all 7211 adverse events) and 80 serious adverse events were identified, of which two were judged to be related to vaccination (one febrile reaction and one anaphylaxis) and one possibly related to it (influenza-like illness) (Henao-Restrepo et al. 2017).

On May 2017 the WHO declared being ready to deploy Ebola vaccine in the last disease outbreak spread in DRC. To date, the rVSV-ZEBOV vaccine is not yet licensed, because of several steps needed to be taken before made it available to health workers, contacts of those infected, and contacts of those contacts. Further, it still requires a full study protocol approved by the local ethics review board and, importantly, the logistics in place to manage a ring vaccination campaigns. In fact, this vaccine needs to be kept at −80°C, posing an "enormous challenge" in areas with poor telecommunications and road accesses, and without large scale electrification (Gulland 2017).

The chimpanzee-adenovirus ChAd3-Zaire Ebola virus (ChAd3-ZEBOV) began Phase III clinical trials at the beginning of 2015 (M. A. de La Vega, Stein, and Kobinger 2015). Into this platform, the EBOV GP1,2 is encoded by the adenovirus backbone and is therefore expressed upon entry of a target cell by the encoded adenovirion; of note, GP1,2 is not located on the adenovirus particle surface, as in the case of VSIV-based vaccines. As a non-replicating vaccine, ChAd3-EBOZ has not caused the concerning adverse events seen with rVSV-ZEBOV; however, ChAd3-EBOZ also appears to be inadequately immunogenic as a single vaccination. ChAd3-EBOZ is currently being evaluated in clinical trials in Africa, including in Mali, Senegal, Uganda, and Liberia (Martins et al. 2016).

Antibody based therapies

Human survivors to EVD tend to mount an early, vigorous, and long standing neutralizing antibodies (NAbs) that can bind to EBOV structural envelop glycoprotein GP (Shedlock et al. 2010). For this reason, NAbs have been exploited in monoclonal antibody combinations and blood products.

Even in this case, being the only surface-expressed viral protein of EBOV, GP is a common target of such therapeutic antibodies. Moreover, since a single antibody may not be able to neutralize every single viral particle, a cocktail of antibodies is typically

required. Produced *in vitro* from convalescent blood, NAbs are in the form of cocktails of monoclonal antibodies (mAbs) against EBOV GP. Among them, ZMapp a well-known cocktail of 3 chimeric mAbs (c13C6, c2G4 and c4G7), ZMab a cocktail of mouse mAbs (m1H3, m2G4, m4G7), and MB-003 a cocktail of human-mouse chimeric mAbs (c13C6, h13F6, c6D8) (Trad et al. 2017). These Nabs cocktails have demonstrated in animal models some of the most significant therapeutic potential for treating EVD. Of note, ZMapp and ZMAb have been used under emergency compassionate protocols in humans to treat EBOV infections originating from the 2014 EVD outbreak in western Africa. A total of 15 patients were treated with ZMapp or ZMAb under compassionate-use protocols to treat EBOV infections originating from the 2014; at least seven patients have been treated with ZMapp, with five surviving, and six patients have been treated with ZMAb, with all surviving (Davidson et al. 2015). Compared to vaccines that require longer time to induce protection, antibody-based therapies can potentially offer protection immediately after EBOV exposure for up to 120 h in animal models (Pettitt et al. 2013). However, their major drawbacks are a lack of availability and a significantly declining efficacy when given later in the course of experimental infection (Trad et al. 2017).

1.7 EBOV biology

1.7.1 Genome, proteins and structure

Ebola virus particles contain a linear, non-segmented, ssRNA-, therefore classified as a Class V virus (Baltimore 1971). The genome size is of approximately 19 kb in length (Fig. 14) for an average molecular mass of 4×10^3 kDa.

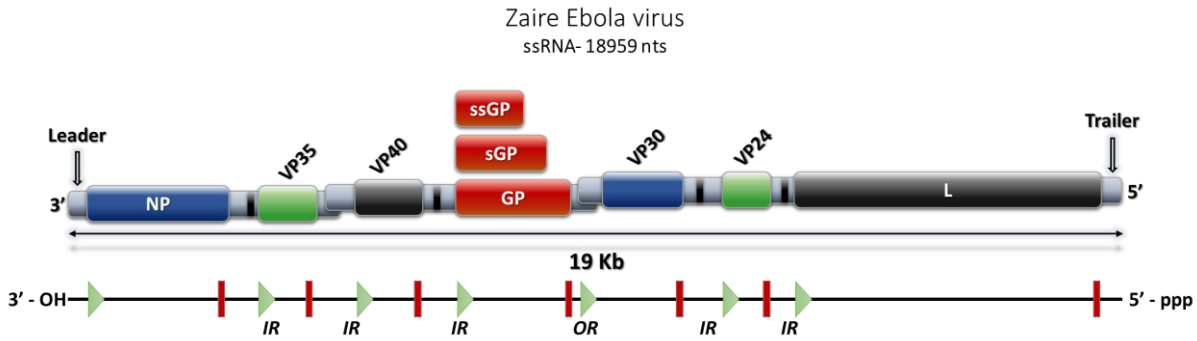

Fig. 14. Organization of EBOV genome. Schematic diagram of the type species Zaire Ebola virus ssRNA- genome with its coding regions. Transcription start signals are depicted as green triangles and stop signals as red bars; leader and trailer (arrows), intergenic (IR) and overlapping regions (OR) are indicated.

Organized in 7 linear genes which encode up to 9 viral proteins, 7 of which are structural proteins found in mature virions, while 2 additional proteins are secreted and do not participate to the formation of viral particles, the viral genome displays the following recurrent structure: 3′-leader ► *nucleoprotein* (*NP*) gene ► *viral protein* (*VP*) 35 gene ► *VP40* gene ► *glycoprotein* (*GP*) gene ► *VP30* gene ► *VP24* gene ► *polymerase* (*L*) gene ► 5′-trailer.

The genome is not polyadenylated at its 3′ terminus and is uncapped at its 5′ termini. At both genomic ends 2 brief and conserved extragenic regions, namely leader (l) and trailer (t) regions, that consist of short non-transcribed regions containing cis-acting signals important for replication, transcription initiation and encapsidation of the genomic RNA are present (Mühlberger 2013).

The coding region of each EBOV gene consists of a central open reading frame (ORF) and is flanked by 3′ and 5′ untranslated regions (UTRs) of highly-conserved transcription initiation and termination sequences that contain the pentameric sequence 3′-UAAUU-5′. Most genes are separated by intergenic regions of variable lengths, although some genes overlap in parts of their UTRs. It is worth of note that all genes are monocistronic with the exception of *GP* gene, for which 3 different ORFs encode a total of 3 viral glycoproteins (GP, sGP, ssGP) that are final products of mRNA

editing event performed by the viral polymerase complex, a feature that distinguishes the ebolaviruses from the marburgviruses. The ORF of each EBOV gene is flanked at both sides by long non-translated sequences, named intergenic regions (IR), which vary in length (from 57 up to 684 bp) and nucleotide composition among EBOVs species, and are apparently not essential for viral transcription. Only one longer intergenic region is located between the *VP30* and *VP24* gene of the different EBOV species. Furthermore, EBOV genes also share overlapping regions (OR), that reside between *VP35* and *VP40* genes. In RESTV species the OR is located between *VP24* and *L* genes, while EBOV, SUDV, TAFV and BDBV species own an additional third OR located between *GP* and *VP30* genes (M.-A. de La Vega et al. 2015; Ning et al. 2017).

EBOV proteins have distinct functions in the life cycle of the virus and, once transcribed and translated, constitute the core structure of filovirus particles, referred to as the nucleocapsid (NC), which is composed by the RNA genome, NP, VP35, VP30, VP24, and L. The trimeric transmembrane glycoprotein (GP), through its carboxyl-terminal end is inserted into the membrane as a type I transmembrane glycoprotein, and forms surface spikes on the virion envelope, while the membrane-associated matrix protein VP40 is associated with the inner surface and is responsible for generating the filamentous structure of viral particles and the connection of NC with the host-derived lipid membrane (Baseler et al. 2017; Beniac et al. 2012).

The first gene on EBOV genome, *NP*, codifies for a nucleoprotein of 739 amino acid residues and a predicted molecular mass of 83.3 kDa. It is responsible for the tight encapsidation of the genome and its preservation from degradation events, and is also a major component of the viral ribonucleoprotein complex (RNP). Moreover, it has been recently showed that NP influences the phosphorylation state of VP30, key protein in regulation of viral RNA synthesis, whose phosphorylation and dephosphorylation take place in viral inclusion bodies that are induced by the nucleoprotein NP (Lier, Becker, and Biedenkopf 2017).

The *VP35* gene, in second position on the genome, leads to the expression of a 340 aminoacid long multifunctional protein, with 35 kDa mass, which acts as a component of the replication and transcription holoenzyme and is also an assembly factor of EBOV viral particles. Moreover, VP35 is a determinant of EBOVs virulence, being a powerful antagonist of the host antiviral innate immune response.

The third gene along EBOV genome, *VP40*, encodes for the viral protein VP40, a major protein consisting of 326 residues and a molecular weight of 40 kDa. As mentioned before, VP40 is the matrix protein and is responsible for the creation of a regular lattice within the envelope (although its contacts with the nucleocapsid are irregular) in which EBOV NCs are assembled into mature virions. The crystal structure of VP40 shows that it is an octamer and forms a pore-like structure that binds RNA. Further, VP40 plays a critical role during virus budding, being crucial for NCs transport to the cell surface and for the incorporation of NCs into virions, event where the interaction between the proteins NP and VP40 is essential (Johnson et al. 2006; Kallstrom et al. 2005; Licata and et al. 2004; Noda et al. 2006).

From the homonymous fourth gene on the viral genome comes the GP protein, that represents the only EBOV structural glycoprotein. Ebolaviruses encode a full-length transmembrane glycoprotein ($GP_{1,2}$), as well as multiple nonstructural glycoproteins (GPs) such as the soluble glycoprotein (sGP), Δ-peptide, small soluble glycoprotein (ssGP), and shed GP. The production of the various GP forms is the result of transcriptional editing (mRNA editing by the viral polymerase-mediated addition or deletion of nucleotides at the specific site) of the *GP* gene and post-translational processing of GP precursors. The *GP* gene encodes three GP precursors (pre-sGP, pre-full-length GP, pre-ssGP) that result in multiple GP protein products. The primary product of the GP gene is pre-sGP (expressed from the majority of RNA transcripts, approximatively 71% of transcripts). It results from no shifting of the ORF and, cleaved by host enzyme furin at its C-terminus, yields an N- glycosylated sGP dimer

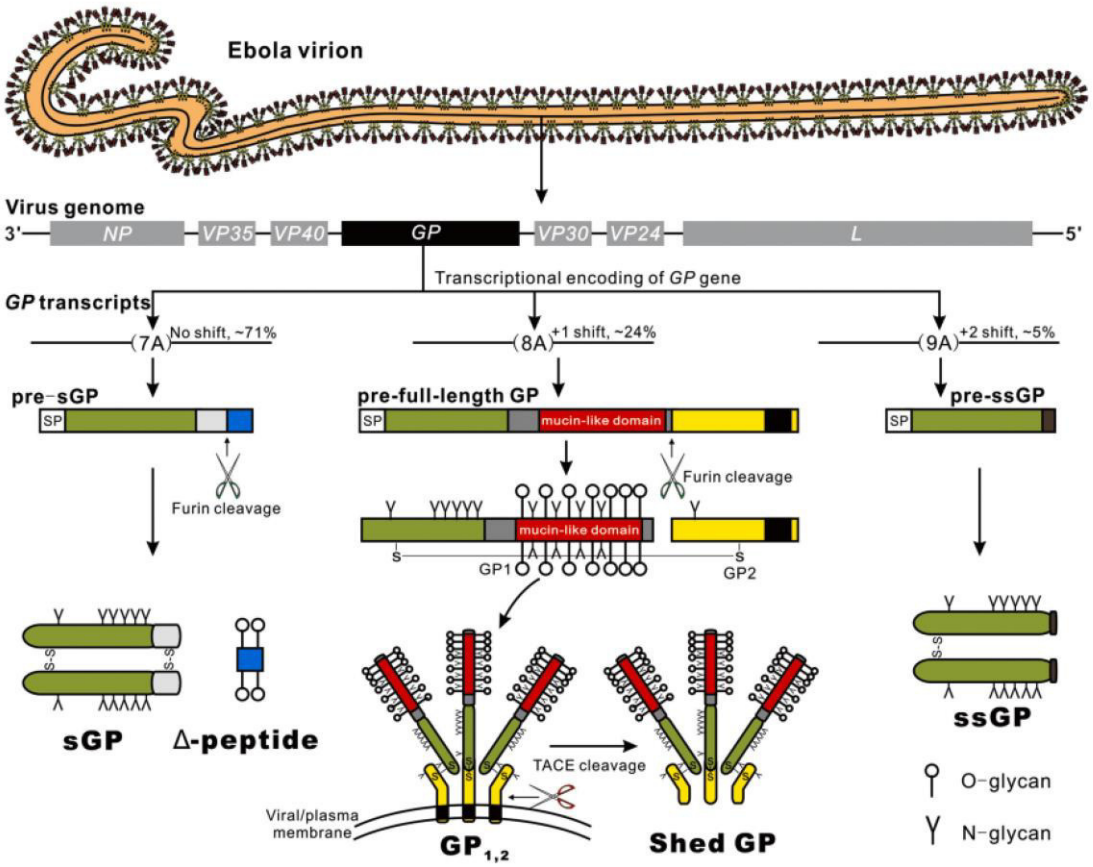

Fig. 15. Encoding strategy of ebolavirus GPs. The ebolavirus genome contains seven genes, which the *GP* gene encodes three GP precursors, resulting in multiple GP protein products. The primary product of the *GP* gene is pre-sGP, which is expressed from the majority of RNA transcripts (e.g., approximately 71% of the total transcripts) with no shift of ORF and can be cleaved by furin at its C-terminus, yielding an N-glycosylated sGP dimer and an O-glycosylated Δ-peptide. Transcriptional editing can occur at a series of seven uridine residues in the GP gene, resulting in corresponding changes in the number of adenosine (A) residues in the transcripts. A +1 ORF shift results the full-length GP, while a + 2 shift leads to the synthesis of the ssGP from the truncated ORF. That the addition of more A residues or the deletion of a single A nucleotide has also been observed. The full-length GP precursor is cleaved by furin to form a disulfide-linked GP1-GP2 dimer, which subsequently assembles into the GP1,2 trimer and locates to the plasma or viral membrane, functioning as virion surface spikes, facilitating virus entry (source: Ning et al. 2017).

and an O-glycosylated Δ-peptide. Both sGP and Δ-peptide can be secreted extracellularly, while Δ-peptide is retained in producer cells for a longer period than sGP. It has been reported that sGP exhibit immunomodulatory and anti-inflammatory functions and appears to be able to assemble with GP2 subunit as a substitute for GP1 (Ning et al. 2017). Importantly, the Δ-peptide has been recently demonstrated to be a

viroporin, thus acting as a permeabilization and disruption agent for host cell membranes (J. He et al. 2017), thereby facilitating virus release from infected cells. Events of transcriptional editing that occur at a series of seven uridine residues in the *GP* gene result in corresponding changes in the number of adenosine (A) residues in the transcripts. A +1 shift results in an extended ORF, encoding the full-length GP (approximately 24% of transcripts), while a +2 shift leads to the synthesis of the ssGP from the truncated ORF (approximately 5% of transcripts). Transcripts containing 7A, 8A, or 9A at the transcriptional editing site are the most common, and encode for sGP, full-length GP, or ssGP, respectively. The 676 aminoacid full-length GP precursor is cleaved by furin to form a disulfide-linked GP1-GP2 dimer, which subsequently assembles into the $GP_{1,2}$ trimer and locates to the plasma or viral membrane. $GP_{1,2}$ trimers on the viral membrane function as virion surface spikes (Sanchez et al. 1998), that facilitate virus entry by mediating receptor binding and membrane fusion (Lee, Road, and Jolla 2010). Moreover, some surface $GP_{1,2}$ can be further cleaved by the TNF-α converting enzyme (TACE) at the membrane-proximal external region leading to the release of shed GP. Likewise sGP, shed GP, acts as a decoy antigen by adsorbing the antibodies against $GP_{1,2}$, thus counteracting antibody-mediated clearance of viral infection, contributing to viral immune evasion (Ning et al. 2017).

The fifth EBOV gene codes for the viral protein VP30, a 288 amino acid residues protein with a molecular mass of 32 kDa. This protein is a component of the EBOV NC and, importantly, is a polymerase co-factor central for EBOV transcription. In fact, VP30 is a transcriptional activator supporting primary transcription as well as RNA editing and its interactions with NP are fundamental in regulating the viral RNA synthesis (Biedenkopf et al. 2016; Kirchdoerfer et al. 2016; W. Xu et al. 2017).

The sixth gene of the genome encodes for VP24, a protein of 251 amino acid residues and molecular weight of 28.2 kDa. EBOV VP24 plays a structural role in viral assembly (its interaction with NP facilitates nucleocapsid assembly and genome packaging) and is a potent antagonist of the host innate immune response to viral infection by

inhibiting IFN-induced antiviral responses and, more recently, it was also found to efficiently inhibit type III IFN-λ1 gene expression (Banadyga et al. 2017; F. He et al. 2017; Mateo et al. 2010; St. P. Reid et al. 2006).

Lastly, the seventh and last gene of EBOV genome encodes for the L protein, the viral polymerase; while several studies have brought insights into the structure/function of NP, VP35 and VP30, much less is known about the essential L protein. This large protein of about 2200 amino acids has an estimated molecular mass of 250 kDa constitutes the catalytic site of the EBOV RNA-dependent RNA polymerase complex.

During their evolutionary history, viruses evolved a number of strategies to maximize their weapon arsenal, in order to efficiently penetrate, infect, replicate and evade from host organisms. The majority of viruses have hollow or (almost) spherical shells because it gives a most efficient packaging of the nucleic acid, with a fixed copy number of coat protein subunits. Most membrane enveloped viruses are also quasi-spherical, but their symmetry is frequently less well-ordered, which is usually described as pleomorphic. This feature allows some flexibility in volume, which could accommodate variation in the size of the genome or its copy number.

Filoviruses, including Ebola virus, show a particular and unusual shape among animal viruses, owning a filamentous morphology. This modular organization accommodates a well ordered and symmetrical nucleocapsid within a flexible, tubular membrane envelope. When produced in tissue culture, EBOV virions are pleomorphic and not only show the well-known filamentous elongated forms but either U-shaped, six-shaped, or circular (torus) configurations. The filamentous morphology may have evolutionary implications by allowing genome length flexibility, but could also enhance the ability for viral dissemination in infected tissues, for example by diapedesis of budding filamentous virions through epithelial layers.

Typically, an EBOV virion is ~982 nm long, with a molecular mass of about 3.82×10^5 kDa, and contains one viral NC that runs through a cylindrical axis of ~80 nm in diameter, the letter being enwrapped by an envelope acquired from the host cell

membrane during the process of virus budding (Fig. 16). In 2012, Beniac et al. reported the three-dimensional structure and architecture of Ebola virus and showed that multiple copies of the RNA genome can be packaged to produce polyploid virus particles, through an extreme degree of length polymorphism. Furthermore, in addition to the common form, other viral particles could be observed, such as "continuous-virions" containing two or more NCs, and "linked-virions" composed of single NCs connected by short sections of an empty envelope (Beniac et al. 2012).

The NC, as observed within intact viral particles, show a uniform helical structure that is enveloped by a membrane coated by an external layer of GP spikes. The EBOV nucleocapsid is a right-handed double-layered helix with an outer diameter of 41 nm and a hollow inner channel 16 nm in diameter. The inner nucleocapsid layer is 22 nm in diameter and consists of a tight association, in its entire length, of the viral genome with regular repeats of the viral nucleoprotein NP, which, in turn, are connected each other and run along the NC axis.

Externally, a 37 nm-wide outer layer protects and stabilize the NP-RNA structure. This layer consists of a series of "boomerang-shaped" protrusions, formed by repeats of an heterodimeric association between VP24 and VP35 (Bharat et al. 2012). The twos are the structural components of a "bridge" located on the periphery of the nucleocapsid and each one independently associates with NP to different sites of two NP subunits. More in particular, each bridge is composed of a VP24-VP35 heterodimer (for a total mass of 60 kDa) that holds horizontally adjacent NP molecules together (Fig. 17).

Finally, the NC internal structure is completed by the other viral polymerase co-factor VP30. This protein lies in the interior of the nucleocapsid and associates with NP but, however, it is non-essential for NCs formation and is not part of the bridge on the

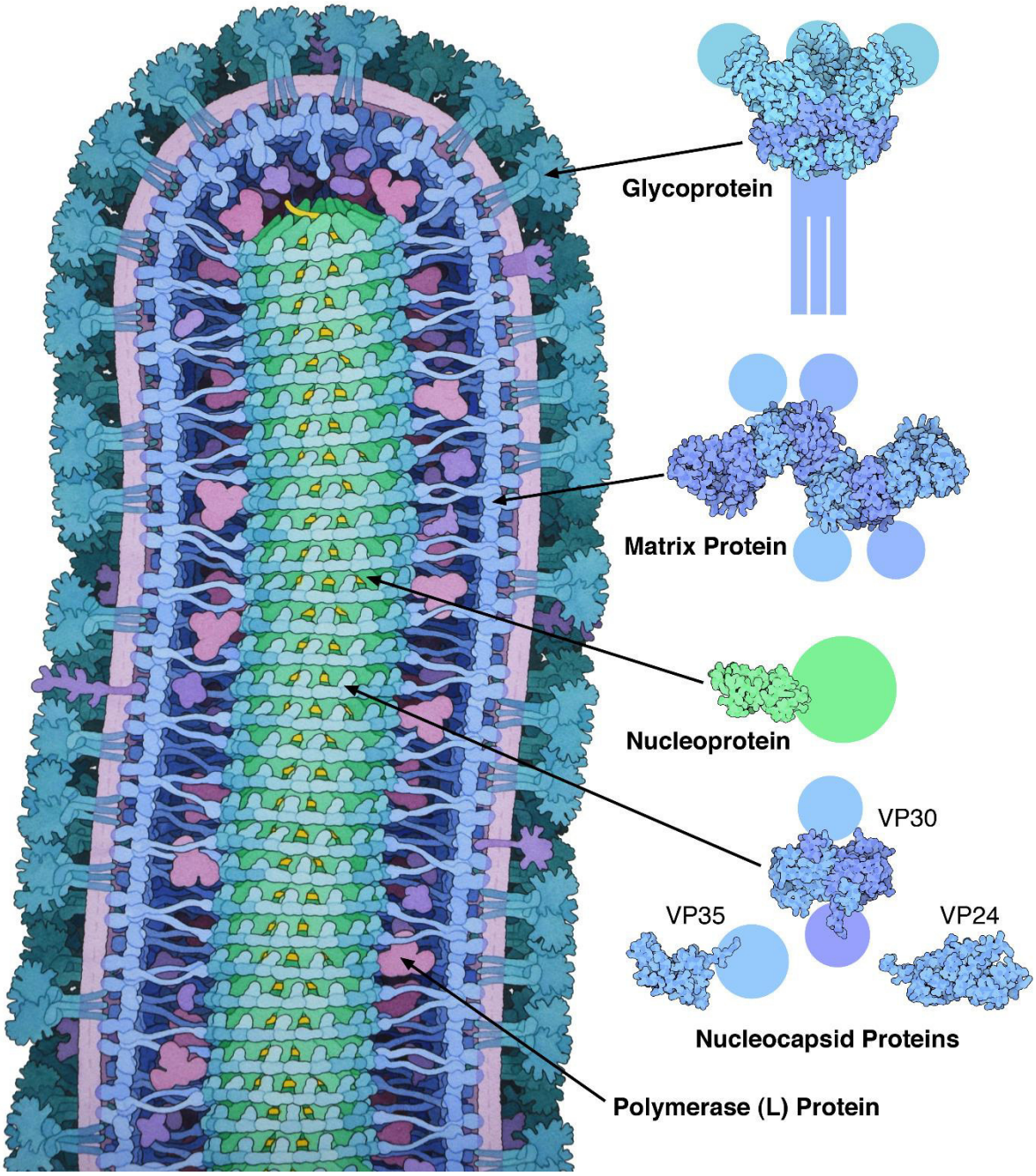

Fig. 16. Structure of an EBOV virion. Ebola virions consist of filamentous-shaped particles enwrapped onto a host cell membrane-derived envelope with peplomers of the viral glycoprotein GP trimeric complexes. An outer matrix layer (under the envelope) is formed by the two VP40 and VP24 proteins covering the viral NC. Immature NC consists on a ribonucleoprotein complex formed by a ssRNA- encapsidated by protomers of the NP and associated to the viral proteins VP30 and VP35-L complex, which represent the viral RNA-dependent RNA polymerase holoenzyme (source: Goodsell 2014).

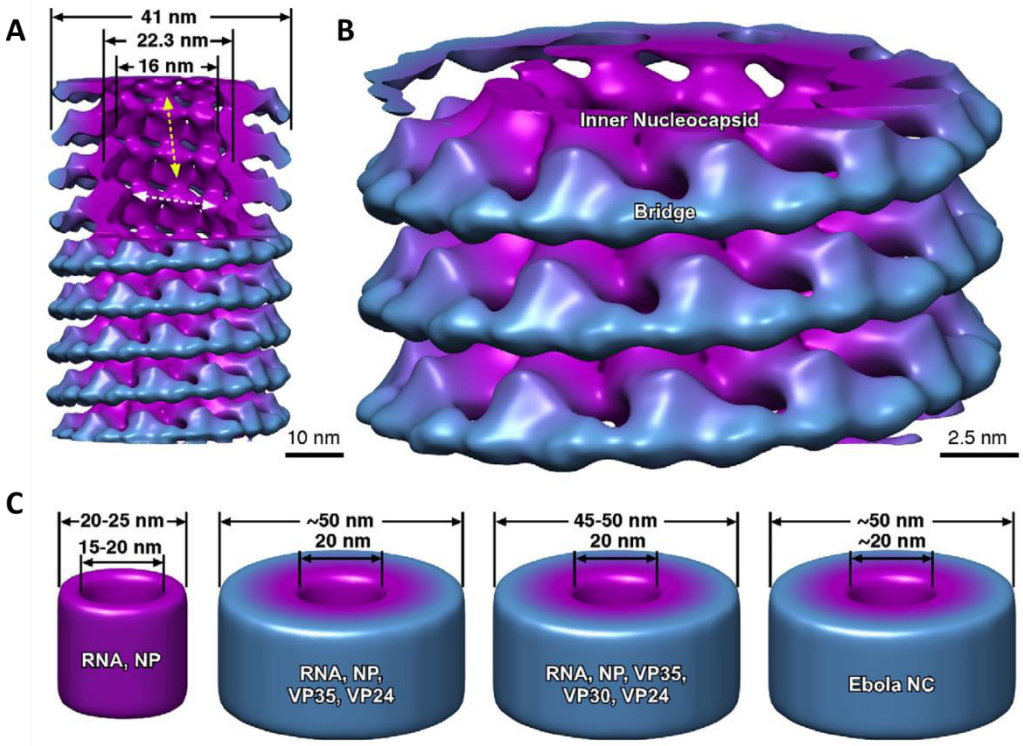

Fig. 17. A 3D reconstruction of EBOV nucleocapsid. The location of the inner nucleocapsid, and the bridge are indicated (A, B). The vertical (protein-protein) and horizontal (protein-RNA) contacts are indicated by yellow and white arrows, respectively. 3D schematics of various recombinant nucleocapsid-like structures, and authentic EBOV (C) highlighting the RNA and protein composition and the diameter of these structures, at the same scale for comparison to (A) (source: Beniac et al. 2012).

periphery of the NCs (Beniac et al. 2012). Instead, copies of VP30 and of the viral RNA-dependent RNA polymerase L protein, bind to NP and VP35 subunits, respectively. The described RNA-NP-VP24-VP35-VP30-L complex forms a soluble-layered helix that necessitates to be condensed into a rigid tubular structure to form the mature EBOV NC. To this purpose, this multiprotein/RNA structure is further surrounded by a 5 nm-wide lattice composed by regular repeats of the matrix protein VP40. The association of VP40 with VP35 and the C-terminus of the NP subunits provide the required stabilization to condensate the NC helix (Fig. 18). Such tubular architecture is then enwrapped by an envelope originating from cellular membrane, in which are mounted repeats of the viral glycoprotein GP, necessary for cellular attachment and fusion of EBOV virions. GPs form spikes that protrude 10 nm from the envelope surface, with

3.5 nm stalk and 6.5 club-shaped head. As mentioned before, every spike is typically composed by a trimeric association of GP subunits, each one consisting of the transmembrane GP2 domain, anchored to the membrane by a hydrophobic membrane spanning domain (msd), and the GP1 mucin-like domain that acts as the receptor binding domain for cell surface ligands (Beniac et al. 2012; Bharat et al. 2012; Vande Burgt, Kaletsky, and Bates 2015).

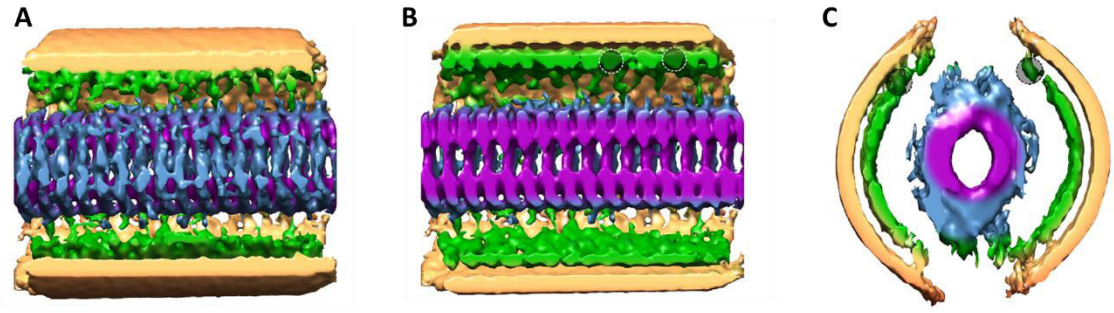

Fig. 18. Sections of an Ebola virion. The image shows different sections of the density map of an Ebola virion. (A–C) Sections of the sub-tomogram average are shown from the top sliced just below the envelope (A), the middle of the virus (B) and an end-on slice (C) of the virus. Color coding as follows; beige, lipid envelope; green, membrane associated proteins (VP40); blue and purple, outer and inner nucleocapsid.

1.7.2 Life cycle of the virus

Once penetrated into the host organism, the virus could exploit all of the weapons at its disposal to mount an efficient infection. EBOV particles can be up to a micron in length, making it difficult for the viruses to enter via classic clathrin- or caveolin-mediated endocytosis pathways.

Like all cellular membranes, enveloped virus membrane comprises phosphatidyl-serine (PS), a lipid that is primarily present on the inner leaflet of plasma membrane (Zachowski 1993). This molecule is actively kept at the cytoplasmic surface of the membrane by an enzyme called flipase through ATP consumption; since enveloped virions do not produce ATP, PS ends up at the surface of the virion membrane. Thus,

an increased amount of phosphatidylserine (PS) may be also present on the surface of Ebola-virus-like particles (Kondratowicz et al. 2011).

In cell death condition via apoptosis, PS is exposed to the outer leaflets of plasma membranes and apoptotic bodies. This circumstance alerts nearby cells, including phagocytic cells, to begin ''eating'' the debris via micropinocytosis, in a process that is mediated by TIM-1 and Axl and, importantly, does not induce an inflammatory response. EBOV, similarly to other large viruses such as vaccinia virus, may induce macropinocytic uptake by appearing to be an apoptotic body to be phagocyted. This event, called ''apoptotic mimicry'', is anti-inflammatory and could induce a rapid uptake of a large virus into cells, thus avoiding humoral and cell surface immunity factors (Misasi and Sullivan 2014).

EBOV uses the GP protein to bind its receptor and virions enter the cell by the process of macropinocytosis. To gain entry into the target cells, EBOV is able to attack a number of host receptors that include: i. the asialoglycoprotein receptor on hepatocytes; ii. the folate receptor α on epithelial cells; iii. C-type lectins, such as DC-specific intercellular adhesion molecule-3-grabbing nonintegrin and its receptor (on DCs, macrophages, and endothelial cells); iv. the human macrophage lectin specific for galactose/N-acetylgalactosamine (on macrophages) (Rivera and Messaoudi 2016).

Subsequently, the virus is released into host cell cytoplasm following the acidification of endocytic vesicles that determines a fusion of virus and host membranes. Recently, an additional entry receptor was discovered in regulating EBOV entry; the endosomal receptor Niemann-Pick C1 (NPC1), a ubiquitously expressed protein with multiple transmembrane domains and resides primarily in the limiting membranes of late endosomes and lysosomes, has been shown to bind EBOV GP through its domain C, resulting in a conformational change in GP that triggers membrane fusion. More in particular, the fusion of the viral and cellular membrane is mediated by GP2, which results from proteolytic cleavage of GP1, to a 19 kDa protein, by the endosomal proteases cathepsin B and cathepsin L (Fig. 19) (H. Wang et al. 2016).

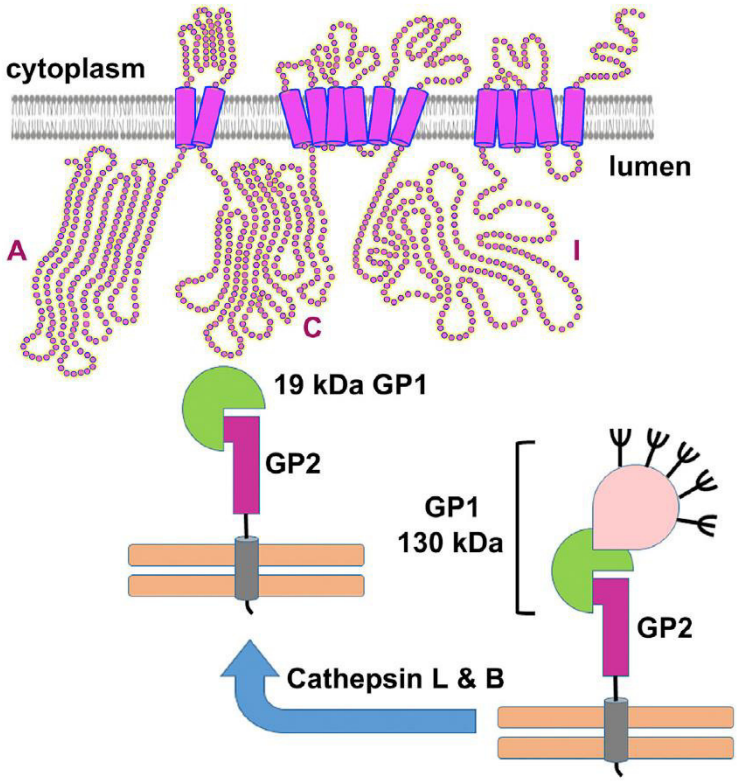

Fig. 19. Model of NPC1 bound to the primed EBOV GP and overall structure of NPC1-C. NPC1 is an endosomal 13-transmembrane protein with three luminal domains (A, C, I). The full-length EBOV GP is primed by cathepsin L and B in the late endosome, and the highly glycosylated 130 kDa GP1 subunit is cleaved into a 19 kDa GP1, generating a primed form of GP which, in turn, binds to the domain C of NPC1 molecule (source: H. Wang et al. 2016).

After ribonucleocapsid (RNC) release into the cytoplasm, mRNA synthesis is detectable at 6–7 h post-infection. The RNA dependent RNA polymerase (RdRp) complex initiates the mRNA transcription by binding to the leader sequence in 3' of the genomic negative strand RNA and slides along the RNA template, transcribing individual genes sequentially in a 3’ to 5’ direction. The viral mRNAs are capped and polyadenylated by polymerase stuttering in the cytoplasm. Precisely, the RdRp transcribes a 5' triphosphate-leader RNA, then stop and restart on a transcription initiation signal; the RNA initiated on this signal is capped. At the end of viral genes is located a transcription stop signal on which the RdRp will produce a polyadenylation signal by stuttering on a U stretch before releasing the mRNA. The initial transcription and translation of EBOV genes generates a buildup of viral proteins (VPs). Amongst

EBOV genes, *NP* is the most transcribed gene, whereas *L* is the least transcribed and, notably, the transcription process is dependent on the presence of the transcription factor VP30 (Hlberger et al. 1999; Rivera and Messaoudi 2016).

When into the host cytoplasm enough NP is present to encapsidate neo-synthetized antigenomes and genomes, the replication process could start. During replication, the promoter at the 3' end of the genomic RNA drives the synthesis of a full-length, positive-sense, antigenomic RNA. In turn, this molecule serves as a template for producing a progeny of ssRNA- genomes. Nucleocapsid proteins (VP35, L, VP30, and NP) associate then with negative-sense genome progeny, whereas GP and sGP are further modified in the endoplasmic reticulum and Golgi body. Once a sufficient expression level of negative-sense genomes and VPs is reached, all the components are assembled at level of the plasma membrane, where VP40 induces budding of filoviruses (Johnson et al. 2006; Noda et al. 2006). VPs are assembled at the plasma membrane with membrane-associated proteins (matrix proteins VP24 and VP40 and GP) and the complete virions can bud from the cell surface (Rivera and Messaoudi 2016).

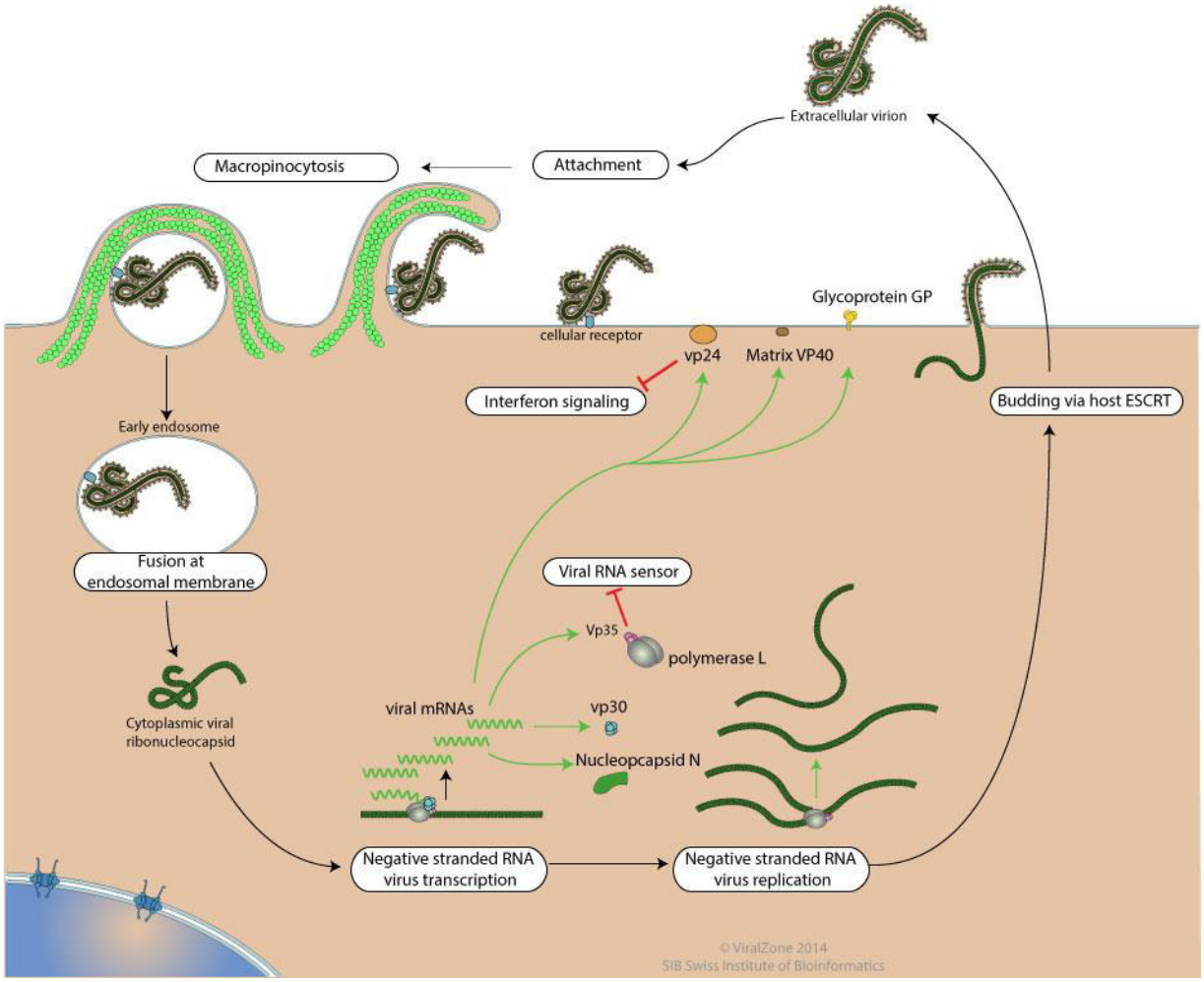

Fig. 20. The life cycle of Ebola virus. After attachment *via* host receptors and macropinocytosis, Ebola virions insinuate into host cell. The fusion at endosomal membrane leads to the uncoating and release of the RNC into host cytoplasm which is now free to be transcribed and replicated. Polyadenylated monocistronic mRNAs are synthesized from the negative-sense genomic RNA template by the replicase-transcriptase VP35-L-VP30 holoenzyme and translation of the viral mRNA genome yields the filoviral structural proteins. Viral replication follows and produces positive-sense antigenomes that serve as template for the generation of the new negative-sense progeny genomes. Prolonged replication produces excessive amounts of viral proteins, which facilitates transition from transcription/translation to replication within host cells. The concentration of NP is the primary trigger that induces this transition between mRNA transcription/translation and genomic replication. Binding of NP to progeny genomic RNA with VP35, VP30 and L result in the formation of immature RNC which, in turn, are enwrapped by VP24 and VP40 onto a matrix layer. Following assembly, virions are released from the host cell by budding of membrane-inserted GP peplomers (source: viralzone.org).

1.8. Viral mechanisms to evade the immune system control

1.8.1. The innate antiviral immune response

Defense mechanisms against infectious pathogens are regulated in concert with innate and adaptive immunity. The innate immune system, in particular, is an aspecific immune response and is the first defense line of the immune system against the activity of invading pathogens thus, it fulfills an essential role in initiating these anti-pathogen immune activities in both peripheral and lymphoid tissues. An efficient and successful activation of the innate response determines the consequential activation of the adaptive immune response that, contrarily to the innate response, is specific and generated in such a way as to induce and maintain the immune memory.

Although viruses are obligate intracellular parasites and rely entirely on the metabolic machinery of the host cell, they usually do not cause much harm; in most instances, patients recover from viral infections and either eliminate the virus or incorporate it in a latent or persistent form without further problems. The main reason is that our body is not defenseless but makes use of numerous measures to keep viruses at bay. However, also pathogens have, in turn, evolved a number of strategies to counteract these responses and evade to the immune system control (Haller, Kochs, and Weber 2006; Ma and Suthar 2015).

1.8.2. The interferon system: the connection between filovirus disease and immune evasion

The severe disease associated with filoviral infection is characterized by a systemic and uncontrolled virus replication, which results in very high viral titers in the blood (Feldmann and Geisbert 2011). This massive replication reflects the ability of EBOV to counteract with extreme efficiency the host antiviral defenses, particularly the IFN responses, which serve as critical innate immune responses regulators toward virus infection (Basler and Amarasinghe 2009; Bray and Geisbert 2005).

Viral infections are detected by sensor molecules which initiate innate antiviral responses. Within this context, the interferon system constitutes a major innate defense against infections by viruses and other pathogens. Upon recognition, virus-infected cells synthesize and secrete type I interferons (IFN-α/β) which warn the body of the dangerous intruders. Secreted IFNs circulate in the body and cause susceptible cells to express potent antiviral mechanisms which limit further viral growth and spread. Three classes of IFNs have been defined, according to the receptors bound by these cytokines. Type I IFN, including IFNα and IFNβ, are produced by many cell types as a direct result of viral infection. IFNγ, the only type II IFN, is generated by activated T cells and NK cells. Type III IFNs, which include IFNλ1–3, that are incompletely characterized but believed to regulate the antiviral response (Haller, Kochs, and Weber 2006; Kühl and Pöhlmann 2012).

Type I IFNs are polypeptides secreted by infected cells with three major functions. First, they induce cell-intrinsic antimicrobial states in infected and neighbouring cells that limit the spread of infectious agents, particularly viral pathogens. Second, they modulate innate immune responses in a balanced manner that promotes antigen presentation and natural killer cell functions while restraining pro-inflammatory pathways and cytokine production. Third, they activate the adaptive immune system, thus promoting the development of high-affinity antigen-specific T and B cell responses and immunological memory (Ivashkiv and Donlin 2015). Most cell types produce IFNβ, whereas haematopoietic cells, particularly plasmacytoid dendritic cells (pDCs), are the predominant producers of IFNα. IFNβ is encoded, in human and mice, by a single *IFNB* gene, whereas 14 distinct genes encode various IFNα isoforms.

When expressed, IFN-α/β are secreted from producing cells and can signal in an autocrine or paracrine manner, binding to a common heterodimeric receptor, the IFN-α/β receptor, found on the cell surface. Type I IFN receptors consist of two subunits, IFN α receptor 1 (IFNAR1) and IFNAR2. Ligands binding to IFNAR1 and IFNAR2 trigger receptor dimerization and signalling. Binding of IFN-α/β to their receptor,

together with the binding of IFNγ to its receptor (IFNGR), induces the phosphorylation, carried out by JAK1 (Janus-activated kinase 1) and TYK2 (tyrosine kinase 2) kinases, dimerization and nuclear translocation of signal transducer and activator of transcription (STAT) factors. Integral components of this signalling pathway induced by IFNs are STAT1 and STAT2 factors; homodimers of STAT1 bind to IFNγ activated sites (GAS), while STAT1/STAT2 heterodimers recognize IFN-stimulated response elements (ISRE), resulting in the transcription of a diverse set of genes that, altogether, establish an antiviral response in target cells. These genes are referred to as IFN-inducible genes or IFN-stimulated genes (ISGs). The ISGs, such as the well-characterized myxovirus resistance guanosine triphosphatases (Mx GTPases) tetherin, IFITM, PKR activity (discussed below) and others, play a fundamental role in host defense and target discrete steps in the viral life cycle, including virus binding to attachment receptors, virus entry, RNA synthesis, progeny virion assembly, and egress. Further, a subset of ISGs can also be induced directly (in an IFN-independent manner) by viral infection, perhaps offering a degree of protection in the primary infected cells, although the dramatic viral sensitivity of IFN-α/β receptor-knockout mice suggests that this is much less effective than the IFN response itself. In addition to the cell-autonomous activities of IFN-α/β, these cytokines modulate the immune system by activating effector-cell function and promoting the development of the acquired immune response. Hence, the type I IFN system is indispensable for vertebrates to control viral infections. The importance of type I IFNs is further demonstrated in instances where disruption of a single IFN effector gene causes a complete loss of innate immunity against a particular type of virus, leading to overwhelming infection and rapid death (Basler 2017; Haller, Kochs, and Weber 2006; Ma and Suthar 2015).

In cells exposed to viruses, the activation of the host innate immune response begins with recognition of pathogen-associated molecular pattern (PAMP) by pattern recognition receptors (PRRs), that sense the presence of the invading pathogens. Viral

PAMPs mainly consist of nucleic acids that may originate from the uncoating process of newly-infecting virions, the transcription of viral genes and the replication of genomic intermediates. Among these, double-stranded RNA (dsRNA) moieties, especially those with the atypically-featured 5′-triphosphate (5′-ppp) termini, have no homologues in the cytoplasm and therefore represent the most efficient triggers for PRRs activation (Gerlier and Lyles 2011). Activation of host PRRs by non-self nucleic acids such as those found in RNA viruses trigger a signaling cascade resulting in the production of IFN-α/β and the expression of hundreds of ISGs (Kühl and Pöhlmann 2012; Ma and Suthar 2015).

Given the central dsRNA role in stimulating IFN-α/β induction, a subset of PRRs is specifically dedicated to its detection and, depending on their cell compartments localization, can be ascribed to two families. The recognition of dsRNA in endosomes, lysosomes and even at the extracellular surface is accomplished by a member of the Toll-like receptor (TLR) family, the TLR-3, while dsRNA recognition in the cytosolic environment is carried out by RNA helicases belonging to the retinoic acid-inducible gene I (RIG-I)-like receptors (RLRs) family, named after the first characterized member, RIG-I (Yoneyama et al. 2004; Zinzula and Tramontano 2013).

The IFN-α/β gene expression preempts the activation of several different pattern recognition receptor pathways, including the RLR pathways, select TLR pathways and the STING/cGAS pathway. Most likely, two RIG-I-like receptors, the retinoic acid-inducible gene I (RIG-I) and melanoma differentiation-associated gene 5 (MDA-5), are the most relevant for filoviruses (Basler 2015). Upon recognition of their ligand, these receptors initiate signaling pathways that result in the translocation of interferon regulatory factor 3 (IRF-3) and other transcription factors to the nucleus. Once in the nucleus, these transcription factors activate expression of IFN-α/β which, in turn, by signaling in autocrine or paracrine fashion, initiate the antiviral response in the infected cells and prime neighboring cells for a rapid response to viral invasion (Hastie et al. 2013). IFNs are released from the producing cells and bind the IFN alpha receptor

(IFNAR), activating a JAK-STAT signaling pathway and inducing the expression of numerous ISGs, triggering an antiviral state that renders cells refractory to viral infection (Basler 2017).

For RNA viruses that replicate in the cytoplasm, the RLRs RIG-I and MDA5 are major sensors of infection, as they detect RNA products of viral replication that possess atypical features that mark them as "foreign", such as 5'ppp-ended RNA, that are specifically sensed by RIG-I (Gerlier and Lyles 2011; Seth et al. 2005). RIG-I and MDA5 helicases have been shown to preferentially sense different types of dsRNA PAMPs, based on their length, bluntness and end overhangs. RIG-I optimal ligands are short 5'-ppp containing dsRNA molecules of less than 20 bp in length, a feature that is essential for its proper activation, but can also bind 5'-hydroxyl (OH) blunt-ended dsRNA. Instead, since MDA5 lack the residues responsible for 5'ppp binding, their optimal ligands are long dsRNA (>1 kb) (Kato et al. 2008) with complex structures, and are selectively activated by mRNA with a cap devoid of ribose 2' O methylation, which appears to be a major MDA5 agonist motif (Gerlier and Lyles 2011; Zinzula and Tramontano 2013).

Because RNA viruses tend to accumulate nucleic acid intermediates and byproducts in the host cytoplasm during their replication cycle, preventing recognition by host PRRs of such PAMPs is of crucial importance. Therefore, most, if not all, RNA viruses encode proteins that display IFN-antagonism properties aimed to circumvent the host innate immune system. Among those proteins, most have been revealed as involved in targeting the RLR pathway at several levels (Versteeg and García-Sastre 2010). The impact of this counteraction becomes particularly evident for those RNA viruses, such as Ebola, that cause severe diseases in humans, since in several cases the fatal outcome has been related to their ability to subvert the type I IFN-mediated innate immune response (Bray, 2005).

Numerous viruses have developed multiple strategies for attenuating the initial innate immune response mounted by their hosts and to overcome the immune response. Suppression of these responses allows the virus to gain an early foothold during infection, replicating to a high titer before an effective adaptive immune response can be mounted. This is particularly true for certain hemorrhagic fever viruses, such as the filoviruses (Basler 2015; Hastie et al. 2013; Zinzula and Tramontano 2013).

1.8.3. The great escape: how Ebola virus eludes the immune response

Evading from host innate immune responses is of particular importance to viruses, and many have evolved mechanisms to circumvent innate immunity. As previously mentioned, Ebola inhibits both type I and type II interferon responses in target cells, especially its preferred target cells: macrophages, monocytes, and dendritic cells. The ultimate result is a defect in dendritic cell maturation and diminished T-cell activation and proliferation along with apoptosis, leading to lymphopenia, a key characteristic of EVD. To ensure an extensive replication and dissemination, EBOV employs multiple mechanisms (Fig. 21).

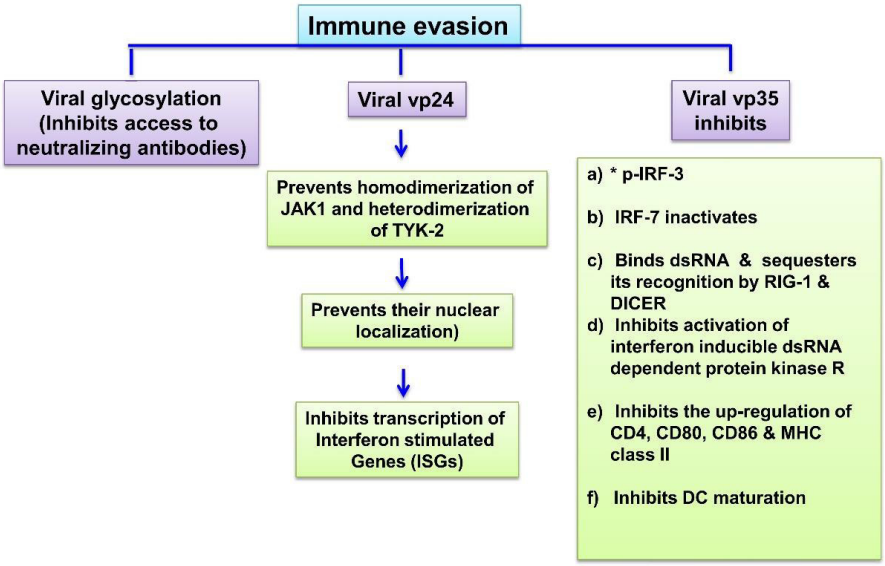

Fig. 21. Ebola virus immune evasion. The potential mechanisms by which the various components of EBOV evade host innate and acquired immunity systems.

The role of viral glycoproteins and cellular factors

On the outside of the battlefield represented by the invaded host cell, EBOV exploits the abundance of sGP during acute illness (and thus circulating at high levels in the serum) as a decoy by binding EBOV-neutralizing antibodies to impair a protective humoral immune response (Ito, Watanabe, and Takada 2015). Moreover, it is hypothesized that glycosylation of GP may sterically impede the binding of neutralizing antibodies to it (Francica et al. 2010). Although lymphocytes are not infected by EBOV, in fatal EVD cases lymphocyte apoptosis results in early lymphopenia and lymphoid depletion in the spleen and lymph nodes, further affecting adaptive immune response. The mechanism underlying lymphocyte apoptosis is not well understood, although intrinsic and extrinsic apoptotic pathways are both thought to be involved (Baseler et al. 2017). Recently, it has been observed that EBOV-stimulated CD4+ T cells were upregulated of both Toll-like receptor 4 (TLR4) and cell death associated pathways, indicating that that EBOV increases the susceptibility of monocytes to infection by promoting cellular differentiation. Interestingly, EBOV glycoprotein directly triggered T lymphocyte death despite of the lack of infection, with both EBOV-induced monocyte differentiation and cell death of T lymphocytes that resulted from a direct interaction between GP and TLR4 (Iampietro et al. 2017).

Recent research revealed that expression of the host cell IFN-inducible transmembrane proteins 1–3 (IFITM1–3) and tetherin is induced by IFN and restricts EBOV infection, at least in cell culture model systems. Tetherin exhibits an unusual topology and restricts release of several enveloped viruses and filovirus-like particles from infected cells (Douglas et al. 2010; Neil, Zang, and Bieniasz 2008), while IFITM proteins inhibit infection by filoviruses and other enveloped viruses at the stage of viral entry (Huang et al. 2011; Kühl and Pöhlmann 2012).

IFITM proteins

IFITM proteins have been defined as the cell's first line of antiviral defense (Bailey et al. 2014). IFITMs 1, 2 and 3 are ubiquitously expressed proteins in human cells and tissues upon exposure to type I (α) and type II (γ) IFN and play a role in early development, cell adhesion and control of cell growth. Their antiviral activity, in particular that of IFITM3, was discovered in a siRNA screen designed to identify host cell factors modulating Influenza A virus (FLUAV) infection and were subsequently identified as able to limit infection in cultured cells by many other viruses, including vesicular stomatitis Indiana virus (VSIV), severe acute respiratory syndrome coronavirus (SARS-CoV), FLUAV , filoviruses and members of the family Flaviviridae, West Nile virus and Dengue virus serotype 2, but not hepatitis C Virus (Brass et al. 2009; Huang et al. 2011; Wrensch et al. 2015). It is thought that IFITM block cellular entry after transport of viruses into endosomal compartments, particularly interfering with NPC1 expression or activity, that is required for endosomal fusion after cathepsin-mediated processing of GP1,2. In this regard, a recent study showed that the type I interferon induces IFITM protein expression in macrophages, that are EBOV major viral targets, so inhibiting host cell entry of the virus driven by GPs (Wrensch et al. 2015). However, the exact mechanisms underlying inhibition of filoviruses (and other viruses) remain to be defined, including the possibility that IFITMs require cellular cofactors to exert their antiviral effects (Ning et al. 2017).

Theterin/BST-2

The tetherin protein (HM1.24, BST-2, CD317) was first identified as a type I interferon-inducible host cellular factor which restricts release of progeny HIV-1 particles from infected cells; its function is counteracted by the HIV-1 accessory viral protein u (Vpu), which allows efficient HIV-1 release form tetherin-expressing cells (Van Damme et al. 2008; Neil, Zang, and Bieniasz 2008). However, the antiviral action of tetherin is not limited to HIV-1 but several studies found that tetherin restricts release of viral-like

particles (VLPs) and progeny particles of several enveloped viruses, included filoviruses (Kühl and Pöhlmann 2012). VLPs are used for the study of early viral-host cell interactions because of their capability to stimulate immune response likely mimic the initial interaction of DCs with infectious pathogens.

The broad spectrum antiviral action of tetherin is intimately linked to its unusual structural organization. Tetherin encodes a short cytoplasmic domain at its N-terminus, followed by a single transmembrane (TM) domain, an extracellular coiled-coil region and a C-terminal glycosylphosphatidylinositol (GPI) anchor (Kupzig et al. 2003). This peculiar structure renders the protein capable to span the membrane twice, inserting one end into the cell membrane and the other end into the viral envelope. By this mechanism, the protein physically "tethers" and retains the budding virions to the cell surface of the infected cell and inhibits their transmission to new target cells (Hammonds et al. 2010). In addition, tetherin/BST-2 has two putative N-linked glycosylation sites in the extracellular domain and forms a homodimer by intermolecular disulfide bonds. More importantly, this molecule is localized to membranes of the *trans*-Golgi network and recycling compartments and, especially, lipid rafts at the cell surface, which are the same sites used by EBOV as platforms for budding (Yasuda 2012).

Kaletsky et al. (2009) demonstrated that EBOV GP directly interacts with tetherin/BST-2 and abrogates the inhibition of VP40-induced VLP release by tetherin/BST-2 (Kaletsky et al. 2009). As described, the EBOV glycoprotein is the only viral surface protein and mediates viral entry into the host cell that requires binding of GP1,2 to the endosomal membrane protein NPC1. The large and heavily glycosylated extracellular domain GP1 mediates attachment to the host cell; the smaller TM unit GP2 facilitates fusion of the viral envelope with the membrane of host cell endosomes (Kühl and Pöhlmann 2012).

It is supposed that EBOV-GP1,2 might relocalize tetherin within the plasma membrane or interfere with the structural integrity of tetherin through its degradation. Further,

abrogating the inhibition of VP40-induced VLP release it is thus possible that the EBOV-GP1,2 rescues the block to particle release by interfering with the integrity of tetherin at filoviral budding sites. However, the exact mechanism by which EBOV GP antagonizes tetherin/BST-2 remains unclear so far (Vande Burgt, Kaletsky, and Bates 2015; Kühl and Pöhlmann 2012). Moreover, unlike other known viral tetherin antagonists, the features within EBOV GP needed to overcome tetherin are not well characterized. Specific EBOV GP domains have been implicated in interacting with or counteracting tetherin. Within GP1, the mucin domain can be removed without affecting EBOV GP anti-tetherin activity; instead, sGP is unable to affect tetherin antiviral function (Kaletsky et al. 2009). Furthermore, FRET analysis of the interaction between EBOV GP and tetherin has suggested that the GP2 subunit appears to interact with tetherin (Kuhl et al. 2011). Similarly, recent chimeric protein analysis demonstrated a role for the EBOV GP msd within GP2 in tetherin antagonism (Gnirss et al. 2014).

Recently, the sequences within the EBOV GP ectodomain and membrane spanning domain (msd) were described as necessary to relieve tetherin restriction of viral particle budding. The domains required to antagonize tetherin antiviral activity within the EBOV GPs were characterized, and it was shown that a minimal 320 AA residue portion of the Ebola glycoprotein ectodomain, containing the receptor binding domain and glycan cap regions of EBOV GP, that when anchored to the cell surface is sufficient to antagonize tetherin activity. Moreover, the deletion of the glycan cap region by proteolytic processing rendered EBOV GP unable to promote viral budding, thus suggesting that the glycan cap is important for tetherin antagonism (Vande Burgt, Kaletsky, and Bates 2015).

Another cellular role of tetherin/BST-2 is to induce the activation of a proinflammatory transcription factor, the nuclear factor-kB (NF-κB). The exact mechanism by which BST-2 initiates NF-κB activity in response to viral infections is unknown, but it was recently demonstrated that EBOV GP and VP40 cooperate with BST-2 to activate NF-

κB independently of VLP trapping, converging on an intracellular signaling pathway that depends on a protein modification termed "neddylation" (a process similar to ubiquitination) and induce or amplify proinflammatory signaling during Ebola virus infection, potentially contributing to the dysregulated cytokine response that is a hallmark of EVD (Rizk, Basler, and Guatelli 2017).

Instead, inside the battlefield, pathogenesis and interferon antagonism are linked to the molecular action of two VPs, VP35 and VP24, that act together for counteracting the host immune defenses (Misasi and Sullivan 2014).

1.8.3.1. VP24

As previously mentioned, VP24 is the smallest of the seven EBOV-encoded structural proteins and constitutes the minor matrix protein relative to the major matrix protein VP40. Furthermore, it has been demonstrated the ability of VP24 in shutting down the host's IFN-α/β and IFN-γ response to viral infection by preventing the dimerization of tyrosine kinases and nuclear translocation of STAT1 (St. P. Reid et al. 2006). Upon activation, STAT1 is tyrosine-phosphorylated (PY-STAT1) and either heterodimerizes with PY-STAT2 for type I IFN signalling or homodimerizes with PY-STAT1 for type II IFN signalling.

The dimerization leads to the exposition of a nuclear localization signal (NLS) in STAT1, which is recognized by members of the family of NLS receptors, particularly, the nuclear import adaptor protein importin α, specifically importin α5, α6 and α7 (also known, respectively, as karyopherin α1, α5, α6; NP-1 subfamily of importins). Importin α is then bound by the nuclear import factor importin β, which facilitates import of STAT dimers into the nucleus (Sekimoto et al. 1997). However, in the presence of VP24, which like STAT1 binds to importins α5, α6 and α7, the recognition of the PY-STAT1 NLS by these importins is disrupted. As a consequence, PY-STAT1 is

not regularly imported and accumulated into the nucleus. Notably, PY-STAT1 nuclear transport blockade is not because of a global inhibition of nuclear import, as VP24 does not bind to importin α1 (karyopherin α2; RchI subfamily), α3 or α4 (karyopherin α4, α3; Qip1 subfamily) and does not affect nuclear import mediated by these factors. Thus, VP24 specifically interacts with karyopherin α1 (importin α5), the NLS for PY-STAT1, but not with karyopherin α2, α3, or α4. The interaction with karyopherin α1 prevents the nuclear accumulation of these STAT1-containing complexes, impeding the activation and nuclear accumulation of these complexes and the specific transcriptional regulation of numerous genes, some of which have antiviral properties. In this way VP24-karyopherin α1 interaction contributes to the block to IFN signaling, and this suggest that VP24 is an important virulence determinant that allows EBOV to evade the antiviral effects of IFNs (Kühl and Pöhlmann 2012; Mateo et al. 2010; St. P. Reid et al. 2006).

1.8.3.2. VP35

EBOV VP35: the gene, the protein and the core domains

The EBOV-encoded protein VP35 is a dsRNA binding protein that fulfils several important functions in the viral life cycle. During EBOV infections, the multifunctional properties of VP35 are used to allow an efficient inhibition of the host defenses and viral replication. As mentioned, EBOV VP35 is an essential polymerase cofactor, is required for nucleocapsid assembly, is involved in the formation of the EBOV RNP complex and therefore it is crucial for transcription and viral replication (Leung, Prins, et al. 2010; Muhlberger et al. 1998). In addition, VP35 blocks multiple steps of the innate antiviral defence, such as the signalling pathways leading to the expression of type I IFNs and type I IFN-induced genes.

Product of the homonymous gene *VP35* (of ~1000 nucleotides in length), whose locus represents the second ORF in the EBOV genome (Fig. 22 A), VP35 is a protein that in

Zaire subtype is 340 amino acid residues long (341 in TAFV and BDBV, 329 residues in SUDV and RESTV) with a molecular mass of ~ 35 kDa, from which the name.

Two VP35 domains are fundamental for the molecular properties of the protein (Fig. 22 B). The N-terminal region of the protein is essential for EBOV replication and transcription. A region within the first 220 residues encompasses a domain of two flexible and disordered regions that flank a putative coiled-coil domain (CCD) that is required for VP35 homo-oligomerization, a process that leads to the formation of presumed homo-trimers and/or tetramers that was demonstrated to be indispensable for the polymerase co-factor role of the protein (Moller et al. 2005).

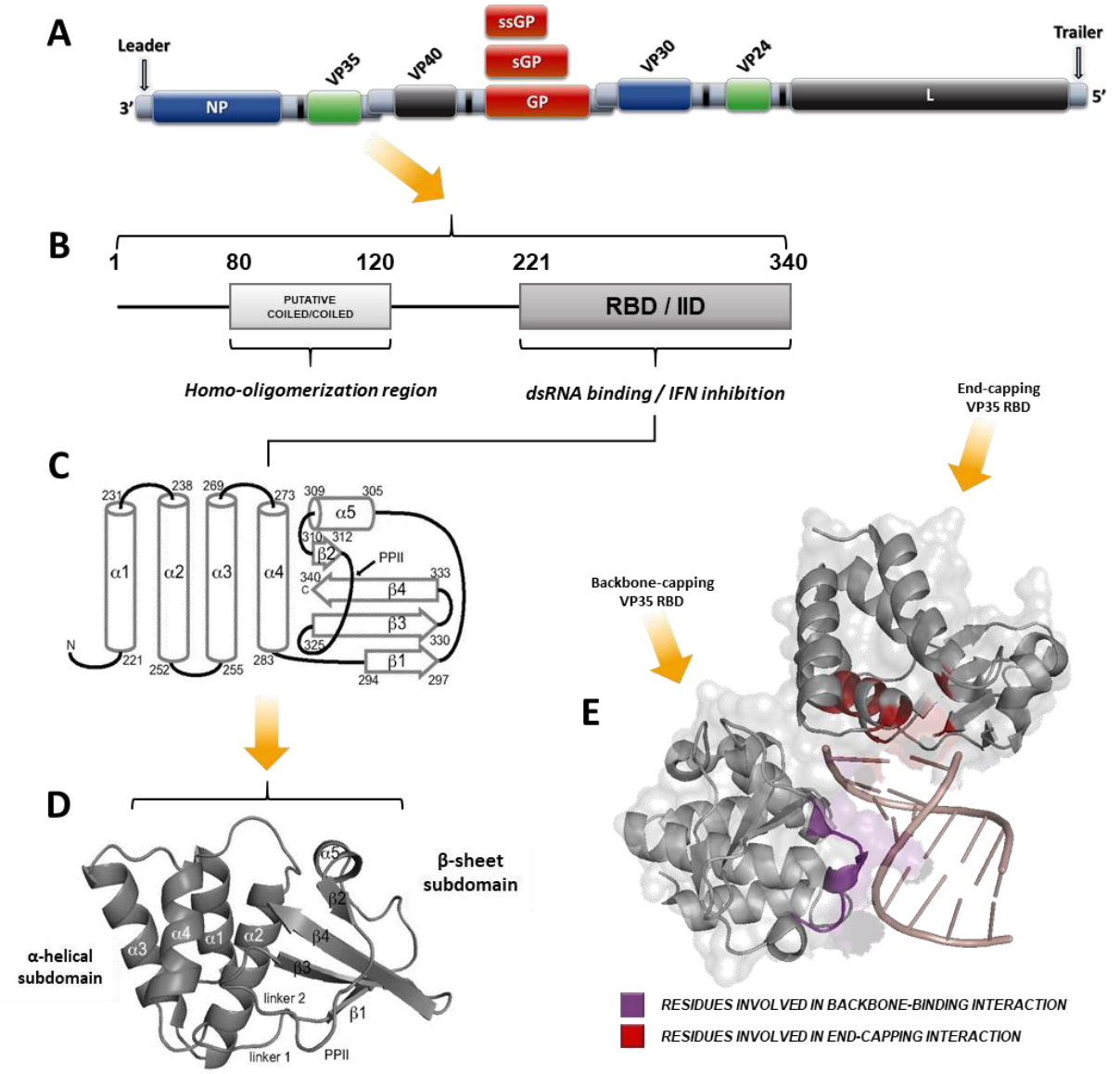

Fig. 22. EBOV VP35 protein. Encoded by the second ORF within the EBOV genome (A), VP35 is a multifunctional protein of 340 amino acid residues and a molecular weight of ~ 35 kDa (B) consisting on an unsolved N-terminal region with a coiled-coil domain (CCD) essential for its homo-oligomerization and replicative function, and a structurally solved C-terminal region that is essential for its anti-IFN properties (C). The C-terminal region consists of two alpha-helical and beta-sheet subdomains; this interferon inhibitory domain (IID) also contains a dsRNA binding domain (D) whose core sequence, named as central basic patch (CBP), is highly conserved among all Ebolavirus species. (E) VP35 binds to blunt-ended or 5'-ppp dsRNA with a bimodal strategy consisting of a monomer binding the nucleic acid phosphate backbone (backbone binding strategy) and another monomer binding to the terminal bases of dsRNA duplex (end-capping strategy).

Instead, the C-terminal domain is the fundamental region important for the powerful suppression of the host innate immune response, as demonstrated by the fact that this domain alone is sufficient to exert such property; therefore, it was named interferon inhibitory domain (IID) (Leung, Ginder, Fulton, et al. 2009). The EBOV VP35 IID comprehends the last 120 C-terminal residues (for an estimated molecular mass of ~16 kDa) and is further divided into two independently folded units (Fig. 22 C). Within this region, an N-terminal α-helical subdomain is connected to a C-terminal β-sheet subdomain. More in particular, the α-helical subdomain encompasses four α-helices (residues 221-283) arranged in two layers that pack against the C-terminal β-sheet, to which it is connected through a short, flexible, 10 residues-long linker region. The following C-terminal β-sheet subdomain comprises residues 294-340 and is folded into four stranded β-sheet and a brief, fifth α-helix (Leung et al. 2009) (Fig. 22 D).

Further, the VP35 C-terminal domain includes two basic patches that, among filoviruses, reveal a high degree of sequence similarity: a first basic patch (FBP) that is important for interactions with EBOV NP and VP35 polymerase cofactor function (Prins et al., 2010) and central basic patch (CBP) important for VP35-dsRNA binding and IFN inhibition (Leung et al., 2009). The CBP is located at the very C-terminus (304-340 residues) and has been found essential for binding of VP35 to dsRNA, a property of the protein that is strongly correlated with its innate immune antagonism. This feature led to term the VP35 IID also as RNA binding domain (RBD) and shows a unique fold that does not follow the α-β-β-β-α organization observed for canonical RBDs.

EBOV replication and transcription are primer-independent processes and synthesis of viral RNA during these phases starts with a single nucleoside triphosphate, resulting in production of genomes, antigenomes and viral transcripts that bear 5'-ppp ends (Hastie et al. 2013). As mentioned, this feature is a strong inducer for RLRs-mediated IFN-α/β response. To avoid their recognition, viral mRNAs are capped shortly after their initiation, while 5'-ppp motifs in genomes and antigenomes are immediately and

tightly bound by NP-protein protomers to avoid the annealing of template and de novo synthesized viral RNAs into dsRNA, which is a major ligand of RLRs. However, RNA-dependent RNA polymerase machinery is not perfect and might produce a variety of defective interfering (DI) RNA particles, such as read-through transcripts that remain uncapped or abortive genomes, antigenomes and small non-coding RNAs that fail to be encapsidated. These molecules may undergo self-hybridization to form secondary structures or could anneal to complementary sequence resulting in dsRNA with blunt ends or exposed 5′-ppp, thus representing the perfect agonist for the RIG-I pathway (Gerlier and Lyles 2011). Therefore, being these molecules a strong "non-self" signal for the host, EBOV exploits the VP35 protein to bind dsRNAs in a sequence-independent manner and to avoid RLRs recognition. VP35 hides such DI particles wrapping about its blunt or 5′-ppp-exposing ends (Hastie et al. 2013). Thanks to crystallographic analyses, that solved the structures of Zaire EBOV IID in complex with 8 bp dsRNA (Leung, Borek, et al. 2010) and RESTV IID bound to an 18 bp dsRNA (Kimberlin et al. 2010) it has been revealed that VP35 uses a bimodal strategy to bind the dsRNA. With one VP35 monomer binds the terminal nucleotides and the RNA phosphate backbone, and with a second monomer binds the dsRNA sugar-phosphate backbone.

These two binding modalities, termed as "end-capping" and "backbone-capping" respectively, lead the two VP35 monomers to assemble an asymmetric dimer. The functional meaning of this "capping process" is to generate a continuous and positively charged pocket specifically designed for receiving dsRNA (Fig. 22 E).

Within the sequence of the VP35 RBD/IID, a number of fundamental residues are involved in this interaction. In particular, the end-capping VP35 packs against the terminal bases of dsRNA with a non-polar face of hydrophobic residues as well as by a hydrogen bond from the carboxyl group of the very C-terminal I340. At the same time, it binds to the dsRNA phosphate backbone through the basic residues K282, R312 and R322, which all lie within the highly conserved CBP of VP35 RBD. On their part,

the R312 and R322 residues of the CBP, together with a third residue (K339), form the dimer interface with the end- capping VP35. The residues I340, S272, R305 and Q274 are among those that make hydrogen bonds with the dsRNA backbone in this VP35 monomer (Leung, Ginder, Fulton, et al. 2009). Importantly, it must be highlighted that the same amino acid residues involved in both dsRNA and dimer-interface interaction (R312, R322 and K339), are those that were previously found as critical for EBOV immune suppression and VP35 dsRNA binding (Hartman et al. 2004; Cárdenas et al. 2006; Leung et al. 2009).

Approaching this peculiar molecular action, the backbone- and the end-capping binding VP35 monomers efficiently mimic the shape and way to approach of the RLRs, efficiently binding and hiding the dsRNA so preventing the type I IFN innate immune response (Kimberlin et al. 2010; Daisy W Leung et al. 2010).

Typically, the activation of RLRs results in a signaling pathway, the RLR pathway, that is essential to prevent and limit viral spread as much as possible. As described, the multifunctional VP35 protein has been implicated in a variety of molecular mechanisms by which EBOVs counteracts the type I IFN antiviral response (Basler and Amarasinghe 2009). However, according to the current knowledge, EBOVs strategies seem to mainly consist in targeting RLRs pathways.

1.8.4. The RIG-I-like receptors (RLRs) pathway

The intracellular RIG-I-like receptors (RLRs: retinoic acid-inducible gene I, RIG-I; melanoma differentiation associated gene 5, MDA-5; and laboratory of genetics and physiology 2, LGP2) are sensory molecules responsible for the recognition of viral RNAs as PAMPs and respond to invading pathogens, initiating an antiviral immune response.

RLRs are a set of cytosolic sensors for dsRNA belonging to the superfamily 2 (SF2) clade of RNA helicases (Fairman-Williams, Guenther, and Jankowsky 2010) that share

a similar structural organization. They consist of an RNA-binding C-terminal domain (CTD) and a central DExD/H-box helicase domain comprising two RecA-like helicase domains, namely Hel1 and Hel2, separated by the insert domain Hel2i. Moreover, in RIG-I and MDA5, but not in LGP2, the helicase domain is preceded by two tandemly-repeated N-terminal caspase activation and recruitment domains (CARDs) (Luo et al. 2011). The helicase domain also appears to have an important role in RNA binding (Versteeg and García-Sastre 2010).

Unlike other members of the SF2 helicases, which bind one strand of the nucleic acid to unwind its double helix, RLRs have double-strand specificity, and do not seem to display an unwinding activity (Fairman-Williams, Guenther, and Jankowsky 2010).

Typically, physiologically inactive RIG-I is found in an auto-inhibited state, in which the two CARDs are kept engaged in intramolecular interactions with the Hel2i domain by a repressor pincer motif located between the CTD and the helicase domains. Upon dsRNA binding to the CTD, the pincer motif is relieved from CARDs that are then displaced from the Hel2i allowing its binding to dsRNA. Subsequent to dsRNA enwrapping to Hel domains, RIG-I dimerization and activation of its ATPase activity take place; ATP hydrolysis propels the translocation and binding of the RIG-I dimer along both dsRNA strands. Further, an overall conformational change releases the N-terminal CARDs for signaling; freely exposed RIG-I CARDs interact with unanchored Lys-63-linked poly-ubiquitin (poly-Ub) chains. Next, RIG-I homo-oligomerization and ATP-ase-driven translocation along dsRNA take place, leading to additional conformational changes that provide the signaling platform for interaction with the CARDs of the adaptor IFN-β promoter stimulator 1 (IPS-1), a mitochondrion-associated protein, now called mitochondrial antiviral signaling protein (MAVS) and formerly also known as IFN-β inducing CARD adaptor (Cardif) or virus-induced signaling adaptor (VISA) (Luo et al. 2011; Seth et al. 2005; Zinzula and Tramontano 2013).

Signalling prosecution involves the recruitment of two adaptors, tumor necrosis factor (TNF) receptor-associated factor 3 (TRAF3) and the nuclear factor-kB (NF-κB) essential modifier (NEMO), which connect and regulate signaling between the upstream sensory domain of MAVS and the downstream complex formed by TRAF family member-associated NF-κB activator (TANK)-binding kinase 1 (TBK-1) and inducible IkB kinase epsilon (IKK-ε). The TBK1-IKK-ε complex interaction with MAVS involves another adaptor, the stimulator of interferon genes (STING), also known as mediator of IRF-3 activation (MITA) or endoplasmic reticulum IFN stimulator (ERIS), that acts as an RLR signaling enhancer.

In turn, TBK-1 and IKK-ε kinases carry out the phosphorylation of latent IFN regulatory factors 3 and 7 (IRF-3/7), leading to their dimerization and nuclear translocation (Fitzgerald et al. 2003; L. Wang, Li, and Dorf 2012). Once in the nucleus, IRF-3 and 7, both in the form of homo- or hetero-dimers, associate into an enhanceosome that involves other transcription factors, such as cAMP response element-binding (CREB) binding protein/p300, NF-κB, activating transcription factor 2 (ATF-2) and c-Jun to drive the transcription of IFN-α/β genes (Panne, Maniatis, and Harrison 2007). As previously described, secreted IFNs act towards the same cell or the neighboring ones, and by binding their ubiquitous receptors activate a signaling cascade that at last leads to the expression of hundreds of ISGs with antiviral properties. Some ISGs encode for effectors that directly interfere with the viral replication cycle, such as the interferon-induced transmembrane (IFITM), the ribonuclease L (RNase L), 20, 50-oligoadenylate synthetase (OAS), the dsRNA-dependent protein kinase R (PKR), Viperin, myxovirus resistance 1 (Mx1) and interferon stimulated gene 15 (ISG15) proteins. Importantly, since among the ISGs products are also the PRRs, their adaptor molecules and transcription factors such as the IRFs, the expression of these proteins determines an amplification loop that increases both IFN-α/β and ISGs production, thereby establishing the overall antiviral

state that is fundamental to limit virus spread and eventually clear the infection (Zinzula and Tramontano 2013).

1.8.5. How VP35 counteracts the RLRs pathway

One major mechanism by which filoviruses evade innate antiviral defenses is by blocking the RLR pathways that would otherwise trigger IFN-α/β production (Fig. 23). This mechanism is carried out by the VP35 proteins of both Ebola viruses and Marburg viruses (Basler 2015). However, between the two filoviral proteins, EBOV VP35 is a more potent inhibitor of the response. This is due, in part, to more efficient RNA recognition by Ebola virus VP35 and blocking of the RIG-I signaling (Edwards et al. 2016). VP35 exerts its IFN-antagonism by targeting the RLR cascade at several points, both "hiding" and directly "hitting" the components of the pathway.

EBOV VP35 was found to act at the upper levels of the RIG-I signalling pathway, hiding the presence of dsRNA replicative intermediates to the sensory action of PRRs RIG-I and MDA5. In fact, VP35 is able to interact with dsRNAs approaching a bimodal strategy, generating an asymmetric VP35 dimer that binds to both blunt-ended and 5'-ppp dsRNA molecules with very high affinity and in a sequence-independent manner (Cardenas et al. 2006; Feng et al. 2007; Kimberlin et al. 2010; Zinzula et al. 2009, 2012). Notably, mutational studies revealed that an N-terminal coiled-coil domain in VP35 mediates this homo-oligomerization, which was found to be essential for IFN antagonism exhibited by the C-terminus of the protein (St Patrick Reid, Cardenas, and Basler 2005).

Two dsRNA-dependent mechanisms of VP35 function have been proposed: i. the sequestration and hiding of RLR-activating RNAs, ii. the interaction of VP35 with cellular protein PKR activator (PACT), another dsRNA binding protein involved in the activation of RIG-I and stimulation of its ATPase activity thus facilitating RIG-I activation by dsRNA (Leung, Prins, et al. 2010; Priya Luthra et al. 2013). EBOV VP35

interacts with PACT in such a manner that PACT is unable to interact with RIG-I; as a consequence, PACT activation of RIG-I and induction of IFN-α/β gene expression is impaired. Interestingly, point mutations in VP35 that disrupted dsRNA binding abrogated VP35-PACT interaction and VP35 became unable to disrupt PACT–RIG-I interaction. This suggests that the same VP35 aminoacidic residues that mediate interaction with dsRNA also contribute to direct interaction with PACT (Priya Luthra et al. 2013).

The interaction of PACT with VP35 has a second functional consequence. Since EBOV VP35 exerts multifunctional tasks in the viral life cycle, it plays a crucial role in filoviral genome replication and mRNA synthesis, because of its interaction with L and NP, bringing L to the NP-encapsidated RNA templates. It has been demonstrated that when PACT is co-expressed with the filoviral RNA polymerase complex it impairs viral RNA synthesis and this impairment requires the interaction with VP35 (Priya Luthra et al. 2013; Muhlberger et al. 1998).

Further, although the biological significance of this observation is unclear, VP35 has been showed also to suppress gene silencing by small interfering RNAs (siRNA), suppressors involved in disabling viral replication (Fabozzi et al. 2011; Haasnoot et al. 2007).

In line with the other viral IFN-antagonist redundancy observed to concomitantly target multiple levels of the RLRs pathway, VP35 also employs several "hit" strategies to suppress the downstream RIG-I pathway and IFN-α/β induction (Zinzula & Tramontano, 2013). VP35 was found to inhibit the virus-induced activation of type I IFN promoters by targeting the transcription factor IRF-3 in different ways. In contrast, activation of IFN promoters through exogenous IFN was not modulated by VP35 (Basler et al. 2003; Kühl and Pöhlmann 2012).

EBOV VP35 was shown to block IRF-3 phosphorylation and nuclear translocation induced by TBK1 and IKK-ε overexpression; these two kinases are essential components of the IRF-3 signaling pathway and are required for IRF3 activation by

dsRNA (Fitzgerald et al. 2003). Significantly, co-immunoprecipitation (co-IP) studies revealed its ability to directly interact with TBK1 and IKK-ε, *via* their more conserved kinase domains located within the N-terminal domain of the two proteins, decreasing their catalytic activity and, acting as a decoy, being phosphorylated by these kinases. In addition, the overexpression of VP35 resulted in a disruption of IKK-ε interactions with IRF-3, IRF-7 and MAVS (C F Basler et al. 2000; Kathleen C Prins, Cárdenas, and Basler 2009).

The two IRFs are also directly targeted by VP35 that prevents their migration to the nucleus. It was demonstrated that VP35 interferes with IRF-3 production, acting on ISG54 and ISG56 promoters, and directly interacts with IRF-3 by blocking its phosphorylation, dimerization and nuclear accumulation (Basler et al. 2003). Further, IFR-7 but not IRF-3, seems to be critical for the production of type I IFNs (Honda et al. 2005). IRF-7, although similar to IRF-3 in structure, differs in its expression and its mode of action, and the dominant role that IRF-7 plays in IFN production is in DCs, particularly the pDCs, which produce the largest amounts of type I IFNs and express IRF-7 at high levels, an expression further enhanced by IFN produced by positive feedback circuit. In light of this evidence, and considering that DCs are a primary site of early EBOV infection, a recent study showed that VP35 inhibits IRF-7 by promoting its SUMOylation (Chang et al. 2009). EBOV VP35 exploits the cellular SUMOylation machinery for its advantage, forming a complex with IRF-7 and PIAS1 (the small ubiquitin-like modifier (SUMO) E3 ligase protein inhibitor of activated STAT) and promotes IRF-7 SUMOylation via PIAS1. This study also revealed that VP35 displays an IFN inhibitory activity independent of its ability to recognize dsRNA, and this activity was mapped, once again to the VP35 N-terminus, which is essential for interactions with IRF-7 and PIAS1. In fact, EBOV VP35 was found to physically interact with both IRF-3 and 7 and to promote their Ub-like modification by the two members of the small Ub-like modifier cascade PIAS1 and Ubc9, thereby inhibiting the IRFs

transcriptional function and subsequently suppressing the activation of IFN-β promoter (Chang et al. 2009; Kühl and Pöhlmann 2012).

Recent studies suggest that other host factors may modulate VP35 function, regulating viral RNA synthesis (P Luthra et al. 2015; Shabman et al. 2011). However, the mechanisms by which the host influences VP35 activity are poorly defined and whether VP35 undergoes other post-translational modifications is not known. Ubiquitination of proteins is a conserved post-translational modification important in many cellular functions, including immune signaling (Z. J. Chen and Sun 2009; Oudshoorn, Versteeg, and Kikkert 2012). However, viruses have adapted to evade ubiquitin (Ub)-dependent antiviral responses and, in many cases, hijack the Ub system to enhance their own replication (Rajsbaum and García-Sastre 2013). Similarly, EBOV evolved a strategy to counteract Ub system and contextually enhance its replication. In fact, has been recently demonstrated that TRIM6, a member of the E3-ubiquitin ligase tripartite motif (TRIM) family, is an important host cellular factor that promotes EBOV ubiquitination and replication. TRIM6 normally promotes the synthesis of unanchored K48-linked poly34 ubiquitin chains, which are not covalently attached to any protein, activating the IKKε kinase to induce efficient antiviral IFN-I-mediated responses (Rajsbaum et al. 2014). VP35, ubiquitinated on a lysine residue located in position 309 (K309) of its IFN antagonist domain, interacts with TRIM6 promoting its ubiquitination; thus, non-covalently associating with poly-ubiquitin chains, VP35 inhibits TRIM6-mediated IFN induction. Intriguingly, it was also found that TRIM6 enhances EBOV polymerase activity, suggesting that VP35 hijacks TRIM6 to promote EBOV replication through ubiquitination and stimulation of viral polymerase activity (Bharaj et al. 2017).

In addition to suppressing IFN-α/β production, VP35 functions a step after the interferon production. In fact, it inhibits the activation of the IFN-induced, dsRNA-activated kinase PKR, a well-characterized kinase with antiviral activity. In normal cells, PKR is present at a low level, but its expression is upregulated by IFNs. Upon

binding to dsRNA, PKR is activated to phosphorylate the α subunit, on serine 51, of translation initiation factor eIF-2 (eIF-2α), which arrests protein synthesis and thereby inhibits viral replication (Feng et al. 2007). To date, the mechanism of inhibition remains to be defined, although it was interestingly shown that the C-terminal interferon inhibitory domain (IID) of VP35 that is required for dsRNA binding and IRF3 inhibition also mediates the inhibition of PKR and enhances the synthesis of coexpressed proteins (Schumann, Gantke, and Muhlberger 2009), but appears to be dsRNA-binding independent. It is suggestive that PACT is a PKR activator, but a direct connection between VP35–PACT interaction and VP35–PKR inhibition has not been demonstrated (Basler 2015).

Finally, VP35 also interferes with development of adaptive immune responses. As mentioned above, DCs are early targets of Ebola virus, that can impair DC maturation and function. DCs serve as a critical link between innate and adaptive immunity and, physiologically, they function to present antigen and promote adaptive immunity. The VP35-mediated suppression of RLR signaling makes a major contribution to DC inhibition. In fact, infection of DCs with Ebola virus disrupts normal DC maturation processes that are required for efficient DC maturation (Yen et al. 2014). Expression of VP35 alone in DCs reproduces the inhibition of maturation seen with wild-type Ebola virus, while dsRNA binding mutants lose this suppressive capacity, indicating that VP35 inhibition of RLR signaling is the major mechanism by which Ebola virus inhibits DCs (Hartman, Bird, et al. 2008; Jin et al. 2010). Furthermore, by interfering with the RIG-I signaling pathway VP35 prevents the upregulation of major histocompatibility complex I and II (MHC I, MHC II) and the costimulatory molecules CD40, CD80, and CD86, thus impairing antigen presentation to CD8+ and CD4+ T cells and T-cell activation (Jin et al. 2010; Yen et al. 2014) and thereby impeding linkage of the innate and adaptive immune responses. It has also been observed that DCs are activated by Ebola virus-like particles (EVLPs) containing the viral matrix protein (VP40) and the viral glycoprotein (GP), that were found to induce a proinflammatory response. This

response included the production of several proinflammatory cytokines and activation of numerous transcription factors including NF-κB, with the GP mucin domain found required for EVLPs to stimulate human dendritic cells through NF-κB and MAPK signaling pathways (Martinez et al. 2007).

Thus, acting in this primary site of infection and impairing the maturation of DCs, EBOV cuts off the communications between innate and adaptive immune response and prevents the establishment of an efficient adaptive immune response, an important feature of EVD pathogenesis.

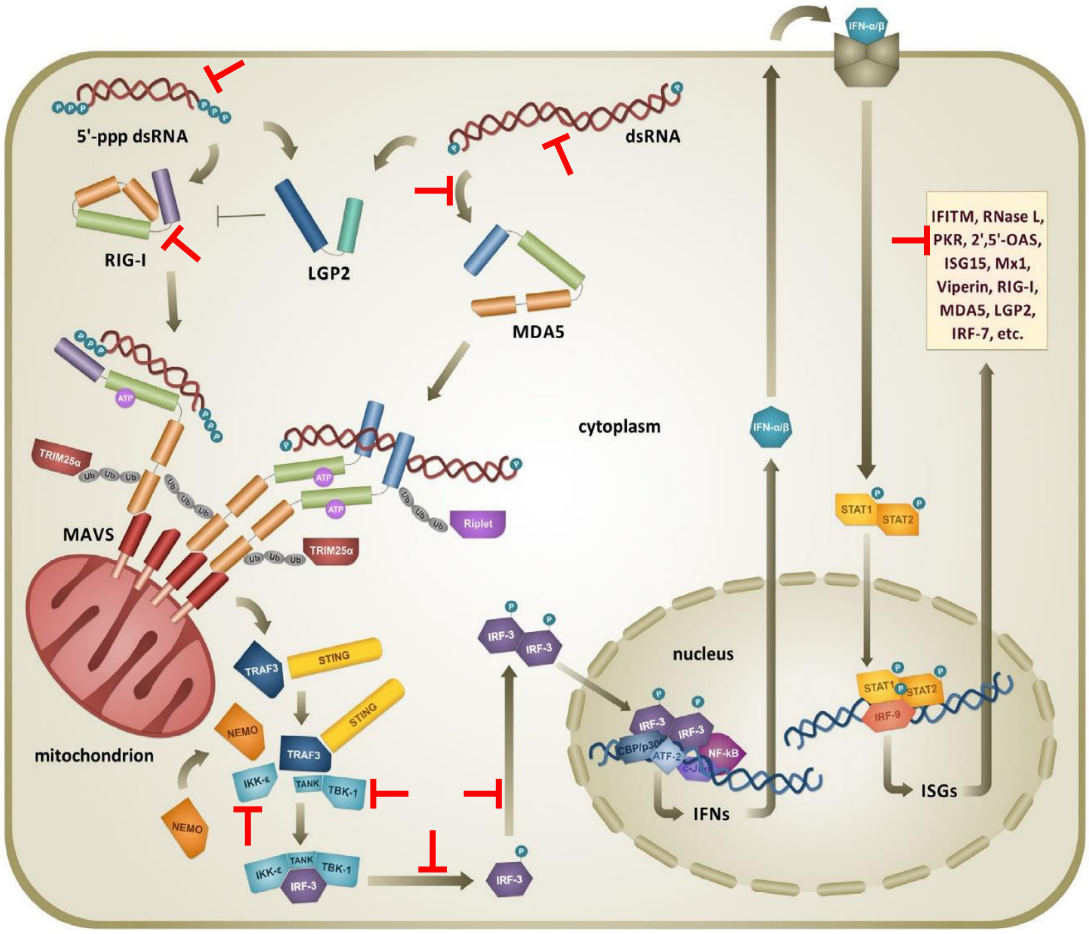

Fig. 23. Suppression of type I IFN antiviral response triggered by the RLRs pathway upon dsRNA detection by EBOV VP35. Viral short 5'-ppp dsRNA and long dsRNA are preferentially recognized by the CTD of RIG-I and MDA5, with LGP2 modulating the activity of RIG-I helicase. VP35 (red t-bars) sequesters dsRNA to RIG-I and MDA5 recognition and binds to PACT impairing its interaction with RIG-I and with PKR. Downstream VP35 interacts with the IRF-3 kinases IKK-ε and TBK-1, preventing phosphorylation of IRF-3 and its translocation to the nucleus and inhibiting in this way the expression of IFN-α/β (source: Zinzula and Tramontano, 2013).

1.9 Aim of the research

On the base of the knowledge gained to date of the strategies employed by EBOV to evade the host innate immune response, it is clear that EBOV VP35 protein is a leading factor for the viral evasion of the host defenses and therefore represents a key viral player for the high pathogenicity of the virus. Correspondingly, for a pharmacological research point of view, EBOV VP35 undoubtedly represents a primary target for the development of effective countermeasures against EVD.

Within this context, the present research work was aimed to develop efficient strategies for subverting the inhibitory blockade of host immune response, with particular interest to: i) searching for molecules, synthetic as well as of natural origin, capable to stimulate the innate immune response of the host organism as well as to counteract the inhibition of the immune response mediated by EBOV VP35; ii) searching for molecules, synthetic as well as of natural origin, capable to directly interfere with a specific domain of the EBOV VP35 protein and inhibiting its biological anti-immunity function; iii) developing an antibody-based approach to directly inhibit the anti-immunity activity of the VP35 protein.

2. MATERIALS AND METHODS

2.1 Cell lines

Adenocarcinoma human alveolar basal epithelial (A549) cells and African green monkey kidney Vero cells were grown at 37 °C in humidified atmosphere with 5% CO_2 and 95% air in Dulbecco's modified Eagle's medium (DMEM) by Life Technologies, supplemented with 10% heat-inactivated fetal bovine serum (Life Technologies).

2.2 Viral infections

Viral RNA extraction for luciferase reporter gene assays. For production of viral RNA (vRNA) to be used in the luciferase reporter gene assays, A549 cells were infected with Influenza virus A/Puerto-Rico/8/34 (H1N1) strain (IAV/PR/8/34) with a multiplicity of infection (MOI) of 5. Five hours after infection, total RNA was isolated using the RNeasy Kit (Qiagen).

EBOV replication BSL-4 experiments. All of the EBOV replication experiments were conducted at the BSL-4 laboratory of Karolinska Institutët in Stockholm, Sweden. EBOV from the recent outbreak (Ebola virus/H.sapiens-tc/SLE/ 2014/Makona) was isolated and cultured, and infectivity was quantified by fluorescence forming units as previously described (Weidmann et al. 2011).

Infection of Vero cells with the Ebolavirus strain Makona was performed by adding the virus at MOI of 0.05-0.005 FFU/cell diluted in the culture medium with the appropriate drug concentration. After 24 h, cells were fixed ON with ice-cold methanol/acetone at −20 °C and processed for immunofluorescence using an antibody targeting the viral glycoprotein GP, as previously described (Rosenstierne et al. 2016; Salata et al. 2015). The number of infected cells, expressed as percentage (%) of those obtained from infected with viral suspensions without any compound treatment, was

set as 100%. IFN-α at 2000 IU/mL was used as positive control of viral infection inhibition.

2.3 Plasmid constructs

The construct pGL IFN-β luc was kindly provided by Prof. Stephan Ludwig (Institute of Molecular Virology, Münster, Germany).

Cloning of the EBOV VP35 gene in pcDNA3 plasmid (Invitrogen) and production of pcDNA3-EBOV-VP35 plasmid for the transfection of rVP35 was performed as previously described (Cannas et al., 2015).

The constructs of scFv mAbs were kindly provided by Dr. Paola di Bonito from the Istituto Superiore di Sanità (ISS) - Department of Infectious, Parasitic and Immune-mediated Diseases of Rome (Italy).

2.4 Plant extracts

Plant extracts preparation. Collected plant materials were washed with deionized water, frozen at -80 °C and then lyophilized. The dried plant was stored at - 80° C until required. Alternatively, the collected plants were dried in a ventilated stove, then their aerial parts were macerated in ethanol for the raw extract preparation, while for the process of extraction of the various fractions other solvents were also employed.

Extraction procedures. For extraction, the crushed aerial parts were placed in a container and let stand in the dark for a period of 2-8 days, which is necessary to dissolve the soluble material. After filtering, solvent was removed by rotary dryer (rotavapor) and the obtained crude extract was subsequently dissolved in dimethyl sulfoxide (DMSO) for storage at -20 °C. Fractions were obtained by chromatographic separation from the crude extract by the use of different solvents, such as water, ethyl acetate, ethanol and n-butanol in various percentages. The separation was monitored by thin layer chromatography (TLC). The compounds isolated from the fractions are identified

through the use of spectroscopic methods, mainly the nuclear magnetic resonance spectroscopy (NMR).

The lyophilized plant materials (10 g) of *A. microcarpus* were extracted in 50 mL of ethanol for 24 h at room temperature under continuous stirring. After filtration, ethanol extract was diluted 10-fold with water and then lyophilized. Dried powder was dissolved in 10% DMSO for antimicrobial activity tests. For HPLC–DAD–ESI/MS analyses, dried extract was dissolved in 1 mL of 0.1% formic acid: acetonitrile (70:30, v/v) and filtered through a 0.22 μm disposable LC filter disk for HPLC analysis.

In order to evaluate the effects of plant extracts, fractions and compounds on the *in vitro* fluorescent dsRNA-VP35 binding assay, dry plant extracts were resuspended in DMSO at concentration of 2.5 mg/ml at first and then tested at the concentration of 100 μg/ml. A short dsRNA oligomer was used as positive control of inhibition.

For the luciferase reporter gene assays, plant extracts, fractions and compounds were first resuspended first in DMSO at a stock concentration of 2.5 or 5 mg/ml, then serial dilutions (ranging from 100 μg/ml to 0,03 μg/ml) were assayed on cells. Purchased Virtual Screening selected drugs were first resuspended in DMSO, according to manufacturer's instructions, at concentration of 100 mM and then serial dilutions compounds (ranging from 300 μM to 0,3 μM) were assayed on cells.

2.5 Cytotoxicity of extracts, compounds and drugs

The effect of natural extracts on A549 cells proliferation was determined in 96-well plates (Spectra Plate, PerkinElmer). Cells were seeded at initial density of 10^5 cells/mL and cultured in DMEM (Life Technologies) supplemented with 10% Fetal Bovine Serum (E.U.-approved, South America Origin, Life Technologies), in the presence or absence of serial dilutions of extract (ranging from 100 μg/mL to 0.03 μg/mL). Camptothecin was used as positive control. Plates were incubated for 72 h at 37 °C in humidified atmosphere of 5% CO_2 and 95% air. Cell viability was determined adding

PrestoBlue™ Cell Viability Reagent (Invitrogen). Following 1 h incubation at 37°C, relative fluorescence was read with a Victor3 (Perkin Elmer). The percentages of cell viability were calculated on the amount of living cells in extract treated cells relative to untreated control cells (defined as 100% viability). The concentration required to reduce cell growth by 50% (CC_{50}) was calculated using regression analysis of cytotoxicity curves.

The cytotoxic activity of VS-selected compounds was determined on exponentially growing cells in complete medium at 24 hr. Cells were plated in quadruplicate at a density of 1 x 10^^{4} cells per well, in 96-well plate. On the following day compounds were added to the experimental final concentrations in fresh medium. Twenty-four hours later, cells were incubated with MTT dye (Cell Proliferation Kit I, Roche Life Science) according to the manufacturer's instructions. Optical density was determined by measuring absorbance at 550 nm and 650 nm.

2.6 Luciferase reporter gene assays

IFN-β induction luciferase reporter gene assay. A549 cells (5 x 10^4 per well) were transfected in 48-well plates with T-Pro P-Fect Transfection Reagent (T-Pro Biotechnology) with the construct pGL IFN-β luc kindly provided by Prof. Stephan Ludwig (Institute of Molecular Virology, Münster, Germany). Twenty-four hours after transfection cells were additionally transfected with IAV PR8 vRNA and incubated for further 6 hours at 37 °C with 5% CO_2. Cells were harvested with lysis buffer (50 mM Na-MES pH 7.8, 50 mM Tris-HCl pH 7.8, 1 mM dithiothreitol, 0.2% Triton X-100). The crude cell lysates were cleared by centrifugation and 50 µL of cleared lysates were added to 50 µL of luciferase assay buffer (125 mM Na-MES pH 7.8, 125 mM Tris-HCl pH 7.8, 25 mM magnesium acetate, 2.5 mg/ml ATP) in a white 96-well plate. Immediately after addition of 50 µL 1 mM D-luciferin into each well, the luminescence was measured in

Victor3 luminometer (Perkin Elmer). The relative light units (RLU) were normalized as the fold activity of the unstimulated control. Each assay was carried out in triplicate.

EBOV VP35 luciferase reporter gene inhibition assay. The above described luciferase reporter gene assay was also performed for evaluating the IFN-β induction inhibition mediated by EBOV VP35 protein. When the pcDNA3-EBOV-VP35 was used as control, it was co-transfected with the pGL IFN-β luciferase plasmid. Inhibition of luciferase expression was indicated either as the fold activity of the unstimulated control or as percentage of induced control. Each assay was carried out in triplicate.

2.7 dsRNA-EBOV VP35 *in vitro* binding assay

Plasmid construction, cloning and protein expression. Cloning of the EBOV VP35 gene in pET45b(+) vector (Novagen) and production of pET45b-EBOV-VP35 plasmid for the expression of recombinant N-terminal His6-tag-VP35 protein was performed as previously described (Zinzula et al. 2009). Competent BL21AI *E. coli* cells (Invitrogen), were prepared and transformed with pET45b-EBOV-VP35 plasmid. Transformants were selected on Luria-Bertani (LB) medium agar plates containing 150 μg/ml of ampicillin. A single transformed bacterial colony was inoculated in 50 ml of LB medium with the same quantity of antibiotic and left to grow overnight (ON) at 200 rpm at 37 °C. Bacterial culture was transferred in 4 liters of LB medium containing 150 μg/ml of ampicillin and 0.1 % (w/v) glucose, then incubated at 37 °C with 200 rpm shaking until OD_{600} reached 0.6. Protein expression was inducted adding 0.4 % (w/v) arabinose and 0.65 mM IPTG and culture was incubated ON at 200 rpm at 18 °C. After incubation, the cell culture was centrifuged at 4500xg at 4 °C for 20 min and bacterial pellets were collected and then frozen at -80 °C.

EBOV VP35 protein purification. The bacterial pellet was re-suspended in 5 ml lysis buffer (with 6 M urea) per 1 ml of pellet. The suspension was incubated on ice for 15

min and subsequently sonicated on ice. The cell lysate was centrifuged at 32000xg at 4 °C for 45 min. Supernatant was slowly loaded (0.5 ml/min) to an IMAC Econo Column (Biorad) prepared with 3 ml of Ni-Sepharose High Performance (GE Healthcare) resin, pre-equilibrated in binding buffer (with 6 M urea). The column was connected to the BioLogic LP Chromatographic System (Biorad) for the management and the reading of the purification. Urea content was gradually removed from the column by a decreasing gradient of concentration from 6 up to 0 M with a flow rate of 0.5 ml/min for around 130 column volumes (800 minutes). The column was washed for several bed volumes with Washing buffers at increasing concentrations of imidazole (70 mM - 150 mM - 250 mM imidazole). Refolded recombinant proteins were eluted using 90 ml of the same buffer having 1M imidazole and collected in fractions. Significant eluted fractions, selected on IMAC chromatogram, were analyzed running on 12 % SDS–PAGE. Fractions containing rVP35 protein were gathered and dialyzed against Dialysis buffer (50 mM sodium phosphate pH 8.0, 800 mM NaCl, 1 mM 2-mercaptoethanol, 10 % glycerol). Afterwards, protein concentration was determined by Bradford assay with the Protein Quantification Kit-Rapid (Fluka – Sigma Aldrich).

Preparation of dsRNA substrates. A 500 bp dsRNA was produced by in vitro transcription using the T7 MEGAscript RNAi kit (Ambion) from the linearized DNA provided with the kit as template, according to manufacturer's instructions. IVT oligomers were purified from transcription reaction with Quick Spin G25 columns (Roche), and quantified by spectrophotometry.

A fluorescent dsRNA oligomer of 30 bp in length and a not fluorescent 30 bp oligomer were prepared by annealing from three different ssRNA purchased from Metabion International AG (Germany).

2.8 Molecular Modeling

Complex preparation. The coordinates of VP35-dsRNA homodimer structure were taken from the RCSB Protein Data Bank (PDB ID: 3L25). The protein was prepared by using the Maestro GUI Protein Preparation Wizard module (Schrödinger LLC. 2014. Maestro GUI, New York, NY, USA). Bond orders and formal charges were added for hetero groups, and all the hydrogen atoms were added in the structure. After preparation, the structures were refined to optimize the hydrogen-bond network by using OPLS2005 force field. The minimization was terminated once the energy converged or the RMSD reached a maximum cut off of 0.30Å. The wt model was generated introducing 5'-ppp dsRNA as terminal portion using build module in Maestro GUI available in Schroedinger Suite 2014 (Schrödinger LLC. 2014. Maestro GUI, New York, NY, USA). The protein was then minimized with the Polak-Ribiere conjugate gradient minimization allowing 10000 iterations and a convergence threshold of 0.01 in GB/SA implicit water. Since the model misses the coil-coil tail portion and dsRNA is likely to be open during the simulation, force constraints were applied around residue Asp218 and dsRNA terminal bases (C1-G8). The rest of the complex was left free to move. Minimized complex was then used as initial structure for MD simulation, where the same constraints were maintained.

Pharmacophore generation. The frame with the lowest energy of wt 3P-VP35 coming from the MD was considered for pharmacophore generation. Only end-capping interacting monomer was selected. The two terminal bases and the triphosphate portion were considered as core molecule and the pharmacophore was automatically generated by *Ligandscout*. This original pharmacophore was modified with the introduction of hydrophobic feature in correspondence of Guanine aromatic portion and used to screen the database allowing 2 omitting features.

Database preparation. FDA Drugs .sdf file was downloaded from IPMC (Institut de Pharmacologie Moléculaire et Cellulaire). This file contains one conformer for each

drug with indication of chiral centers or list of possible diastereoisomers if the drug possesses more than one chiral center. Compounds were prepared with Ligprep using the right ionization at 7.4 and allowing possible tautomers. This file was then converted in a multiconformer .ldb database with ldbgen by LIgandScout and screened with the pharmacophore.

Docking. Selected compounds were then minimized and docked considering 3 docking protocols: GlideXP, QMPL and Autodock. Grid was centered considering the residue F239 located in the middle of end-capping surface and it was wide enough to contain the whole monomer (36 x36 x36) Å. For Glide and QPLD, extra-precision (XP) mode was selected. All the other settings were left as default as well as for Autodock, where the files were generated with Raccoon. The best poses of each compound were then subjected to a post-dock eMBrAcE protocol. For each ligand, the protein-ligand complex, the free protein, and the free ligand were all subjected to energy minimization in implicit solvent (generalized Born). A traditional molecular mechanics (MM) method to calculate ligand–receptor interaction energies was used, with a Gaussian smooth dielectric constant function method for electrostatic part of solvation energy and solvent-accessible surface for the nonpolar part of solvation energy. A conjugate gradient minimization protocol was used in all the performed minimizations. The compounds with the best consensus scoring were then clustered for diversity and analyzed by visual inspection. Nine compounds were selected and purchased.

2.9 ScFv antibodies generation

A library of antibodies in scFv format designed for phage display on bacteriophage M13 was used to select antibodies against EBOV VP35 protein.

Isolation of scFv antibodies from antibody phage display library. Immunotubes (Nunc Maxisorp) were coated overnight (ON) at room temperature (RT) with 15 μg/ml of recombinant purified EBOV VP35 protein in PBS. An aliquot of the library, containing

about 10^{12} cfu phage displaying scFv was added to immunotube, after panning, phages were eluted with 1 ml of 100 mM triethylamine and the solution was immediately neutralized by adding 0.5 ml of 1 M Tris-HCl pH 7.4. Eluted phages were used to infect log phase TG1 *E. coli* bacteria and amplified for the next round of selection. Briefly, 50 ml of 2 × YT with 100 μg/ml ampicillin (2 × YTA medium) and glucose 1% were inoculated with enough bacterial suspension to yield an OD600 nm ≅ 0.05–0.1. The culture was grown up to OD600 nm 0.4–0.5 and infected with M13 K07 helper phage in a ratio of around 20:1 phage/bacteria. Rescued phages were concentrated by precipitation with PEG 6000 and used for next round of panning).

For soluble scFv preparation, individual colonies were grown in 96 flat bottomed wells (Nunc) for 2 hours at 37 °C in 180 μl 2 × YTA medium and glucose 0.1% in 96 well plates and inducted with 50 μl 2 × YTA medium and 6 mM IPTG. The following day, plates were spinned-down at 1800 g for 10 minutes and the supernatants containing soluble scFvs were recovered and tested for specificity.

ELISA assays. Positive scFv clones were analyzed by ELISA for reactivity with the EBOV VP35 antigen. To this aim, 96 well ELISA-plates (Nunc Maxisorp) were coated ON at RT with 0.5 μg of antigen in PBS. The following day, a blocking solution consisting of 2% non-fat dry milk in PBS (MPBS), was added; plates were washed with PBS containing 0.05% Tween 20 (TPBS) and incubated for 2 hours at RT with 50 μl of supernatants containing soluble scFv antibody, anti-Flag M2 antibody (1.6 μg/ml Sigma-Aldrich; MO, USA) and anti-mouse HRP conjugated antibody (1.6 μg/ml Dako; Denmark).

The reaction was developed using 3, 31-5, 51-tetramethylbenzidin BM blue, POD-substrate soluble (Roche Diagnostics; IN, USA) and stopped by adding 50 μl of 1 M sulfidric acid. The reaction was detected with an ELISA reader (Biorad; CA, USA), and the results were expressed as A (absorbance) = A(450 nm) – A(620 nm).

DNA characterization and sequences. Plasmid DNA from individual bacterial colonies of 8 scFv clones was digested with specific endonucleases and sequenced with an automated DNA sequencer (M-Medical/Genenco, Pomezia, Italy).

Cloning of scFv anti-VP35 in pTarget. The 8 scfv clones positive for VP35 were PCR amplified using opportune primers containing at reverse primer a 6His tag. Amplimers were cloned in pTarget (an expression vector for transient and stable expression in eukaryotic cells) under a viral strong promoter (Cytomegalovirus immediate early enhancer). The 8 clones obtained in pTarget were sequenced to monitor mutations introduced by PCR.

2.10 Statistical analysis

Data are expressed as mean ± standard deviation (SD). Differences were analyzed by a Student's 't' test. The level of accepted significance was $P < 0.05$.

3. NATURAL EXTRACTS AS POTENTIAL INHIBITORS OF EBOV VP35

3.1 Introduction

Strategies to prime the immune response: searching for new IFN-stimulating molecules

Defense mechanisms against infectious agents and tumors critically rely on type I IFN response. This system is based on the induction of both IFN-α/β cytokines and ISGs, both contributing to the activation of innate and adaptive immunity. Once secreted, IFN-α/β bind to their membrane receptor at the surface of both IFN-producing and neighboring cells to amplify the immune response (Khiar et al. 2017). Type I interferons have been long widely used as an immunomodulatory therapy in the treatment of many viral and malignant diseases but the side effects of protein-based IFN therapy severely limit their clinical use. Therefore, the discovery of small molecules able to reinforce the activation of the immune response, acting as more subtle immunomodulatory agents, avoiding directly administering IFNs, could be the first step for the development of new drugs which have similar pharmacological function to IFNs but with fewer side effects.

In addition, since infections by RNA viruses such as influenza virus, measles virus, dengue virus or respiratory syncytial virus, represent a major burden for public health and are responsible for hundreds of thousands of human deaths every year, there is an urgent need for the development of novel broad-spectrum antivirals. Although efficient prophylactic treatments, and in particular vaccines, can be used to protect individuals from some of these pathogens, our therapeutic arsenal remains extremely limited. Importantly, RNA viruses tend to escape drugs that target viral proteins through mutations, thus calling for innovative therapeutic approaches. Among them, searching for stimulators of the innate antiviral response is an appealing approach to develop novel therapeutics against viral infections (Lucas-Hourani et al. 2013). In fact, an improved interferon signaling system might better protect against viral infection and the identification of small molecular weight compounds mimicking its beneficial

effects might crucially improve our antiviral defenses (Martínez-Gil et al. 2012; Patel et al. 2012).

The quest for small compounds activating the type I interferon response is a field of intense researches in academic laboratories and pharmaceutical companies (Guo et al. 2012; Harvey et al. 2009; Khiar et al. 2017). The key point is to develop innovative therapies that stimulate the immune system against infections or tumors, avoiding the deleterious over activation of this system.

The biggest Ebola outbreak occurred across the years 2014-2016 pointed out to an urgent need to develop specific drugs for EVD treatment. To date, there is no univocally-defined drug as the leading treatment for treating EVD and that, in particular, is able to interfere with the immune-inhibitory functions of EBOV VP35 over the IFN signaling cascade.

Within this context, a robust cell culture gene reporter assay has been developed to assess both IFN-α/β activation after viral dsRNA RIG-I recognition and EBOV VP35 inhibition of this IFN-α/β activation (Cannas et al. 2015). In fact, screening procedures aimed to identify small molecule enhancers of the interferon signaling pathway represent a powerful approach in drug discovery, especially for the treatment of viruses that strongly inhibitor the immune response such as EBOV. In particular, this assay allows to measure the ability of small molecules to increase the IFN-α/β activation following viral dsRNA RIG-I recognition and subsequently to verify whether the same molecule is also able to directly induce IFN-α/β activation even in the absence of viral stimuli. Overall, the system is able to discriminate between molecules reinforcing IFN-α/β activation or inducing it. Such discrimination should allow the potential identification of molecules able to support the immune response in the presence of an infection avoiding to over stimulating it in the absence of a pathogen.

Plants as a source of antiviral molecules

The use of plants as a healing remedy dates back to ancient times. Their usage for medicinal purposes is described as early as 3000 BC; also Egyptian documents dated back form 1500 BC reported the use of a number of drug cures, mostly of plant origin, until arriving to the well-known traditional Chinese and Ayurvedic medicines (Cragg and Newman 2013). Ethnopharmacological studies have shown that a number of plants were used until less than 100 years ago in folk medicine (Bruni, Ballero, and Poli 1997) and some of them were reported to have therapeutic effects on inflammations and immune system reinforcements (Schafer and Kaschula 2014).

However, in the early 19th century the development of the chemical analysis offered the possibility to obtain active molecules extracted from plants up to, in the recent decades, directly synthetizing the isolated molecules identified as plant metabolites. Therefore, the possibility to explore libraries of synthetic compounds, together with the easiness of production and resupply, became the main drug discovery source for pharmaceutical industry over time. As a consequence, the use of herbal medicines declined in favor of drugs. Nevertheless, the exploitation of this screening approach coincided with a declining trend in the number of new produced drugs (Atanasov et al. 2015). Hence, recently, the interest for plant-originated constituents considerably increased in the attempt of identify new active substances with therapeutic properties. As further proof of this, it is worth noting that more than the half of the new chemical small molecules that had been approved between 1981 and 2010 were derived or inspired from nature (Cragg and Newman 2013).

The clinical usage of modern natural-origin products often resides in traditions and popular customs. A perfect example is represented by China that has been using molecules of natural origin for healing purposes for thousands of years, in what is called traditional Chinese medicine (TCM). TCM is now gaining popular interest worldwide and is practiced by more than 140 countries, which is primarily used as a complementary health approach (J. Chen et al. 2017). India has also a rich heritage of

traditional system of medicine and is a home for a large variety of plants with remarkable medicinal and pharmacological value. Ayurveda is the traditional Indian system of medicine which is meant not only for curing the diseases but also for prevention of the occurrence of illnesses and provides a plethora of information on ethnic folklore practices and traditional aspects of therapeutically important medicines (Mukherjee et al. 2017). Also in Europe plants were used for a long time as therapeutic approach. In particular, the Mediterranean area offers a great variety of endemic plants and, due to its geographical isolation, the island of Sardinia provides an even greater plant biodiversity, with significant variations in genetic and molecular characteristics as compared to plants grown in other regions.

Many plants have been used in traditional medicine for their antibacterial, antifungal, antiprotozoal, antiviral, antidiarrheal, analgesic, antimalarial, antioxidant, anti-inflammatory and anticancer activities. This has brought attention also in the antiviral field. As an example, just limited to the Sardinian plants, it is worth mentioning, the flavonoid *quercetin* that is present in the *Hypericum hircinum* L., that was shown being able to inhibit the HIV-1 integrase (Vandegraaff et al. 2001); the *Plagius flosculosus*, known for its anti-inflammatory activity, was associated with NF-κB inhibition (Calzado et al. 2005) and the *Salvia desoleana*, whose leaves are still used for the anti-inflammatory properties, have showed antimicrobial activities (Peana, Moretti, and Juliano 1999).

Due to the wide variety of secondary metabolites, plant extracts show many concomitant biological activities (Kumar and Pandey 2013; Pintus et al. 2015, 2017; Rosa et al. 2017) and they stand as an infinite source for drug development, novel pharmacophores, and scaffolds to be amplified into efficacious drugs for a multitude of diseases (Fang et al. 2017; Sharma and Gupta 2015). To date, while a number of small molecules extracted from plants are known for their antiviral effects, no antiviral drug coming from plant constituents have been approved. For instance, flavonoids and anthraquinones showed inhibitory activity against different viruses, such as Influenza

A virus (Derksen et al. 2016), Herpes Simplex virus types 1 and 2 (Petrecca et al. 2012), Hepatitis C virus (Wahyuni et al. 2013) and HIV (Esposito et al. 2012; L. Xu et al. 2015). However, none of them ever enter a clinical trial.

Therefore, in the quest to identify new molecules that may be used as antiviral agents by stimulating the innate antiviral response and improving the IFN signaling system, we screened in the present study 76 natural extracts and, in some cases, their constituents, to exploring their ability both to reinforce the IFN response and to subvert the EBOV VP35 inhibitory effects, and to stand as core compounds for further drug development. In particular, in cooperation with a number of scientists that provided us the extracts, we tested herbal extracts, and in some cases their constituents, coming from plants of the Italian and Sardinian flora (Prof. Mauro Ballero and Dr. Cinzia Sanna from the University of Cagliari), of African origin, and plants commonly utilized in Indian Ayurvedic (Prof. Poli from the "Alma Mater Studiorum" University of Bologna) and Chinese traditional medicines (Prof. Min Ye from Peking University, Beijing, China, and Prof. Xu Lijia from the Institute of Medicinal Plant Development (IMPLAD), Beijing, China).

3.2 Results

With the aim to identify molecules able to reinforce the dsRNA-dependent RIG-I-mediated IFN-β induction, we tested the extracts in the previously described luciferase reporter gene assay and the same assay was used to verify the extracts ability to subvert the EBOV VP35 inhibition of the IFN-β induction, as described in chapter 2 (Cannas et al. 2015).

To ensure that marginal cytotoxic effects could not influence the data, all extracts were primarily tested for cytotoxicity as described. Since the extracts showed minimal cytotoxicity with a CC_{50} values > 50 μg/ml, an initial concentration of 30 μg/ml was chosen to investigate the effects of a possible increase of the dsRNA RIG-I-mediated

IFN-β induction in the presence of viral dsRNA. The extracts that shown to be positive in this first induction assay, were then investigated for their ability to counteract the EBOV VP35 mediated inhibition of the RIG-I activated IFN-β induction.

3.2.1 *Screening of natural extracts for potential boosters of IFN-β production*

In the primary screening we tested 18 extracts from Italian plants, 23 from Sardinian plants, 11 from African plants, 19 from Indian plants and 5 from Chinese plants (Table 4).

The effect of herbal extracts of Sardinian endemic plants

As described, the Mediterranean area offers a great variety of endemic plants in Europe and, due to its geographical isolation, the island of Sardinia provides an even greater plant biodiversity, with significant variations in genetic and molecular characteristics as compared to plants grown in other regions. For this reason, we assayed a series of extracts and molecules of the Sardinian traditional medicine. Among the natural extracts and related compounds tested, the *Asphodelus microcarpus* leaves extract (AE), revealed the ability to significantly potentiate the dsRNA RIG-I-mediated IFN-β induction. *Asphodelus microcarpus* Salzm.et Vivi (*Asphodelaceae*) is a widely distributed plant over the coastal Mediterranean region, traditionally used as an antimicrobial agent. In the ethnobotanical literature, its use for otitis and toothache in Algeria and for lung diseases in Sardinia has been also reported (Di Petrillo et al. 2017). Henceforth, we initially investigated the effects of both the root and leaves ethanol fraction of *A. microcarpus* (Fig. 24, 25).

Results of the luciferase reporter gene assay showed that *A. microcarpus* leaves extract, but not roots, was capable to significantly increase (p value < 0.05) the production of IFN-β at the concentrations of 10 μg/ml and 3 μg/ml (Fig. 25), increasing the IFN induction as compared to the control (p value = 0,0388 and 0,0484 respectively).

Table 4. Effects of natural extracts on IFN production. The table illustrates the results of the natural extracts assayed both on dsRNA-dependent RIG-I-mediated IFN-β production and inhibition mediated by EBOV VP35. Each data represents the results of three independent experiments. Abbreviations indicate as follows: Italian traditional medicine, IT; Sardinian endemic plants, S; Traditional Chinese Medicine, CH; African herbal extracts, AF; Ayurvedic medicine, IN.

Plant extract			
IT *Agrimonia eupatoria L.*	S *Hypericum scruglii* Bacch.	S *Onopordum illyricum L.* **(●)**	IN *Aconitum heterophyllum*
IT *Alchemilla vulgaris L.*	S *Hypericum hircinum L.* **(●)**	S *Astragalus terracianoi*	IN *Alstonia scholaris*
IT *Althea officinalis L.*	S *Asphodelus microcarpus (leaves)* **(+/●)**	S *Santolina insularis*	IN *Asparagus racemosus*
IT *Asparagus officinalis L.*	S *Plagius fosculosus*	CH *Licorice extract*	IN *Azadiracta indica*
IT *Betula pendula L.*	S *Helichrysum italicum (Roth)*	CH *Scutellaria extract*	IN *Bhoeravia diffusa*
IT *Calendula officinalis L.*	S *Pistacia Lentiscus L.*	CH *Maca tea*	IN *Chlorophytum borivillanum*
IT *Centaurium erythraea Rafn.*	S *Thymus herba-barona*	CH *Scutellaria baicalensis* **(+/●)**	IN *Convolvulus pluricaulis*
IT *Equisetum arvense L.*	S *Stachys glutinosa*	CH *SLF*	IN *Crataeva nurvala*
IT *Medicago sativa L.*	S *Vinca Sardoa*	AF *Butyrospermum paradoxum (leaves)*	IN *Curculigo orchioides*
IT *Galium verum L.*	S *Glechoma sardoa*	AF *Cassia siberiana (roots)*	IN *Embelia ribes* **(+)**
IT *Gentiana lutea L.*	S *Berberis aetnensis*	AF *Chrysantemum afroamericanum*	IN *Emblica officinalis*
IT *Marrubium vulgare L.*	S *Salvia desoleana (various extracts)*	AF *Cochlospermum tinctorum*	IN *Hemidesmus indicus*
IT *Parietaria officinalis L.*	S *Hyoseris taurina*	AF *Cochlospermum planconii*	IN *Moringa oleifera*
IT *Pinus sylvestris L.*	S *Helichrysum saxatile*	AF *Euphorbia paganorum*	IN *Rubia cordifolia*
IT *Primula veris L.*	S *Stachys corsica*	AF *Kaja senegalensis (fruits)*	IN *Swertia chirayita*
IT *Thymus serpyllum L.*	S *Tanacetum audibertii*	AF *Panicum subaldibum (roots)*	IN *Terminalia bellerica*
IT *Thymus vulgaris L.*	S *Seseli praecox*	AF *Gardenia sokotensis (fruits, leaves)*	IN *Terminalia chebula*
IT *Verbena officinalis L.*	S *Bituminaria morisiana*	AF *Vitellaria paradoxa*	IN *Tinospora cordifolia*
S *Limonium morisianum* Arr. **(●)**	S *Limonium morisianum*	AF *Uvaria angolensis*	IN *Withania somnifera*

(+) Plus sign indicates the ability of the extract to prime the IFN production in response to the vRNA stimulation.

(●) Blue dot indicates the ability of the extract to subvert EBOV VP35 inhibition of the IFN production.

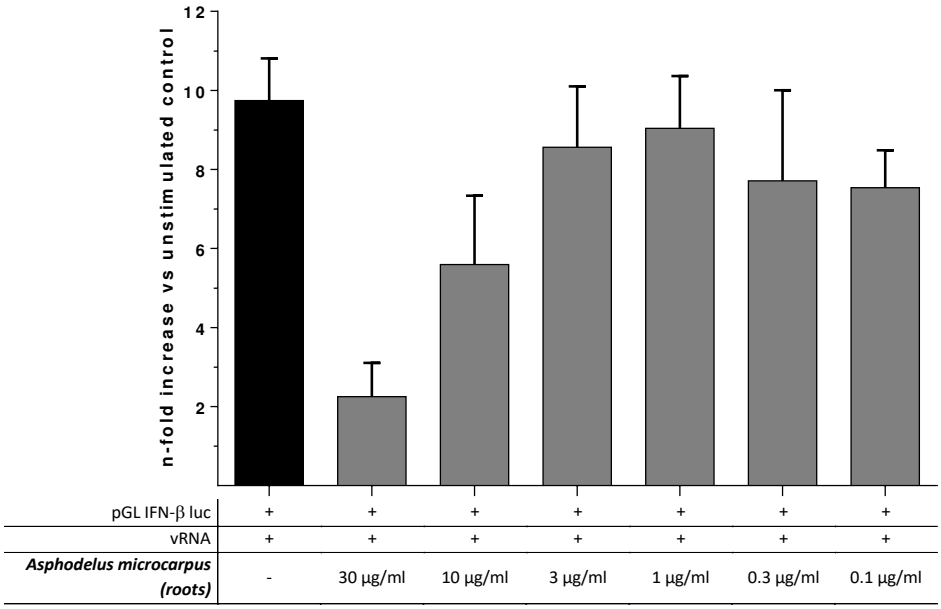

Fig. 24. ***A. microcarpus*** **roots extract effect on the viral dsRNA RIG-I-mediated IFN-β induction.** The *A. microcarpus* roots extract was tested in a RIG-I-mediated IFN-β induction system both in presence and in absence (data not-shown) of the vRNA stimulation, with various extract concentrations (from 30 to 0.1 µg/ml). The histogram illustrates the results of three independent experiments shown in n-fold compared to unstimulated control.

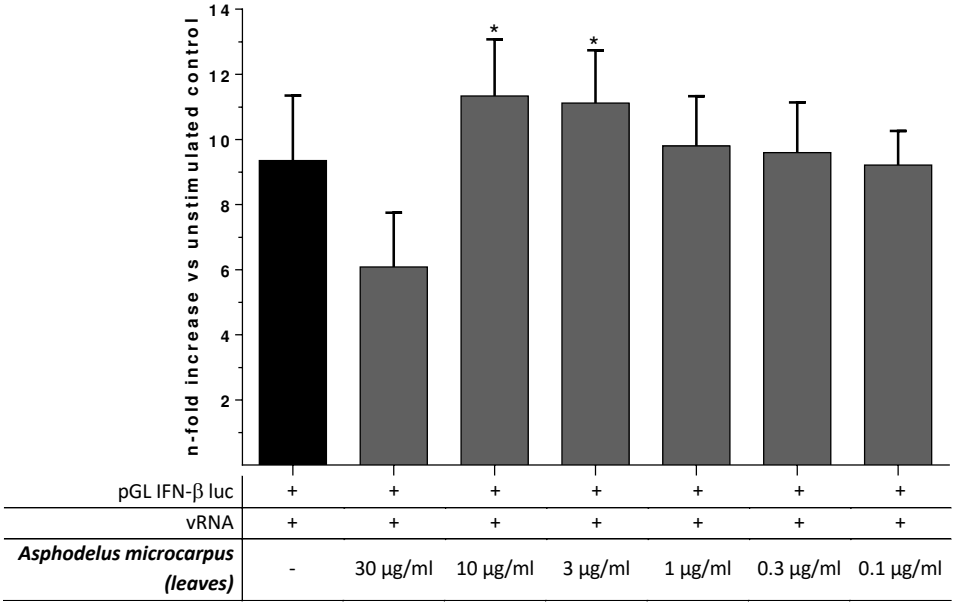

Fig 25. ***A. microcarpus*** **leaves extract effect on the viral dsRNA RIG-I-mediated IFN-β induction.** The *A. microcarpus* leaves extract was tested in a RIG-I-mediated IFN-β induction system both in presence of the vRNA stimulation, with various extract concentrations (from 30 to 0.1 µg/ml). The histogram illustrates the results of three independent experiments shown in n-fold compared to unstimulated control (* p value < 0.05).

Subsequently, we asked whether *A. microcarpus* leaves extract was able to activate the IFN-β induction even in the absence of a viral stimulus, observing that it is not able to activate the IFN-β production (data not-shown).

Hence, we investigated if the AE was capable to potentiate the dsRNA-dependent RIG-I-mediated IFN-β induction to such a level to counteract the inhibition mediated by VP35. Results showed that the AE is able to strongly interfere with the inhibition of the IFN-β induction mediated by EBOV VP35. In fact, results showed that AE significantly reverted the VP35 inhibition of the vRNA induced IFN response at concentrations of 3 - 0.1 μg/ml (p values = 0.0125, 0.0018, 0.0016 and 0.0008 respectively) (Fig. 26).

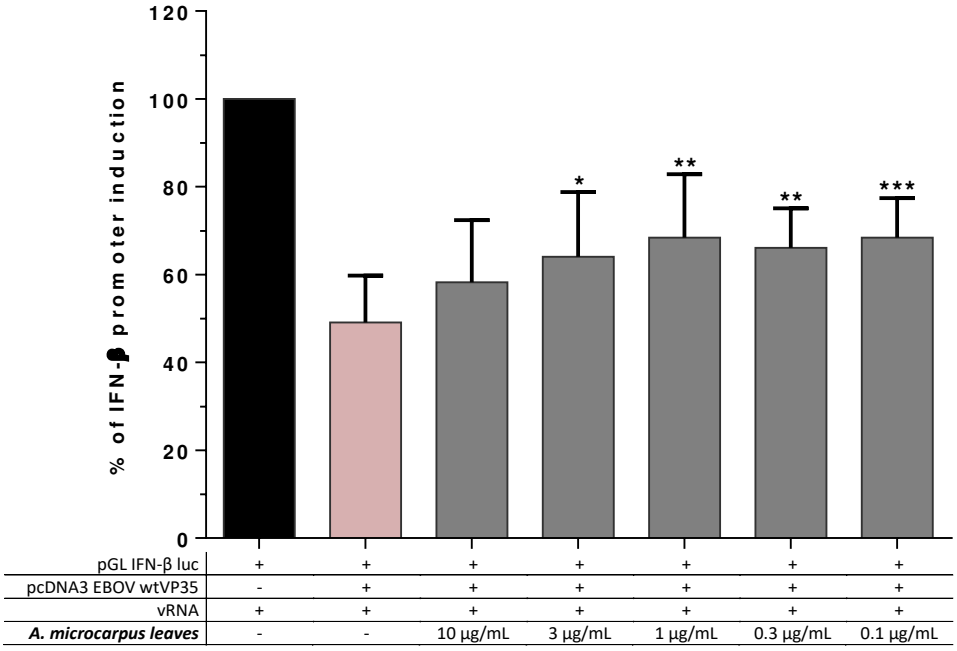

Fig 26. ***A. microcarpus*** **leaves effect on IFN-β induction inhibition of VP35**. The histogram shows the effect of AE on the IFN response inhibition mediated by EBOV VP35. 24 hours post co-transfection with pGL IFN-β luc and pcDNA3 EBOV wt VP35 expression vectors, cells were treated with different AE concentrations (10, 3, 1, 0.3, 0.1 μg/ml) and additionally transfected with IAV vRNA. The results from three independent experiments, displayed as percentage of the IFN-β promoter induction, showed a significant effect from 3 to 0.1 μg/ml concentrations (* p value < 0.05, ** p value < 0.01, *** p value < 0.001).

The effect of herbal extracts from the Indian Ayurvedic medicine

Ayurveda is a traditional healthcare system of Indian medicine since ancient times. Several Ayurvedic medicines have been exploiting for treatment and management of various diseases in human beings (Mukherjee et al. 2017). This prompted us to investigate the effect of 19 natural extracts known in the Ayurvedic medicine (Table 4). Among them the *Embelia ribes* extract (ERE) showed interesting results.

Belonging to the *Primulaceae* family, *Embelia ribes* is one of the important medicinal plants of India. Also known as *Vidang* or *Baibirang*, it produces seeds resembling pepper so much that it is often referred to as false black-pepper. In India it is considered to be beneficial for a number of diseases for its antitumorigenic, hepato- and gastrointestinal protective role. It is worth nothing that its known bioactive molecule, called *embelin*, is a quinone derivative isolated that has been shown to have an important role in cancer. In fact, it has been demonstrated that *embelin* could induce apoptosis in tumor cells via AKT / mTOR pathway activation, leading to the suppression of leukemic, human breast and prostate cancer cells growth (Park et al. 2015; Prabhu et al. 2017; Shah et al. 2016).

When tested in the luciferase gene reporter assay, the total extract of *Embelia ribes* reinforced the viral dsRNA RIG-I mediated IFN production at the concentrations of 3, 1 and 0.3 μg/ml ($p = 0,0449$, $p = 0,0054$, $p = 0,0265$ respectively), as compared to the viral dsRNA stimulated control (Fig. 27). Hence, we tested the extract for its ability to induce by itself the IFN production showing that in this system it is inactive (Fig. 27). Further, since *embelin* is the main constituent of *Embelia ribes*, we investigated the ability of this molecule to reinforce the viral dsRNA RIG-I mediated IFN production. Results showed that, compared to the dsRNA induced control, *embelin* was able to potentiate the IFN production signal at the concentrations of 0.3 and 0.1 μg/ml ($p = 0,0151$, $p = 0,0072$ respectively) (Fig. 28).

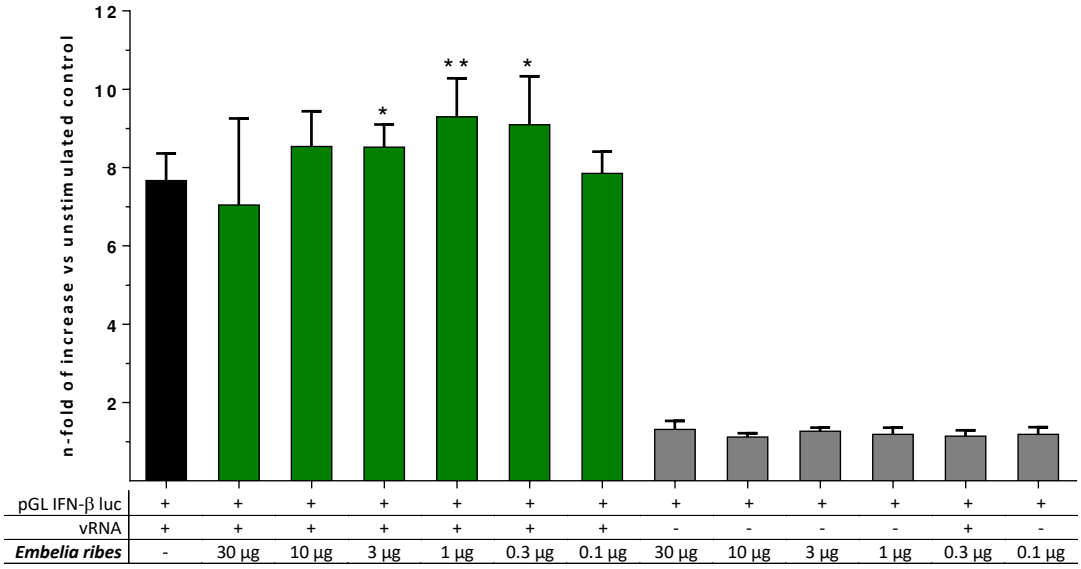

Fig. 27. ***Embelia ribes*** **extract effect on the viral dsRNA RIG-I-mediated IFN-β induction.** The ERE was tested in a RIG-I-mediated IFN-β induction system both in presence and in absence of the vRNA stimulation, with various extract concentrations (from 30 to 0.1 µg/ml). The histogram illustrates the results of three independent experiments shown in n-fold compared to unstimulated control (* p value < 0.05, ** p value < 0.01).

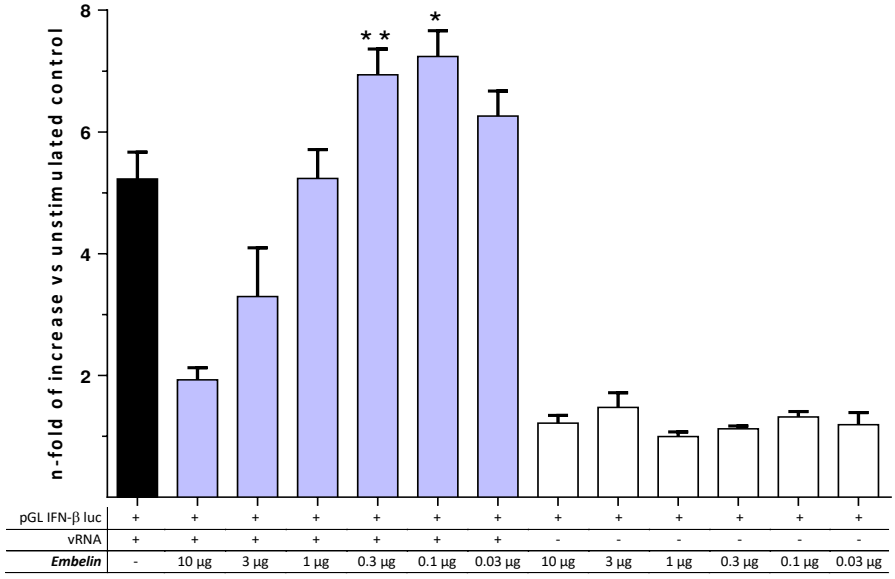

Fig. 28. ***Embelin*** **effect on the viral dsRNA RIG-I-mediated IFN-β induction.** *Embelin* was tested in a RIG-I-mediated IFN-β induction system both in presence and in absence of the vRNA stimulation, with various *embelin* concentrations (10, 3, 1, 0.3, 0.1, 0.03 µg/ml). The histogram illustrates the results of three independent experiments shown in n-fold compared to unstimulated control (* p value < 0.05, ** p value < 0.01).

Similarly to the analysis performed on the *A. microcarpus* extracts, we then investigated whether this effect on the IFN production was able to counteract the inhibition due to the concomitant EBOV VP35 expression. Data showed that *embelin* demonstrated to significantly subvert the EBOV VP35-mediated IFN-β production inhibition (Fig 29). In fact, at 1 and 0.3 μg/ml concentrations, it produced a significant increase of IFN-β induction, as compared to the VP35 inhibition control (p value = 0.0132, p value = 0.0004, respectively). However, contrarily to what was observed for *embelin*, the total extract (ERE) strengthening of the viral dsRNA induced the IFN production was not able to efficiently subvert the EBOV VP35 mediated inhibitory blockade, showing no effect in counteracting its IFN-β production inhibition (data not-shown).

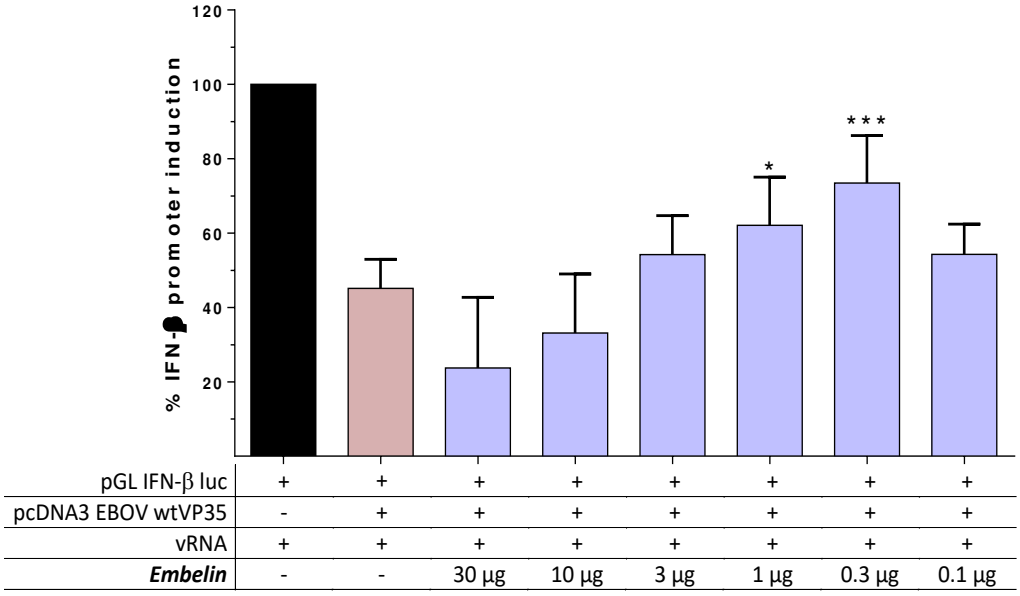

Fig. 29. Embelin effect on IFN-β induction inhibition of VP35. The histogram shows the effect of *embelin* on the IFN response inhibition mediated by EBOV VP35. 24 hours post co-transfection with pGL IFN-β luc and pcDNA3 EBOV wtVP35, cells were treated with different *embelin* concentrations (30, 10, 3, 1, 0.3, 0.1 μg/ml) and additionally transfected with IAV vRNA. The results from three independent experiments, displayed as percentage of the IFN-β promoter induction, showed a significant effect at 1 and 0.3 μg/ml concentrations (* p value < 0.05, *** p value < 0.001).

The effect of herbal extracts from the Traditional Chinese medicine

Together with Indian traditional medicine, TCM grounds its knowledge in a millenary history of usage. Therefore, we investigated a series of TCM extracts with the aim to find molecules able to boost the immune response.

We tested 5 TCM extracts (Table. 4), finding among them interesting results with the extract from *Scutellaria baicalensis* (SBE). *Scutellaria baicalensis* (Huang-Qin or Chinese skullcap) is a very-well known plant of *Lamiaceae* family and is one of the 50 fundamental herbs of TCM. It is commonly used in the East of Asia, including countries such as China, Japan, and Korea, and has been studied thoroughly by many researchers till date for its anti-viral, anti-oxidant, anti-cancerous and neuro-protective properties. When tested in our luciferase gene reporter assay, the SBE showed to be capable to reinforcing the IFN response in a dose-response manner at the 3, 1 and 0.3 μg/ml extract concentrations (p value = 0,0265, p value = 0,0161, p value = 0,0050 respectively), as compared to the IFN-β-stimulated control. On the contrary, it was not able to induce IFN production in the absence of a viral dsRNA stimulus (Fig. 30).

On the basis of the same experimental scheme, the SBE was tested to evaluate its ability to subverting the EBOV VP35 mediated IFN production inhibition. Results showed that SBE is able to counteract the EBOV VP35 inhibition of the viral dsRNA RIG-I-mediated IFN-β induction at 1 and 0.3 μg/ml concentrations (p value = 0.0295, p value = 0.0043 respectively) (Fig. 31).

Previous studies on the root of *S. baicalensis* have identified *wogonin*, *baicalein*, *baicalin* and *wogonoside* as the main active components that have exhibited anti-cancerous properties (Huynh et al. 2017). Indeed, mass spectrometry (MS) analysis confirmed the presence of these main constituents into our SBE, so we also analyzed these single molecules in our cellular assays.

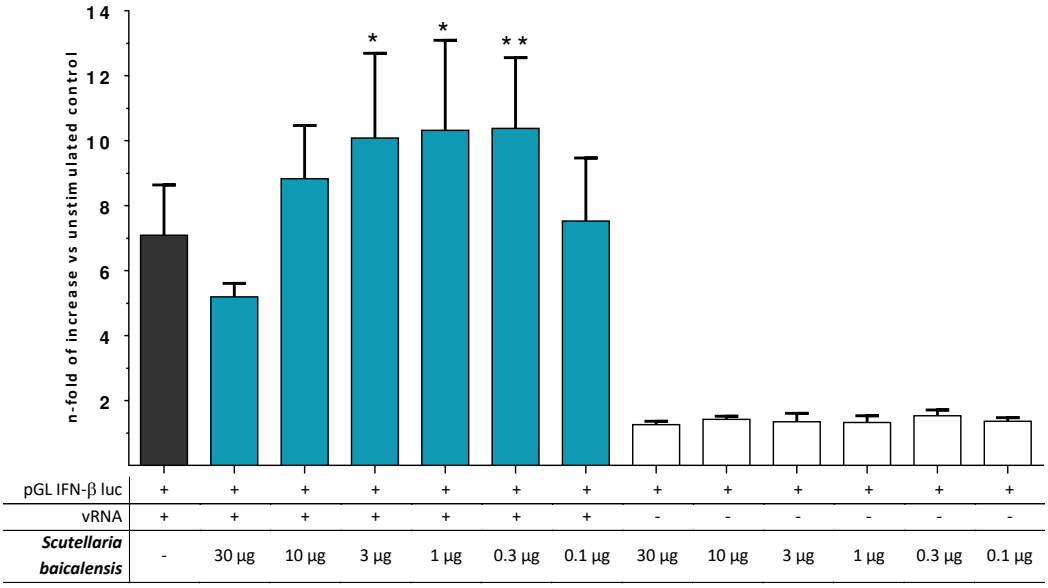

Fig. 30. Scutellaria baicalensis extract effect on the dsRNA RIG-I-mediated IFN-β induction. The SBE was tested in a RIG-I-mediated IFN-β induction system both in presence and in absence of the vRNA stimulation, with various SBE concentrations (30, 10, 3, 1, 0.3, 0.1 µg/ml). The histogram illustrates the results of three independent experiments shown in n-fold compared to unstimulated control (* p value < 0.05, ** p value < 0.01).

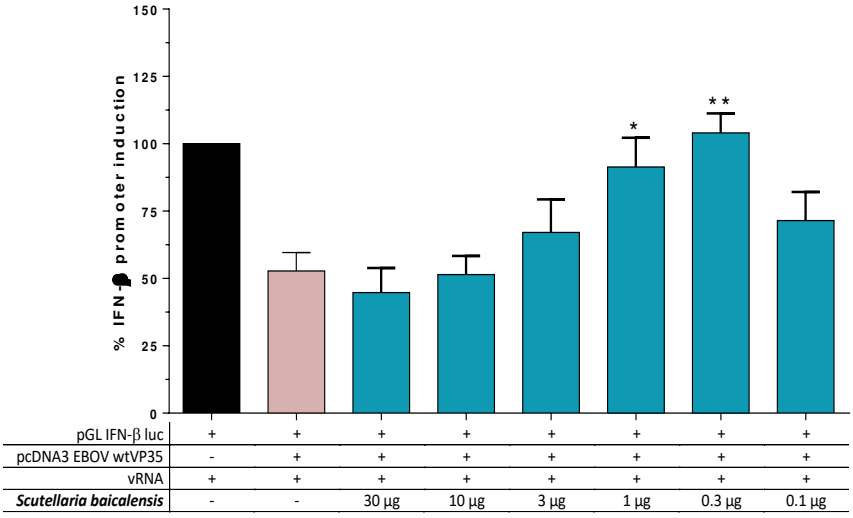

Fig. 31. Scutellaria baicalensis effect on IFN-β induction inhibition of VP35. The histogram shows the effect of SBE on the IFN response inhibition mediated by EBOV VP35. 24 hours post co-transfection of A549 cells with pGL IFN-β luc and pcDNA3 EBOV wt VP35 expression vectors, cells were treated with different SBE concentrations (30, 10, 3, 1, 0.3, 0.1 µg/ml) and additionally transfected with IAV vRNA. The results from three independent experiments, displayed as percentage of the IFN-β promoter induction, showed a significant effect at 1 and 0.3 µg/ml concentrations (* p value < 0.05, ** p value < 0.01).

Hence, we investigated the effect of these 4 main constituents on the dsRNA RIG-I-mediated IFN-β induction showing that only the single compound wogonoside was able to induce a significant increase in IFN-β induction at 1 μg/ml concentration (p value = 0.039), as compared to the control (Fig. 32).

To conclude the analysis, the 4 single compounds constituting the SBE were also assayed. Among them, no compound was able to potentiate the IFN induction to such a level to subvert the VP35 inhibition, showing that induction of the IFN production by the single compound wogonoside was not sufficient to subvert EBOV VP35 IFN production inhibition (data not-shown).

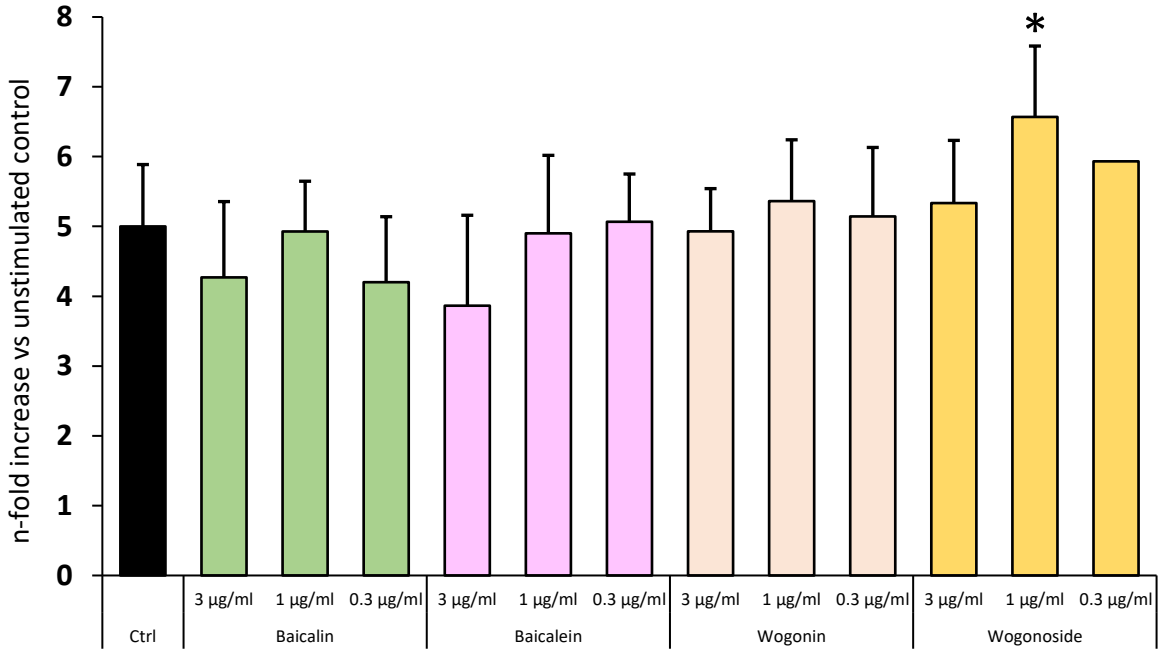

Fig. 32. Scutellaria baicalensis main constituents effect on the dsRNA RIG-I-mediated IFN-β induction. The constituents of *Scutellaria baicalensins* were tested in a RIG-I-mediated IFN-β induction system both in presence and in absence (data not-shown) of the vRNA stimulation, with various concentrations (from 3 to 0.3 μg/ml) of each compound. The histogram illustrates the results of three independent experiments shown in n-fold compared to unstimulated control (* p value < 0.05).

3.3 DISCUSSION

Plants represent an inestimable resource of molecules that can be exploited for a further drug development. The use of plants in traditional medicines grounds its roots in centuries of usage and knowledge of the wide variety of herbal mixtures and constituents, rich in plant metabolites, with curative properties. Medicinal plants have always been a potential source to cure different diseases, either in the form of traditional preparations or as pure active principles, and they are frequently the only source of medicine for the majority of people in the developing world. Often considered as folklore medicine, traditional medicine lives today a period of rebirth in search source of new molecules that can be exploited for their antibiotic, anti-inflammatory, antimicrobial and antiviral properties.

For this reason, we screened 76 natural extracts in search of molecules that could be effective in a context or viral infection, both potentiating the IFN production and counteracting the inhibitory activity of EBOV VP35. Among them, we found some capable to strengthen the IFN-β production.

In particular, we found that *A. microcarpus* leaves extract was capable to modulate both the IFN-β production and the inhibition mediated by EBOV VP35. It is noteworthy that the AE did not stimulate the innate antiviral response when tested in the absence of a vRNA stimulus and showed the ability to potentiate the viral-induced IFN-β production. Significantly, AE showed to be able to subvert VP35 effects at different effective concentrations with an almost similar efficacy between 3 and 0.1 μg/ml and a lower effect at the higher dose of 10 μg/ml. Indeed, it is worth of note that the window of AE efficacy in subverting VP35 inhibition of the IFN production is not completely overlapping with the AE dose-response IFN production shown in (Fig. 25, 26). Even if the reason of this is not clear at the moment, it is possible to speculate that the AE interaction with the IFN production pathways could be different in the presence of the viral protein. Smaller AE concentrations could be effective in reverting the VP35 inhibition but the IFN production system used could not be sensitive enough in the

absence of VP35. The VP35 reverting activity, along with the fact that AE acts only under antiviral response induction, makes this plant extract very attractive for the development of an antiviral drug. Clearly, further studies will be required to: i. identify the constituent of the extract responsible for the antiviral activity and ii. determine the extract's mode of action that, presumably, interacts with one or more components of the RIG-I-mediated IFN signaling pathway increasing IFN production. In fact, as shown by HPLC-DAD- ESI/MS analysis we recently obtained (data not-shown), AE is a complex matrix of several molecules, that could possibly act together inducing IFN production interacting with different cellular targets, as proposed for other synthetic compounds. The phenolic characterization of AE showed high presence of luteolin derivatives. These flavones were extracted from many plants and several studies showed their anti-inflammatory, antibacterial, antioxidant and anti-HIV activity and may be involved in AE biological activity (Bedard et al. 2012; Kanadaswami et al. 2005; Pattabhi et al. 2016; Seelinger, Merfort, and Schempp 2008). In addition, luteolin has been shown to inhibit the kinase activity of TBK (Jeong and Lee 2011) a component of the RIG-I cascade. Hence, it is possible that either luteolin and/or luteolin-*C*-glucoside may modulate dsRNA-dependent RIG-I-mediated IFN-β production. Further studies will be needed to investigate these possibilities. Overall, additional studies will be also needed to characterize extract fractions in order to identify the individual molecules with biological activity.

The Ayurveda medicine plant *Embelia ribes*, together with its main constituent *embelin*, was able to potentiate the IFN production in a dose-response manner, boosting the immune response in a low micromolar range of concentrations, as compared to the IFN stimulated control. When tested in the inhibition assay, we found that main compound *embelin* was able to significantly subvert the EBOV VP35 mediated inhibition of the IFN production. *Embelin* is a well-known bio-active molecule, particularly regarding cancer (Prabhu et al. 2017; Shah et al. 2016). The fact that *embelin* alone was not able to induce any IFN response in the absence viral dsRNA stimulation suggests that this constituent

of the *Embelia ribes* is specifically active only during infection and this render it a suitable molecule for a further development of synthetic derivatives with antiviral action.

Further, we assayed TCM plant extracts finding that the *Scutellaria baicalensis* extract, one of the 50 fundamental herbs in TCM, is able to significantly improve the IFN production with respect to the viral dsRNA stimulated IFN-β control. Furthermore, when assayed in the inhibition assay, the extract potently reverted the inhibitory effect of EBOV VP35 at low concentrations (1 and 0.3 μg/ml). It is worth to note that, when the four main constituents of the SBE were tested, only *wogonoside* was effective in the IFN induction assay. However, when the same compound was evaluated for its ability to counteract the EBOV VP35-mediated inhibition of the dsRNA RIG-I-stimulated IFN-β induction, it was not able to subvert this blockage, suggesting either that its IFN production was not sufficiently strong to subvert EBOV VP35 inhibition.

Overall, these results further underline the importance of traditional medicines and demonstrated the potential of natural extracts as a source of molecules that could be exploited for further drug development. In fact, the huge variety of products of plant metabolism offers an inexhaustible source of small molecules that can be used for the research of new drugs. For this purpose, we tested in our systems the effects of 76 natural extracts and related constituents, searching for new molecules able to interfere with the biological inhibitory activity of EBOV VP35, the perfect example of a viral protein capable to maximize the efficiency of the viral infection *via* immune response inhibition. Like other extracts assayed with this study, all the selected whole extracts assayed contain a number of flavonoids as secondary metabolites. Since flavonoids and anthraquinones showed inhibitory are known for their antiviral and antimicrobial properties (Esposito et al. 2012; Di Petrillo et al. 2017), we evaluated the antiviral potential of the *A. microcarpus*. In this study we found that the methanolic extract of *A. microcarpus* leaves significantly affect the EBOV VP35 inhibition of the viral induced IFN response. Moreover, this extract owns a potent inhibitory activity on Gram-

positive bacteria and an interesting antibiofilm motif on various bacterial strains (*E. coli*, *S. aureus*, *S. haemolyticus* and *B. clausii*) (data not-shown) and, collectively, this data allowed us to recently publish a scientific work about the broad-range potential of *Asphodelus microcarpus* (Di Petrillo et al. 2017).

Similarly to *A. microcarpus*, the *Scutellaria baicalensis* extract showed a similar modality of action. In fact, it positively stimulated the dsRNA RIG-I-mediated IFN-β induction and did not stimulate by itself the innate antiviral response when tested in the absence of a viral RNA stimulus and, very significantly, when tested on VP35 inhibition, showed a potent ability to overcome its effects. Indeed, it must be mentioned that the twos are total extracts and thus a complex mixture of metabolites that possibly could act together in concert to induce such effects or, contrarily, only one or few constituents are responsible for generating this result. The MS analysis data in our possession will allow us to carry out further studies in this perspective and will allow us to investigate this aspect identifying the constituent of these extracts mainly involved in such interactions.

Likewise SBE and AE, we also found that *embelin*, the main constituent of the *Embelia ribes* extract, was capable to generate the same effects in our experimental settings. Although further studies are needed to deeply characterize its molecular action, the fact that this molecule was able to improve the IFN production as well as to subvert the IFN-β induction inhibition mediated by VP35, particularly only in presence of the viral stimulation and with an overlapping window of efficacy in both types of assays we performed, suggests that embelin could be a core molecule from which to start for further drug development of new and effective molecules for the treatment of EVD.

4. NATURAL EXTRACTS AS POTENTIAL INHIBITORS OF EBOV VP35 IDENTIFIED THROUGH A NEW *in vitro* VP35-dsRNA BINGING ASSAY

4.1 Introduction

Discovery of Ebolavirus VP35 inhibitors through a novel fluorescence assay

Among the different pathogenic mechanisms involved in EVD, the suppression of the host innate antiviral response by EBOVs contributes to its high lethality. It is known that the detection of viral components by host PRRs triggers the antiviral innate immune response, with RLRs (and TLRs) having a central role in this recognition phenomenon. The exogenous dsRNAs, in particular those uniquely labelled with a 5'-triphosphate termini, play a key role within this process, being specifically recognized by RLRs and, at the same time, efficiently hidden from such recognition through the EBOV protein VP35 (Christopher F. Basler 2015; Mike Bray and Mahanty 2003; Gerlier and Lyles 2011; Luo et al. 2011; Zinzula and Tramontano 2013).

As described in chapter 1, during EBOV infection VP35 binding to viral dsRNA has been shown to be one of the main determinants of the IFN production inhibition (Cardenas et al. 2006). To do this, VP35 binds the dsRNA uses a bi-modal binding strategy *via* the RBD/IID located at the C-terminal of the protein (Kimberlin et al. 2010; Leung, Ginder, Fulton, et al. 2009), assisted in this interaction by the homo-oligomerization at the N-terminal coiled-coil domain (St Patrick Reid, Cardenas, and Basler 2005). Importantly, it was demonstrated that the sole VP35 RBD/IID, when expressed into cells, it is not able to suppress the type I IFN activation at the same level than the full length protein (Christopher F Basler and Amarasinghe 2009; Feng et al. 2007; Zinzula et al. 2009). This ability to bind viral dsRNA and to prevent the detection by cytoplasmic PRRs is crucial for EBOV VP35 IFN-antagonism and, importantly, is indicated as one of key points for drug discovery; therefore, any molecule able to bind VP35 and to inhibit its binding to the viral dsRNA, could be an interesting molecule for antiviral drug development.

In order to find small molecules able to inhibit dsRNA binding to EBOV VP35, a novel *in vitro* fluorescence-based assay was developed to quantify the VP35-dsRNA binding using a 30 bp 5'-fluorescein-dsRNA as substrate (Daino et al., manuscript under submission). Briefly, a 30 bp long dsRNA oligomer with a triphosphate in a 5' end and a fluorescein molecule in the other 5' end was designed and, together with a full-length recombinant His6-tag-VP35 protein (purified as previously described by Zinzula et al. 2009), was used on a Nickel-coated 96-well plates to quantify the binding VP35-dsRNA. Thus, any molecule capable to interfere with this interaction in the biochemical assay can be an exploitable starting point for exploring the ability of synthetic as well natural molecules to regulate interaction between VP35 protein and the dsRNA genetic elements.

4.2 RESULTS

4.2.1 *Effects of selected natural extracts screened through a novel in vitro dsRNA-EBOV VP35 binding assay*

Simultaneously to the inhibition assays conducted on the selected natural extracts, as described in chapter 3, we wanted to search small natural molecules able to specifically inhibit the interaction between EBOV VP35.

As previously mentioned, Sardinian plants provide a great plant biodiversity region due to the geographical isolation of the island, inducing significant variations in genetic and molecular characteristics as compared to plants grown in other regions. Hence, with the purpose of identifying novel antiviral agents and probing the robustness of the biochemical assay just developed, we tested 11 Sardinian plant extracts in the *in vitro* binding assay.

Among them, on the basis of their potency of EBOV VP35-dsRNA binding inhibition, 4 extracts were selected to continue the investigations: the ones from *Hypericum hircinum*, *Hypericum scruglii*, *Limonium morisianum* and *Onopordum Illyricum* (Table 5).

Table 5. Inhibition of EBOV VP35 binding to dsRNA by screened plants extracts. The table shows the dsRNA-VP35 binding inhibition values resulting from a screening process of whole natural extracts. Based on their potency of inhibition of the VP35 binding to dsRNA and the possibility to further fractionate the extracts, 4 plants were selected (*).

Plant extract	[a]IC_{50} (µg/ml)
Asparagus racemosus	> 100 (63%) [b]
Calamintha nepeta	> 100 (85%) [b]
Centaurea calcitropa	43 ± 21
Euphorbia paganorum	69 ± 3.0
Hemidesmus indicus	69 ± 16
Hypericum hircinum (*)	23.5 ± 2.5
Hypericum scruglii (*)	20.3 ± 3.8
Limonium morisianum (*)	19.2 ± 6.7
Mentha pulegium	> 100 (61%) [b]
Onopordum illyricum (*)	26.9 ± 3.3
Solanum sodomaeum	> 100 (87%) [b]
dsRNA 30 bp	13.9 ± 3.4[c]

[a] Extract/compound concentration (mean ± standard deviation) required to inhibit VP35 binding to dsRNA by 50%.
[b] Percentage of control binding of VP35 to dsRNA in the presence of 100 µg/ml extract concentration.
[c] Concentration expressed in nM.

Hypericum hircinum

The genus *Hypericum* of the *Guttiferae* family comprises mostly herbs widely used in traditional medicine worldwide, producing antimicrobial, antifungal and cytotoxic compounds (Pistelli et al., 2000). The species *Hypericum hircinum* is distributed in the Mediterranean region.

In the binding assay the whole extract of *H. hircinum* showed to inhibit the VP35-dsRNA binding with a IC_{50} of 23.5 µg/ml (± 2.5) (Table 6). Given this effect, the extract was fractioned as previously described (Esposito et al. 2013) and diverse fractions were tested for their ability both to interfere with the dsRNA-VP35 binding and the

Table 6. Inhibition of EBOV VP35 binding to dsRNA by *Hypericum hircinum*.

Compound	[a]IC_{50}
[b] Skicimic acid	67.8 ± 0.6
[b] Quercetin	100.0
dsRNA 30 bp	13.9 ± 3.4[c]

[a] Extract/compound concentration (mean ± standard deviation) required to inhibit VP35 binding to dsRNA by 50%.
[b] Concentration expressed in μM.
[c] Concentration expressed in nM.

VP35 blockade of IFN-β induction (data not shown). Among the active fractions two small molecules were identified as extract constituents: *shikimic acid* and *quercetin.* These compounds were then tested in the biochemical binding assay showing that *shikimic acid* is able to inhibit EBOV VP35 binding to dsRNA with an IC_{50} value of 67.8 μM.

Consequently, we tested the *H. hircinum* extract and the 2 single constituents in the previously described EBOV VP35 based luciferase gene reporter assays. Results showed that the *H. hircinum* extract was able to revert the EBOV VP35-mediated inhibition of the IFN production, with significant efficacy at the concentration of 3 μg/ml (p value = 0,0112) (Fig. 33). Differently, when tested in the same cell culture system, *shikimic acid* did not show any appreciable effect of reversion on the IFN inhibition (data not-shown). Interestingly, however, *quercetin* was able to partially revert it at the concentration of 10 μM (p value = 0,0131) (Fig. 34). Collectively, these data suggest that *quercetin* could be the active component of the *H. hircinum* extract, even though its mode of action seems to be unrelated to the EBOV VP35 dsRNA binding inhibition.

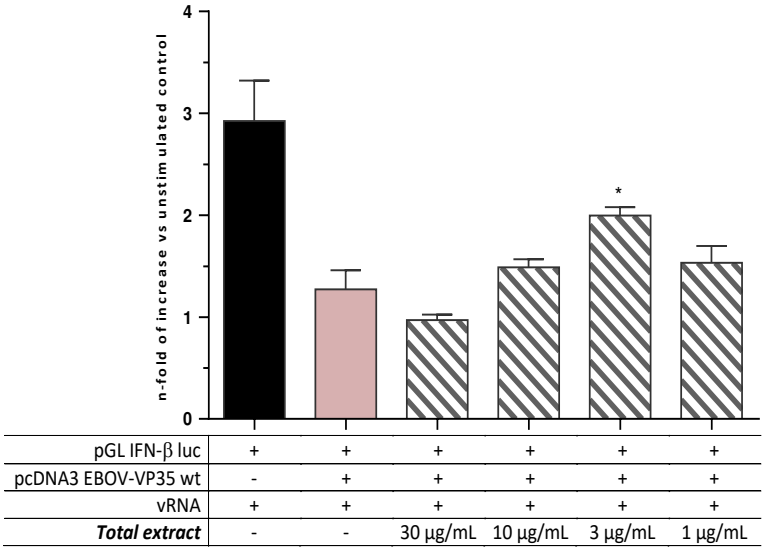

pGL IFN-β luc	+	+	+	+	+	+
pcDNA3 EBOV-VP35 wt	-	+	+	+	+	+
vRNA	+	+	+	+	+	+
Total extract	-	-	30 µg/mL	10 µg/mL	3 µg/mL	1 µg/mL

Fig. 33. *H. hircinum* effect on IFN-β induction inhibition of VP35. The histogram shows the effect of *H. hircinum* on the IFN response inhibition mediated by EBOV VP35. 24 hours post co-transfection of A549 cells with pGL IFN-β luc and pcDNA3 EBOV wt VP35 expression vectors, cells were treated with different *H. hircinum* concentrations (30, 10, 3, 1 µg/ml) and additionally transfected with IAV vRNA. The results from three independent experiments, displayed as percentage of the IFN-β promoter induction, showed a significant effect at 3 µg/ml concentration (* p value < 0.05).

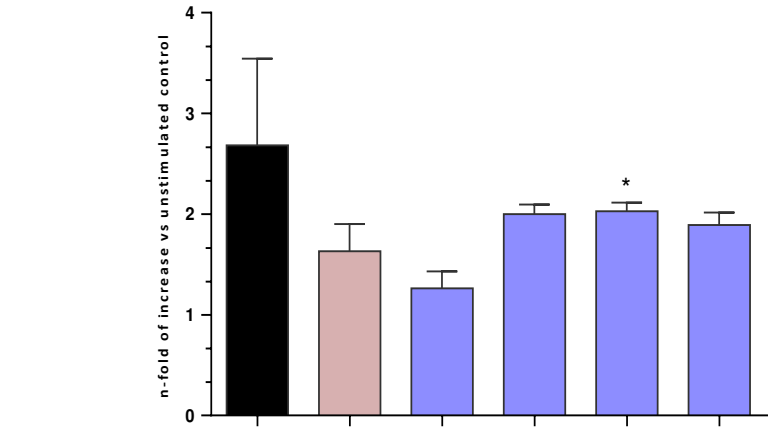

pGL IFN-β luc	+	+	+	+	+	+
pcDNA3 EBOV-VP35 wt	-	+	+	+	+	+
vRNA	+	+	+	+	+	+
Quercetin	-	-	100 µM	30 µM	10 µM	3 µM

Fig. 34. *Quercetin* effect on IFN-β induction inhibition of VP35. The histogram shows the effect of *quercetin* on the IFN response inhibition mediated by EBOV VP35. 24 hours post co-transfection of A549 cells with pGL IFN-β luc and pcDNA3 EBOV wt VP35 expression vectors, cells were treated with different *quercetin* concentrations (30, 10, 3, 1 µM) and additionally transfected with IAV vRNA. The results from three independent experiments, displayed as percentage of the IFN-β promoter induction, showed a significant effect from 10 µM concentration (* p value < 0.05).

Further, in order to verify if the extract of *H. hircinum* and the two consitutents were able to reinforce the viral dsRNA RIG-I mediated IFN production, we also tested them in the IFN-induction assay. Results showed that both the total extract and the two single compounds were not able to prime the IFN-β induction (data not-shown).

Limonium morisianum

Limonium morisianum Arrigoni is an endemic Sardinian species. Even though some beneficial properties are reported in literature, such as cardio-protective, anti-haemorrhagic and antibacterial activity, few information are available on its folk use as medicinal plants and its biology (Aniya et al. 2002; Medini et al. 2011; Murray and Rodriguez 2004).

In the binding assay the whole extract of *Limonium morisianum* showed to inhibit the VP35-dsRNA binding with a IC_{50} of 19.2 μg/ml (Table 7). Given this effect, the extract was fractioned and among the obtained fractions, the fraction 8 was the most potent (Table 7 and data not-shown) in inhibiting with the dsRNA-VP35 binding. Within this fraction two small molecules were identified: a *catechin* and *myricetin.* These compounds were then tested in the biochemical binding assay showing that both of them were able to inhibit EBOV VP35 binding to dsRNA in the low micromolar range (Table 7).

Next, we tested the *L. morisianum* extract, fraction 8 and the two small molecules in the previously described EBOV VP35 based luciferase gene reporter assays. Results showed that the total *L. morisianum* extract was able to revert EBOV VP35 IFN production inhibition at the concentration of 1 μg/ml (p value = 0,0048), with fraction 8 showed only the ability to revert the EBOV VP35 inhibition of at 1 μg/ml concentration (p value = 0,0054) (Fig. 35 and 36).

Differently, when the catechin and myricetin were tested in the EBOV VP35 based luciferase gene reporter assays, they showed no counteracting effect on the VP35 inhibition of the IFN-β induction (data not-shown). This suggests that, even though

Table 7. Inhibition of EBOV VP35 binding to dsRNA by *Limonium morisianum* Arrig.

Compound	[a]IC_{50}
Fraction 8	2.1
[b] Compound 8.2 (catechin)	13.3 ± 1.3
[b] Myricetin	4.2 ± 1.4
dsRNA 30 bp	40.5 ± 14.2[c]

[a] Extract/compound concentration (mean ± standard deviation) required to inhibit VP35 binding to dsRNA by 50%.
[b] Concentration expressed in μg/ml.
[c] Concentration expressed in μM.
[d] Concentration expressed in nM.

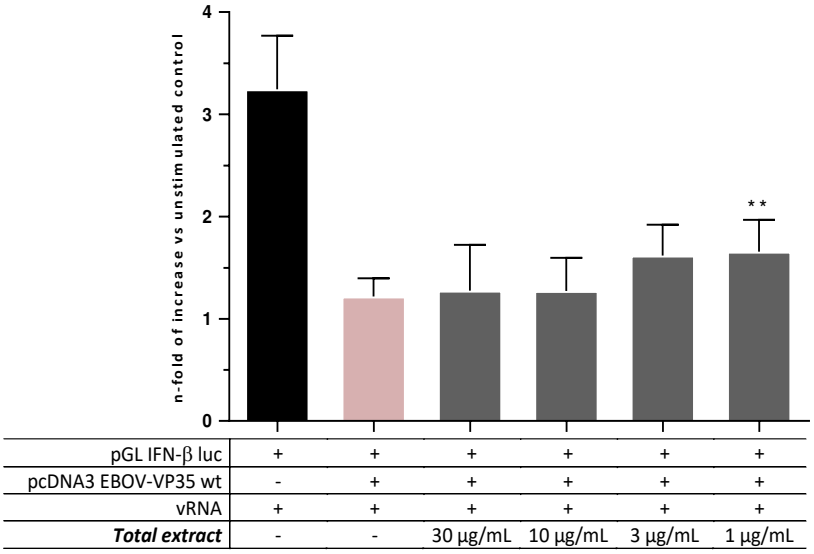

Fig. 35. ***L. morisianum*** **effect on IFN-β induction inhibition of VP35**. The histogram shows the effect of *L. morisianum* on the IFN response inhibition mediated by EBOV VP35. 24 hours post co-transfection of A549 cells with pGL IFN-β luc and pcDNA3 EBOV wt VP35 expression vectors, cells were treated with different *L. morisianum* concentrations (30, 10, 3, 1 μg/ml) and additionally transfected with IAV vRNA. The results from three independent experiments, displayed as percentage of the IFN-β promoter induction, showed a significant effect from 1 μg/ml concentration (** p value < 0.01).

myricetin showed a good ability to inhibit the VP35 binding to dsRNA, however, this interference is not sufficient to efficiently affect the VP35 interaction with the other components of the RLR pathway, leading to an efficient IFN-β induction inhibition of VP35.

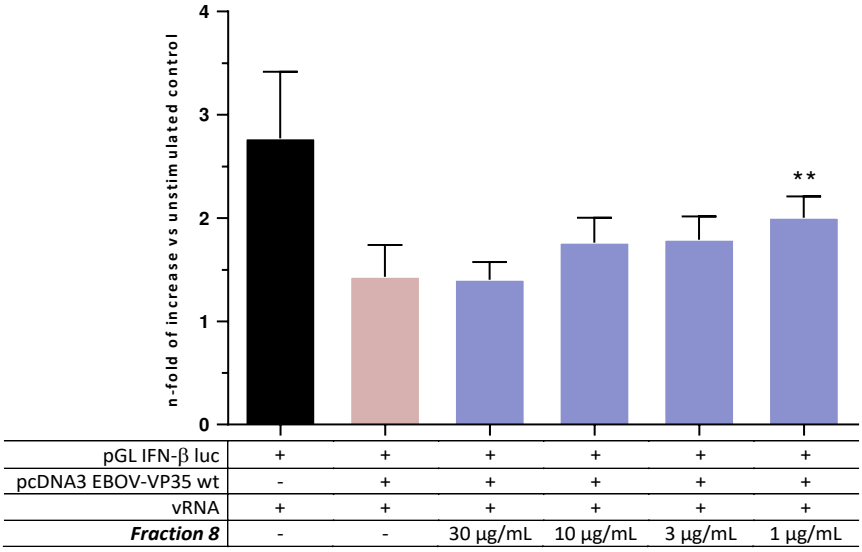

Fig. 36. *Fraction 8* (of *L. morisianum*) effect on IFN-β induction inhibition of VP35. The histogram shows the effect of *fraction 8* from *L. morisianum* on the IFN response inhibition mediated by EBOV VP35. 24 hours post co-transfection of A549 cells with pGL IFN-β luc and pcDNA3 EBOV wt VP35 expression vectors, cells were treated with different fraction concentrations (30, 10, 3, 1 µg/ml) and additionally transfected with IAV vRNA. The results from three independent experiments, displayed as percentage of the IFN-β promoter induction, showed a significant effect from 1 µg/ml concentration (** p value < 0.01).

Onopordum illyricum

Onopordum illyricum is a medicinal plant widely distributed along the Mediterranean coast of Italy, including Sardinia, used in the Mediterranean area as antipyretic for the treatment of respiratory and urinary inflammations and to treat skin ulcers (Formisano et al. 2017). Also in this case, on the basis of the resulting IC_{50} (26.9 ± 3.3) of the whole extract (Table 8), three compounds were isolated from the butanolic extract: Deoxyonopordopricrin, Onopordopicrin and 1,5-dicaffeoylquinic acid.

These 3 small molecules were tested in the *in vitro* EBOV VP35 binding assay. Of note 1,5-dicaffeoylquinic acid inhibited the EBOV VP35 binding to dsRNA with an IC_{50} value of 8.5 μM.

Next, we tested the *O. Illyricum* extract, and 1,5-dicaffeoylquinic acid in the previously described EBOV VP35 based luciferase gene reporter assays. Results showed that the total *O. Illyricum* extract was able to revert EBOV VP35 IFN production inhibition at the concentration of 1 μg/ml (p value = 0.0018). Similarly, 1,5-dicaffeoylquinic acid was able to revert the EBOV VP35 inhibition of at 1 μM concentration (p value = 0.0022) (Fig. 38). Since 1,5-dicaffeoylquinic acid was not able to induce an IFN production by itself (data not-shown), it can be considered the first small molecule of natural origin that is able to revert the EBOV VP35 inhibition of the dsRNA RIG-I mediated IFN production by impeding the EBOV VP35 binding to dsRNA, even if it is also possible that it may also inhibit the interaction between EBOV VP35 and other cellular components of the RIG-I pathway as previously described (section 1.8.4). Further studies will be needed to evaluate this possibility.

Table 8. Inhibition of EBOV VP35 binding to dsRNA by *Onopordum Illyricum* constituents.

Compound	**[a]IC_{50}**
[b] Deoxyonopordopricrin	53.7± 24.2
[b] Onopordopicrin	110.0 ± 20.0
[b] 1,5-dicaffeoylquinic acid	8.5 ± 0.6
dsRNA 30 bp	40.5 ± 14.2[c]

[a] Extract/compound concentration (mean ± standard deviation) required to inhibit VP35 binding to dsRNA by 50%.

[b] Concentration expressed in μM.

[c] Concentration expressed in nM.

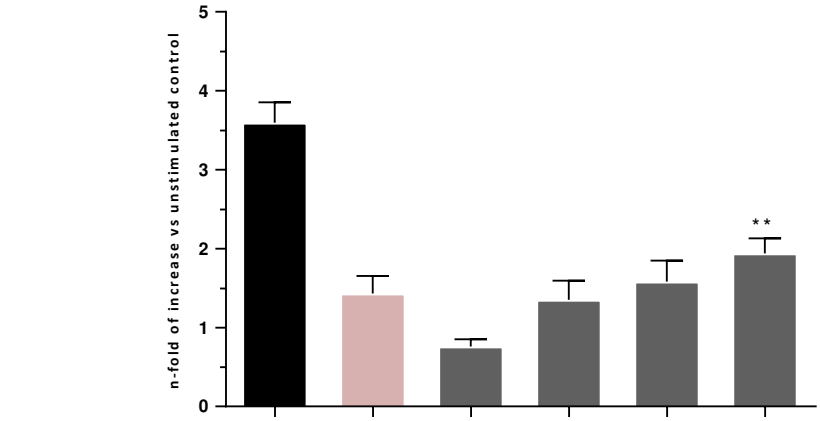

pGL IFN-β luc	+	+	+	+	+	+
pcDNA3 EBOV-VP35 wt	-	+	+	+	+	+
vRNA	+	+	+	+	+	+
Total extract	-	-	30 µg/mL	10 µg/mL	3 µg/mL	1 µg/mL

Fig. 37. *O. Illyricum* effect on IFN-β induction inhibition of VP35. The histogram shows the effect of *O. Illyricum* on the IFN response inhibition mediated by EBOV VP35. 24 hours post co-transfection of A549 cells with pGL IFN-β luc and pcDNA3 EBOV wt VP35 expression vectors, cells were treated with different *O. Illyricum* concentrations (30, 10, 3, 1 µg/ml) and additionally transfected with IAV vRNA. The results from three independent experiments, displayed as percentage of the IFN-β promoter induction, showed a significant effect from 1 µg/ml concentration (** p value < 0.01).

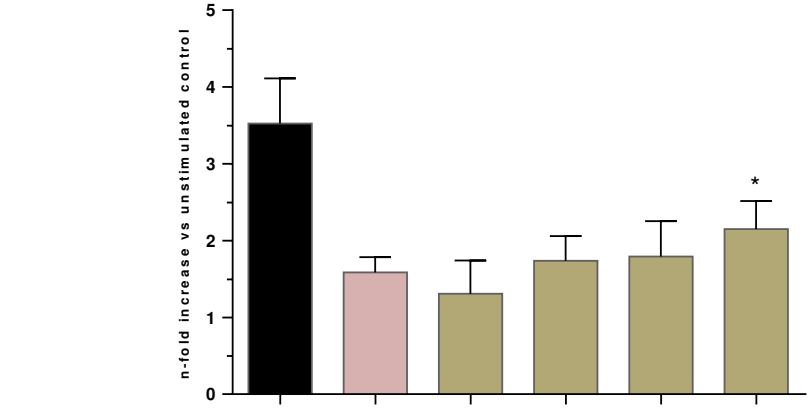

pGL IFN-β luc	+	+	+	+	+	+
pcDNA3 EBOV-VP35 wt	-	+	+	+	+	+
vRNA	+	+	+	+	+	+
1,5-dicaffeoylquinic acid	-	-	30 µM	10 µM	3 µM	1 µM

Fig. 38. *1,5-dicaffeoylquinic acid* effect on IFN-β induction inhibition of VP35. The histogram shows the effect of *1,5-dicaffeoylquicinic acid* on the IFN response inhibition mediated by EBOV VP35. 24 hours post co-transfection of A549 cells with pGL IFN-β luc and pcDNA3 EBOV wt VP35 expression vectors, cells were treated with different *1,5-dicaffeoylquicinic acid* concentrations (30, 10, 3, 1 µM) and additionally transfected with IAV vRNA. The results from three independent experiments, displayed as percentage of the IFN-β promoter induction, showed a significant effect from 10 µM concentration (* p value < 0.05).

4.3 DISCUSSION

The massive diversity of products of plant metabolism represent a great source of molecules that could be studied in search of new drugs. To discover a small molecule capable to reinforce the innate immune system when under viral attack represents is an interesting approach against the inhibitory strategies operated by EBOV through its VP35 protein. At the same time, and with a different approach, also the research of molecules able to directly interfere with EBOV VP35, and in particular with its binding to the dsRNA, can represent an alternative way to achieve the same result, that of subversion of the inhibition of the immune response by the virus.

For achieving this aim and, in addition, with the purpose to prove the robustness of the novel *in vitro* fluorescent binding assay just developed in our laboratory, we tested in our experimental systems the effects of four selected Sardinian plants and some of their constituents. Due to its geographical position in the Mediterranean basin, the island of Sardinia develops and offers a great plant biodiversity; despite the fact that the antiviral activity of these plants we assayed (Table 5) have been previously poorly studied, a number of prior studies reported the biological activity of many compounds isolated from these plants.

For the purpose of the present thesis, four whole extracts and relative fractions with lowest IC_{50} values in the dsRNA-VP35 binding assay were further investigated for evaluating their ability to counteract the VP35-mediated inhibition of the dsRNA RIG-I-mediated IFN-β induction.

Out of the four extracts assayed, the whole extract of *H. scruglii* and the isolated compound *quercitrin*, that displayed to have some effect in the *in vitro* biochemical assay with IC_{50} values of 20.3 and 72.3 μg/ml (the latter corresponding to 161.3 μM) respectively, when tested in the luciferase reporter gene assay showed to be unable to revert the inhibition of IFN production at any tested concentration (data not-shown).

Instead, the total extract of *H. hircinum* and one among the six compounds isolated from the same extract (namely *quercetin*), the total extract and the fraction 8 of *L.*

morisianum, the total extract from *O. Illyricum* and the isolated compound *1,5-dicaffeoylquinic acid*, showed positive results when tested in the luciferase reporter gene assay.

We found that the compound *quercetin* (of *H. hircinum*), a plant polyphenol from the flavonoid group found in many fruits, vegetables, leaves, and grains, showed the ability to inhibit the VP35 inhibition in our cellular assay (Fig. 34). Contrarily, in the biochemical studies it showed no effect on dsRNA-VP35 binding (Table 6). Together, this data suggest that *quercetin* could be the active component of the *H. hircinum* extract and that it may act through a mechanism of action different from the inhibition of the dsRNA sequestration by VP35. Thus, additional studies will be needed to characterize if the extract fractions of *H. hircinum*, beside of *quercetin*, possess a biological activity on the downstream components of the RIG-I pathway.

The whole extract of *L. morisianum* showed to inhibit the VP35-dsRNA binding with a IC_{50} of 19.2 μg/ml (Table 7). Given this effect, the extract was fractioned and the fraction 8 showed to be the most potent constituent in inhibiting with the dsRNA-VP35 binding (Table 7). Within this fraction the two small molecules *catechin* and *myricetin* were able to inhibit EBOV VP35 binding to dsRNA in a low micromolar range and, for this reason, we tested them together with the *L. morisianum* extract and fraction 8 in the EBOV VP35 based luciferase gene reporter assay. We found that only the whole extract and the fraction 8 showed the ability to revert the EBOV VP35 inhibition (Fig. 35 and 36). Instead, the catechin and myricetin showed no in counteracting the EBOV VP35. This result suggests that the two isolated compounds, cathechin and myricetin, although a good ability to inhibit the dsRNA-VP35 binding are not able to interfere sufficiently with VP35 and counteract with efficacy the VP35 blockade of IFN-β induction.

Indeed, the discrepancy we found between the efficacy of the selected extracts and relative compounds to inhibit the rVP35 binding to dsRNA in the biochemical assays with the one of to reverse the VP35 inhibition of the IFN production, was denied in one

case. In fact, one compound was found able to interfere with both processes, the *1,5-dicaffeoylquinic acid*. Also known as *cynarin*, this compound is the active chemical constituent of artichoke (*Cynara cardunculus*) and it is known for its antiviral, antibacterial, and antihistaminic effects, as well as antioxidant, antiradical, and anticholinergic activities (Topal et al. 2016; Xia et al. 2014). In our assays, it was the only capable to inhibit the VP35 functions (Table 8 and Fig 38). This may suggest that *1,5-dicaffeoylquinic acid* could be the active component of the *O. Illyricum* extract and, therefore, its interaction with VP35 and possible other cellular RLR cascade components needs to be further investigated for a better understanding its mechanism of action.

Together, this VP35 overcoming activity of the extracts and compound tested, along with the fact that some act only under the induction of an antiviral response, makes these extracts very attractive for further studies directed to the identification of the molecules having a central role in this phenomenon. In fact, by identifying a compound responsible for such effect, it would be crucial for the development of an antiviral drug. Moreover, further studies will need to be performed to determine the specific target of these extracts that is likely located in one or more components belonging to RIG-I-mediated IFN signaling pathway, and if its VP35 inhibition is sufficient to induce an innate immune response that could be effective in EVD.

5. SYNTHETIC COMPOUNDS CAPABLE TO SUBVERT THE INHIBITION OF THE IMMUNE RESPONSE MEDIATED BY EBOV VP35

5.1 Introduction

Virtual screening approaches for identifying therapeutic drugs

The large 2014/2016 Ebola virus outbreak in West Africa pointed out the urgent need to develop new preventive and therapeutic approaches effective against EBOV that can be rapidly utilized. New drugs for the treatment of EVD should be safe, efficacious, easy to manufacture and inexpensive in order to be successfully deployed in African countries. In contrast to the significant progress recently achieved in development of an effective Ebola virus vaccine (Henao-Restrepo et al. 2017), therapeutic options are still limited (Olszanecki and Gawlik 2014). In fact, despite recent headlines and scientific articles declaring the success of experimental Ebola vaccine and drugs, the world still is not prepared for future Ebola epidemics and is not in position to prevent another deadly outbreak due to limited therapeutic and /or prophylactic options.

The main obstacle in drug development is represented by the identification of an appropriate therapeutic target, and is largely hampered by the time and money-consuming development of new drugs, especially for neglected diseases (Glisic et al. 2015). Thus, the process for drug discovery and development is challenging and time consuming, therefore bringing a pharmaceutical drug to the market is a long-term process that costs billions of dollars. According to a study conducted in 2014 by the Tufts Center for the Study of Drug Development, an increased cost nearly 150% in the last decade was estimated, up to a staggering amount of $2.6 billion dollars. Additionally, the probability of a failure in the drug discovery and development pipeline is high (approximately 75% of the cost is due to failures that happen along the drug discovery and design pipeline) and 90% of the drugs entering clinical trials fail to get FDA approval and reach the consumer market (Leelananda and Lindert 2016).

Nowadays, the faster high-throughput screening (HTS) experiments can assay thousands of molecules with robotic automation. However, HTS is still expensive and

requires a lot of resources of targets and ligands, not available in academic settings. Consequently, HTS is often replaced by computer-aided drug discovery (CADD) tools can act as a "virtual shortcut", assisting in the expedition of this long process and potentially reducing the cost of research and development. Virtual HTS (vHTS) screening is commonly used due to its low-cost and fast prediction rates of the target for small molecules (Jones 2015). With virtual vHTS, where screening is done using computer-generated models, the "docking" of chemical compounds from virtual molecular libraries against a target can be mimicked. Therefore, such CADD has become today an effective and indispensable tool in therapeutic development (Leelananda and Lindert 2016).

CADD technologies are powerful tools that can reduce the number of ligands that need to be screened in experimental assays, identify lead drug molecules for testing, predict effectiveness and possible side effects, and assist in improving bioavailability of possible drug molecules. CADD methods can be broadly classified into two groups, namely structure-based (SB) and ligand-based (LB) drug discovery (DD), and depend on the availability of target structure information.

In order to use SBDD tools, information about target structures needs to be known (information usually obtained experimentally by X-ray crystallography or nuclear magnetic resonance). Knowing the structure makes it possible to use structure-based tools such as virtual screening (VS) and direct docking methods on targets and possible drug molecules. The affinity of molecules to targets can be evaluated by computing various estimates of binding free energies.

VS approaches comprise resource-saving techniques, which are used to identify bioactive hit compounds from large databases by means of computational technologies, either by ligand-based or structure-based approaches to determine novel chemical scaffolds. Therefore, VS can be done either by ligand-based approaches such as chemical similarity, pharmacophore modelling, and Quantitative structure–activity

relationship (QSAR) or structure-based approaches like protein-ligand docking (Jones 2015).

Virtual screening of a drug library in search of small molecules counteracting VP35

If the aim of the first part of the present study was to search molecules able to stimulate the immune response through strengthening and improving the production of IFN-β here, instead, we looked for small and more specific molecules able to directly interact with the EBOV VP35 protein, that stands as a key viral determinant for EBOV biology and a validated drug target (Leung, Prins, et al. 2010).

As mentioned, EBOV VP35 IID forms an asymmetric dimer with dsRNA-end, held together by a network of hydrogen bonds. One VP35 monomer binds the sugar-phosphate backbone of both dsRNA strands through a central basic patch (in a process called "backbone-binding") whereas a second one binds to dsRNA terminal bases and the proximal phosphate backbone capping the ends of dsRNA *via* a hydrophobic pocket (in a process called "end-capping-binding"). Through this peculiar molecular action, the backbone- and the end-capping binding VP35 monomers specifically mimic the RLRs shape, efficiently hiding their 5'-ppp dsRNA ends so preventing to highlight the recognition of this key site (Bale et al. 2013; Cardenas et al. 2006; Kimberlin et al. 2010; Leung, Borek, et al. 2010; Leung, Ginder, Nix, et al. 2009; Luo et al. 2011; Priya Luthra et al. 2013; Zinzula and Tramontano 2013).

The discovery of the structural characteristics of this area, revealed the importance of the contribution of several amino acids for the dsRNA binding function, also showing a differential role between the two VP35 RBD/IIDs. Furthermore, the specificity of 5'-ppp recognition led us to focus on targeting the small surface of VP35 end-capping site that has potentially more implications for small molecule inhibitors design. In fact, side chains of amino acid residues R312 and R322 (EBOV numbering) undertake interactions with dsRNA in the end-capping RBD/IID and, similarly, the amino acid residues F239, Q274, I278, K339 and I340 bind to dsRNA terminal bases in the end-

capping region (Kimberlin et al. 2010; Leung, Borek, et al. 2010). In addition, other amino acid residues such as R305, K309, R312, K319, R322, F239 and K339 have been shown to hold importance for the VP35 RBD/IID. In fact, mutations in this specific aminoacids correspond to a diminished or abolished suppression of IFN-β induction (Cardenas et al. 2006; Hartman, Bird, et al. 2008; Hartman, Ling, et al. 2008; Leung, Borek, et al. 2010; K. C. Prins et al. 2010; Zinzula et al. 2012). Furthermore, as showed by Bale et al. in 2013, the dsRNA binding by the end-capping RBD/IID monomer is the earliest binding event, to which attachment of backbone-binding RBD/IID monomers all along the dsRNA helix follows.

Therefore, this small area interacting with dsRNA terminal bases in the concave surface of the end-capping RBD/IID monomer represents a suitable target for small molecule inhibitors design. Moreover, it is worth noting that specific amino acid residues laying in this area, such as R312, K319, R322, F239 and K339 were found to be critical for RBD/IID dsRNA binding and IFN inhibition, as their mutation into alanine resulted in decrease, or even total loss, of their function (Fig. 39).

Few are the published studies that identified compounds against EBOV and some have highlighted the potential for the repurposing of FDA-approved drugs on different Ebola strains (Johansen et al. 2013, 2015; Madrid et al. 2013; McMullan et al. 2016; Mirza and Ikram 2016; Picazo and Giordanetto 2015); even though these studies were promising, they were not exhaustive screens of all FDA drugs and it was unclear whether these drugs had biological activities when used in combination with therapies to overcome drug resistance, as the virus is a highly variable species. For these reasons, we carried out a VS aimed to find out drug candidates able to interact and interfere with the end-capping RBD/IID VP35 domain and the formation of the complex with dsRNA, and screened the FDA approved drugs Database (Pihan et al. 2012).

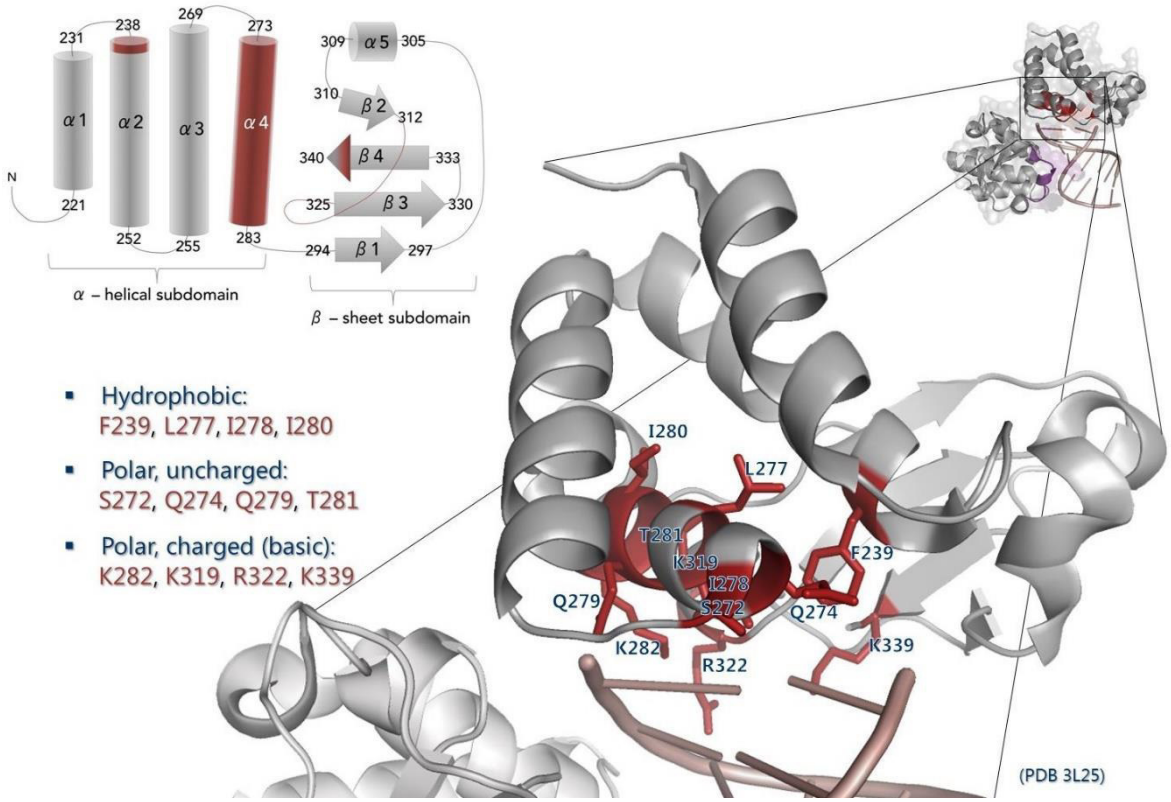

Fig. 39. Important residues in end-capping interface. VP35 residues involved in dsRNA end-capping interaction which can be subjected to structure-based alanine scanning.

Drug repositioning is an attractive approach for drug screening and discovery, with success stories available in literature. In fact, the finding that many drugs interact with more than one target provided the rationale behind the selective optimization of side activities (SOSA) approach recently developed (Ashburn and Thor 2004; Langer and Wermuth 2012; Wermuth 2006). As mentioned, since previous studies highlighted that end-capping RBD/IID monomer constitutes the earliest binding event, to which attachment of backbone-binding RBD/IID monomer follows (Bale et al. 2013; Kimberlin et al. 2010), we applied a pharmacophore filter by means of LigandScout computer software with the aim to find molecules that bind the end-capping region to avoid the dsRNA binding (Wolber and Langer 2005).

Pharmacophore modelling is a powerful VS tool to generate and use ligand chemical information in 3D to search for novel active compounds. With the purpose to find

molecules binding the end-capping region, a structure-based pharmacophore considering the terminal portion of dsRNA as "core molecule" was generated. More in particular, the lowest energetic frame of molecular dynamic (MD) simulation of the wt 5'-pppVP35-dsRNA complex was selected as starting structure (Fig. 40).

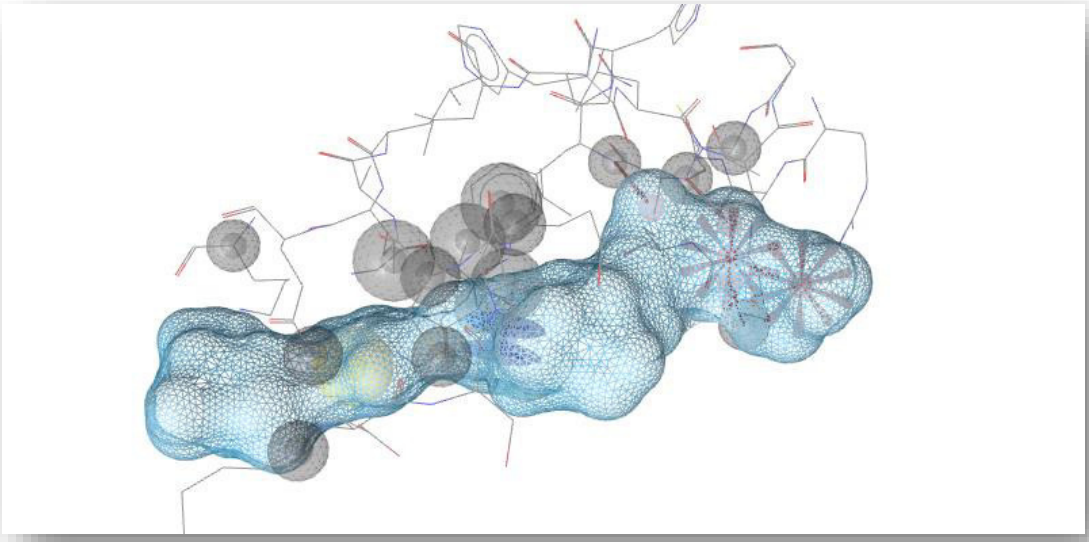

Fig. 40. Pharmacophore generated by LigandScout. The image exemplifies a model of pharmacophore generated with LigandScout software.

The pharmacophore was applied to screen the FDA Database containing all the approved drugs available in the market. Selected compounds were then minimized and docked considering three different protocols: GlideXP, QMPLD and Autodock (Chung, Hah, and Cho 2009; Friesner et al. 2006; Morris et al. 1998, 2009). Best pose of each compound was then subjected to a post-docking procedure considering eMBrAcE (Guvench et al. 2002). eMBrAcE applies multiple minimizations, during which each of the specified pre-positioned ligand is minimized with the receptor. By calculating a consensus score (CS) we ranked the compounds with the best CS, then clusterized for diversity and analysed by visual inspection, finally selecting 9 hits (Fig. 41).

The selected compounds were then purchased and tested both in biochemical and cellular assays for evaluating their ability to inhibit EBOV VP35 or the intracellular cascade in which VP35 is involved. Among them, 4 compounds were selected for further studies on EBOV replication.

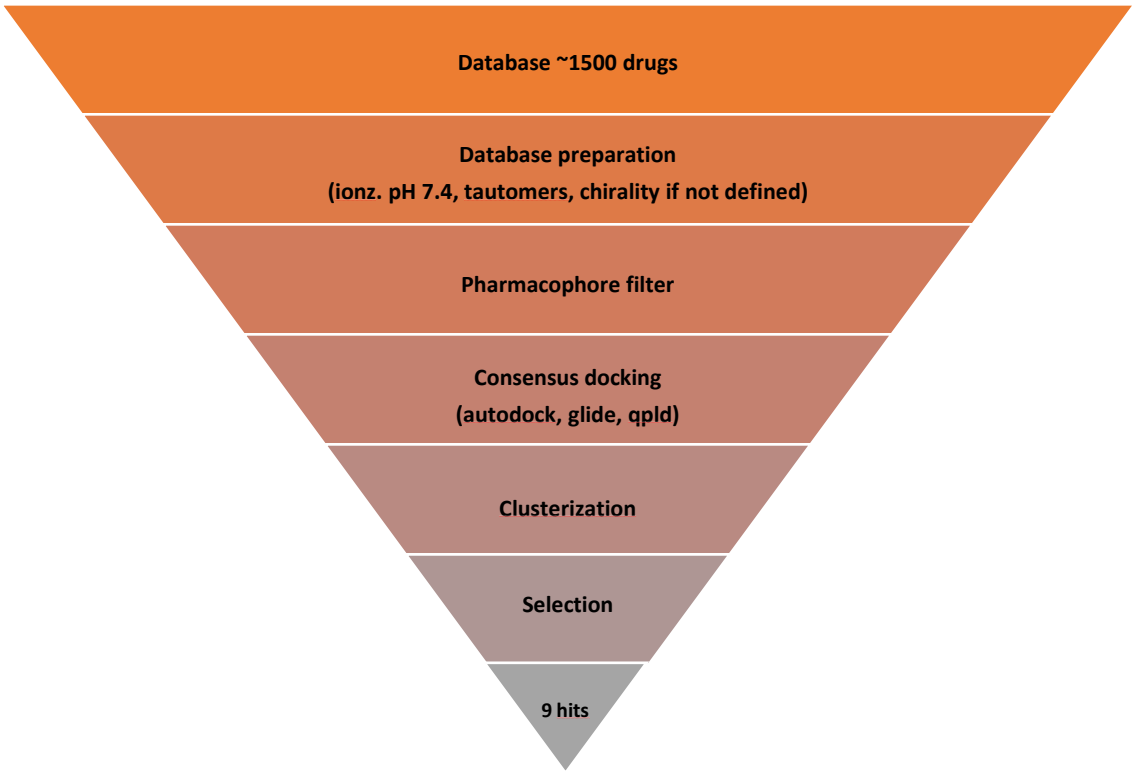

Fig. 41. Virtual screening procedure workflow. The FDA Database, containing all the approved drugs available in the market, was screened in search for molecules potentially inhibiting the dsRNA-EBOV VP35 RBD/IID interaction. More than 1500 drugs were screened and results filtered *via* 3 different docking protocols to ensure. Compounds with the best consensus scoring were then clusterized for diversity and analysed by visual inspection. Nine compounds were purchased and further analysed trough *in vitro* binging- and cellular assays.

5.2 Results

As mentioned, different strategies can be exploited to overrun EBOV VP35 inhibitory functions of the IFN signalling cascade. A first strategy, put in place in the first part of the present thesis, is to identify molecules that could potentiate or activate the IFN signalling pathway, increasing IFN production in response to viral infections to a level able to subvert VP35 inhibition, even not by physically interacting with it. Instead, an alternative approach is to develop molecules that directly bind to VP35 inhibiting its functions.

Bearing in mind these strategies, the nine compounds identified from the VS procedure were tested both in the novel *in vitro* dsRNA-VP35 binding assay and in a luciferase reporter gene assay (Cannas et al. 2015), for investigating their capability to potentiate the IFN-β production as well as their capability to ameliorate the dsRNA-dependent RIG-I-mediated IFN-β induction inhibition in the presence of EBOV VP35.

5.2.1 *Effect of VS compounds in the in vitro binding assay*

Once again, in parallel to the cellular assays performed on the selected synthetic molecules, we have exploited the recently developed *in vitro* fluorescence-based binding assay to measure the ability of these molecules to interfere with the VP35 binding to the dsRNA.

Thus, with the aim to find a novel antiviral molecule able to directly regulate the interaction between EBOV VP35 and the dsRNA genetic elements *via* interference with the binding, we tested the nine VS compounds.

Out of the nine compounds assayed, only the compound A displayed to have some effect in the *in vitro* biochemical assay with IC_{50} value of 28.3 μM (±0.9). Instead, the other compounds tested IC_{50} values close to or higher than 100 μM, as in the case of compound C (99.8 μM) and of compounds D, F, G and H. The compound B was the sole to show an IC_{50} higher than 200 μM, whereas the compounds E and I showed IC_{50} values higher than 300 μM (Table 9).

Table 9. Inhibition of EBOV VP35 binding to dsRNA by screened VS-selected compounds. The table shows the dsRNA-VP35 binding inhibition values resulting from a screening process of VS compounds.

Compound	[a] IC50 (μM)
A	28.3 ± 0.9
B	220.8
C	98.4
D	> 100 (57,7 %) [b]
E	> 300 (69.2 %) [b]
F	> 100 (79.5 %) [b]
G	> 100 (76.2 %) [b]
H	> 100 (62.0 %) [b]
I	> 300 (84.6 %) [b]
dsRNA 500 bp	36.9 ± 2.1 [c]

[a] Compound concentration (mean ± standard deviation) required to inhibit VP35 binding to dsRNA by 50%.
[b] Percentage of VP35 control binding to dsRNA in the presence of 100 μM extract concentration.
[c] Concentration expressed in nM.

5.2.2 *Effect of VS compounds on IFN-β induction*

Compounds were first dissolved in 100% DMSO at 100 mM stock concentration and firstly assayed for the ability to improve the dsRNA-dependent RIG-I-mediated IFN-β induction, using a range of concentrations from 100 to 0.3 μM. Data showed that only compounds F and I induced a significant increase of the IFN-β induction. In particular, compound F showed a significant increase of IFN signals at 3 and 1 μM concentrations from 4.7 to 5.3 folds ($p = 0.0384$ and $p = 0.0062$ respectively), and compound I showed a significant increased induction at 10 and 3 μM concentrations from 5.1 to 6.8 and 8.0 folds respectively ($p = 0.0073$ and $p = 0.0123$, respectively), as compared to the unstimulated control, while others compounds did not show any significant increase in the dsRNA-dependent RIG-I-mediated IFN-β induction (Fig. 42 and 43, Table 10).

Further, in order to verify if all the compounds were able to induce by itself the IFN signalling cascade even in the absence of a vRNA stimulus, they were also tested, in the same system and in the same experiment, in the absence of the IAV RNA stimulation. Results showed that compounds alone did not induce the IFN response (Fig. 42 and 43). The fact that the selected compounds were not able to induce IFN response by itself is very important; in fact, the identification of possible antiviral drugs that enhance the IFN response only during infection, avoiding the harmful effects of uncontrolled IFN stimulation, is a priority in the perspective of drug development. Therefore, we next investigated the action of the compounds in conditions of viral inhibition, particularly in their ability to subvert the EBOV VP35 inhibition of the RIG-I signalling cascade.

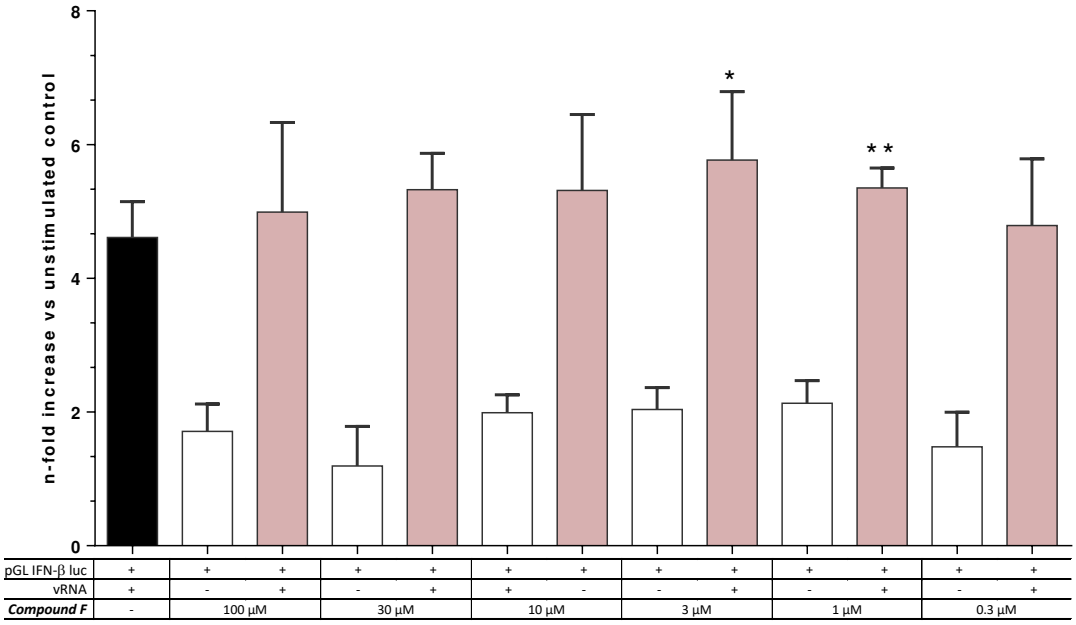

Fig. 42. Compound F effect on the dsRNA RIG-I-mediated IFN-β induction. The compound F was tested in a RIG-I-mediated IFN-β induction system both in presence and in absence of the vRNA stimulation, with various compound F concentrations (100, 30, 10, 3, 1, 0.3 μM). The histogram illustrates the results of three independent experiments shown in n-fold compared to unstimulated control (* p value < 0.05, ** p value < 0.01).

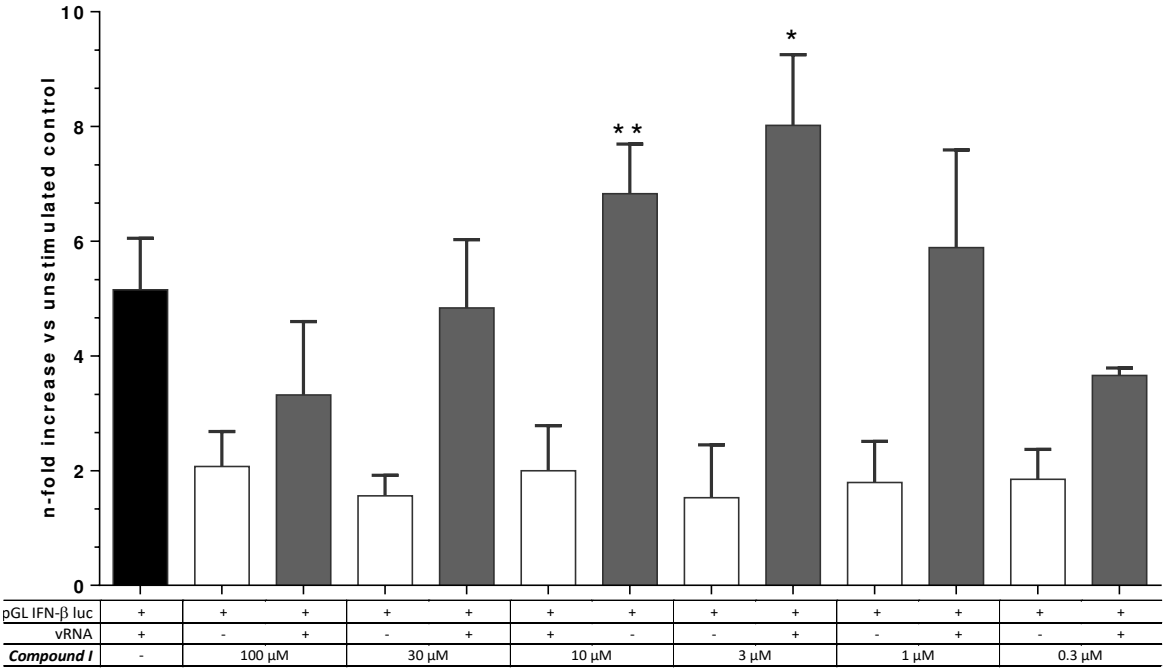

Fig. 43. Compound I effect on the dsRNA RIG-I-mediated IFN-β induction. The compound I was tested in a RIG-I-mediated IFN-β induction system both in presence and in absence of the vRNA stimulation, with various compound I concentrations (100, 30, 10, 3, 1, 0.3 μM). The histogram illustrates the results of three independent experiments shown in n-fold compared to unstimulated control (* p value < 0.05, ** p value < 0.01).

5.2.3 Effects of VS compounds on the IFN-β induction inhibition of EBOV VP35

To assess whether the IFN-β response induction of the VS-selected compounds was capable to counteract the EBOV VP35 inhibitory functions, the compounds were tested on IAV RNA-stimulated A549 cells in presence of the viral protein expression.

When added to cells in presence EBOV 35 inhibition, of the nine compounds only compounds A, B, F and I determined a significant increase of IFN signals. In fact, compound A at 30 and 10 μM concentrations induced a fold increase from 1.96 to 3.6 and 2.8 respectively ($p = 0.0042$ and $p = 0.0235$, respectively) (Fig. 44) and compound B showed a significant increased luciferase signals at 30 and 10 μM concentrations from 1.93 to 3.2 and 4.9 folds respectively ($p = 0.0022$ and $p = 0.0002$, respectively) (Fig. 45), when compared to the VP35 control. Further, also compound F showed to be effective

in subverting the inhibitory effect of VP35 of the IFN production at the concentration of 3 μM, with a fold induction ranging from 1.5 to 1.97 (p value = 0.023) (Fig. 46), as well as compound I which showed to be effective at the concentration of 1 μM increasing from 1.8 to 2.6 (p value = 0.0264) with respect to their VP35 stimulated control (Fig. 47). Conversely, the remaining five VS compounds did not show any significant reversion of the dsRNA-dependent RIG-I-mediated IFN-β induction inhibition.

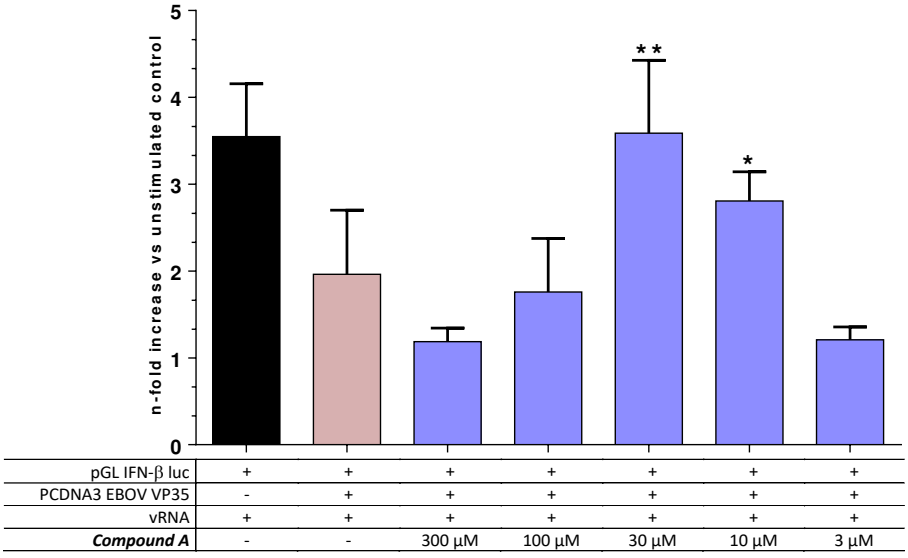

Fig. 44. Compound A effect on IFN-β induction inhibition of VP35. 24 hours post co-transfection of A549 cells with pGL IFN-β luc and pcDNA3 EBOV wt VP35 expression vectors, cells were treated with different compound A concentrations (300, 100, 30, 10, 3 μM) and additionally transfected with IAV vRNA. The results from three independent experiments, displayed in n-folds compared to the unstimulated control, showed a significant effect at 30 and 10 μM concentrations (* p value < 0.05, ** p value < 0.01).

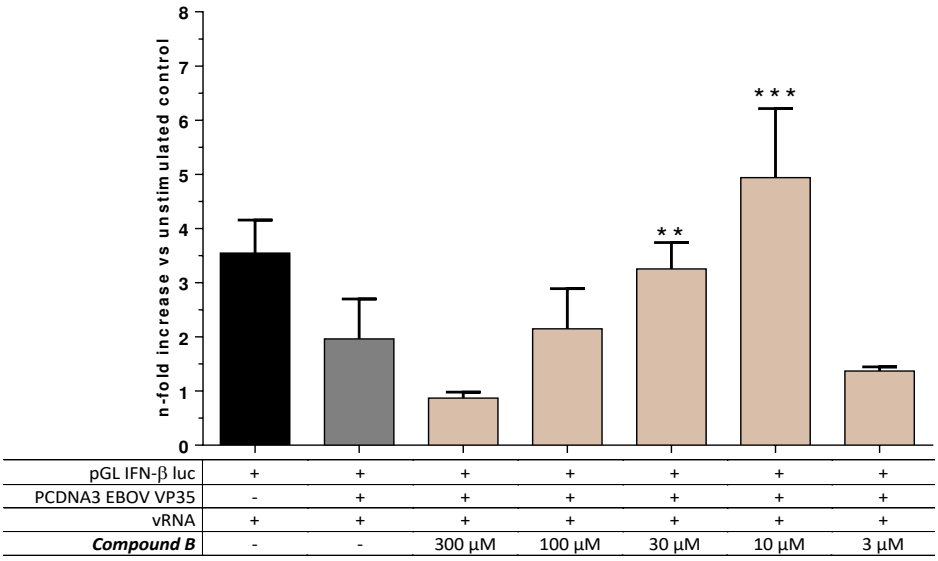

Fig. 45. Compound B effect on IFN-β induction inhibition of VP35. 24 hours post co-transfection of A549 cells with pGL IFN-β luc and pcDNA3 EBOV wt VP35 expression vectors, cells were treated with different compound B concentrations (300, 100, 30, 10, 3 µM) and additionally transfected with IAV vRNA. The results from three independent experiments, displayed in n-folds compared to the unstimulated control, showed a significant effect at 30 and 10 µM concentrations (** p value < 0.01, *** p value < 0.001).

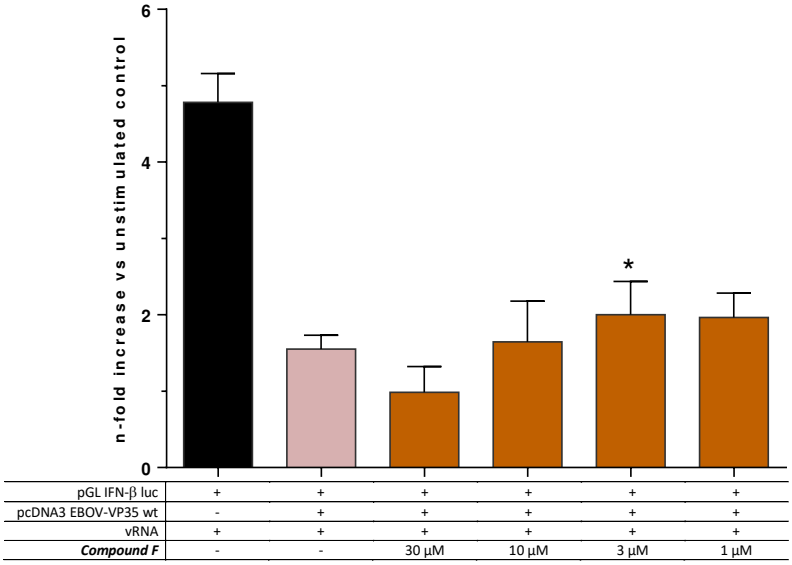

Fig. 46. Compound F effect on IFN-β induction inhibition of VP35. 24 hours post co-transfection of A549 cells with pGL IFN-β luc and pcDNA3 EBOV wt VP35 expression vectors, cells were treated with different compound F concentrations (30, 10, 3, 1 µM) and additionally transfected with IAV vRNA. The results from three independent experiments, displayed in n-folds compared to the unstimulated control, showed a significant effect at 3 µM concentration (* p value < 0.05).

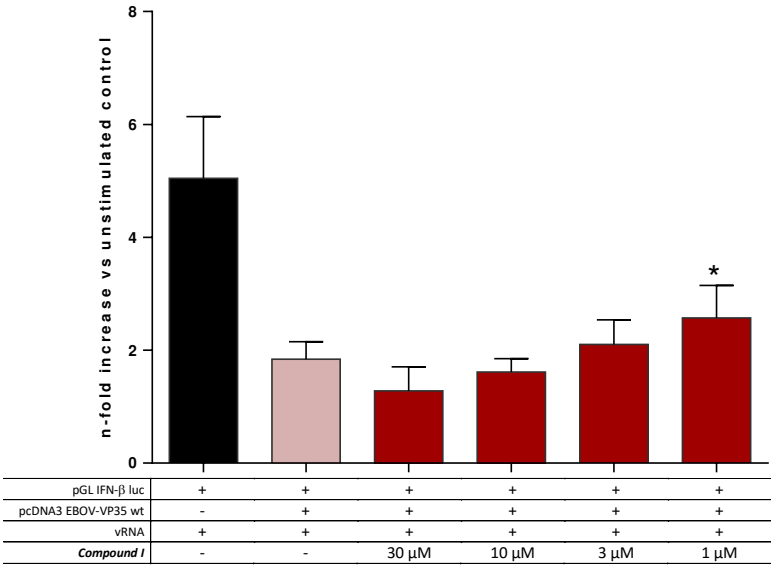

Fig. 47. Compound I effect on IFN-β induction inhibition of VP35. 24 hours post co-transfection of A549 cells with pGL IFN-β luc and pcDNA3 EBOV wt VP35 expression vectors, cells were treated with different compound I concentrations (30, 10, 3, 1 µM) and additionally transfected with IAV vRNA. The results from three independent experiments, displayed in n-folds compared to the unstimulated control, showed a significant effect at 1 µM concentration (* p value < 0.05).

Collectively, among the nine compounds, four molecules (namely compound A, compound B and compound F and compound I) showed the ability to positively interfere with EBOV VP35 inhibition of the dsRNA stimulated RIG-I signalling pathway.

5.2.4 *Effects of VS compounds on EBOV replication*

Since EBOV VP35 is a multifunctional protein involved not just in immune response suppression but also in viral replication, we next investigated if the selected compounds could have any detrimental effect over this fundamental step of EBOV biology. To this aim, thanks to the precious collaboration of the laboratory of microbiology leaded by Prof. Ali Mirazimi at the Karolinska Institutet (Sweden), the *in vitro* analysis of EBOV replication in presence of the four selected compounds was performed in BSL4 settings.

In order to evaluate the potential antiviral effect of the identified compounds against Ebola virus, as viral prototype, we selected an Ebola virus isolated (strain Makona) from a clinical sample derived from the latest Ebola virus outbreak in West Africa. After assessing, by MTT assay, that no significant cytotoxicity was observed in A549 cells (data not-shown), a panel of different concentrations of compounds was combined with viral suspensions and inoculated on target cells (at MOI = 0.005-0.05), as described in materials and methods section. Twenty-four hours post-inoculation infected cells were identified by staining with an anti-Ebola virus glycoprotein (GP).

Among the selected compounds, the compounds A, B and F were capable to influence EBOV replication. More in particular, the compound A was effective in potently inhibiting the viral replication of 75.44% at 100 μM concentration (Fig. 48 and table 10). Importantly, was the compound B to exhibit the most powerful effect on EBOV replication at lower concentrations. In fact, it was able to reduce the viral replication already at 10 μM concentration (71.93%), reaching a peak of inhibition at 30 μM concentration (87.72%) (Fig. 49). Diversely, the compound F was able to influence the EBOV replication only at the concentration of 1 μM of 35.44% (Fig 50).

By contrast to the other VS compounds tested in the luciferase assays that showed to be effective in subverting the EBOV VP35 inhibition of the IFN-β induction, compound I was uncapable to counteract the viral replication.

As clearly shown in Fig. 48 and 49, the compounds A and B reduced the number of infected cells in a dose dependent manner, while compound F did not show a clear antiviral effect (Fig. 50). In particular, the stronger antiviral effect was observed in the case of compound B treatment, with an IC_{50} of 5 μM.

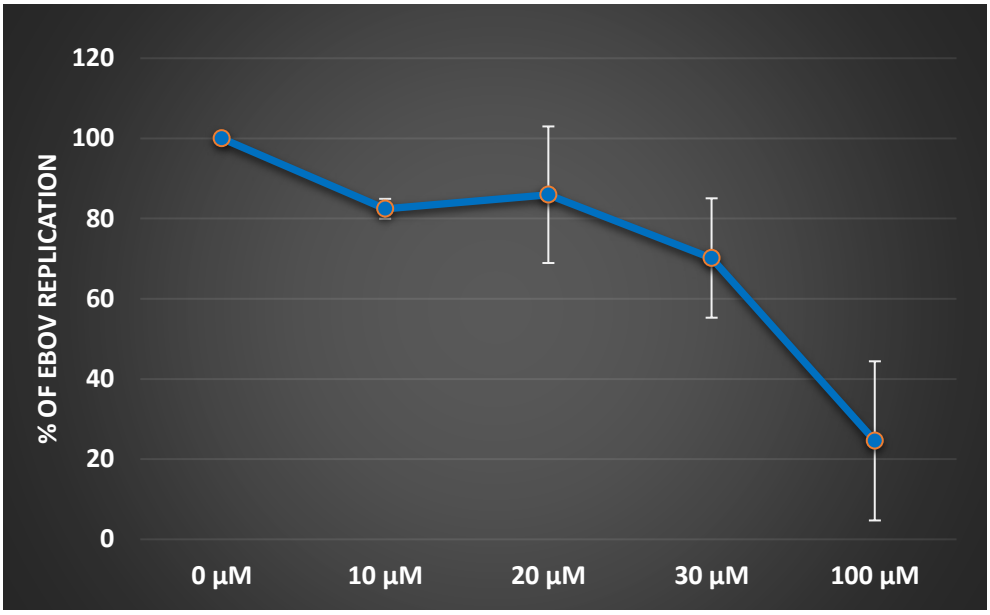

Fig. 48. Compound A evaluation of anti-Ebola virus infection. A549 cells were infected with roughly 0.005-0.05 FFU/cell of virus in the presence of the appropriate compound concentration and analyzed after 24 h. Data (mean ± SD,) are percentages of Ebola virus infected cells with respect to untreated cells, set as 100%.

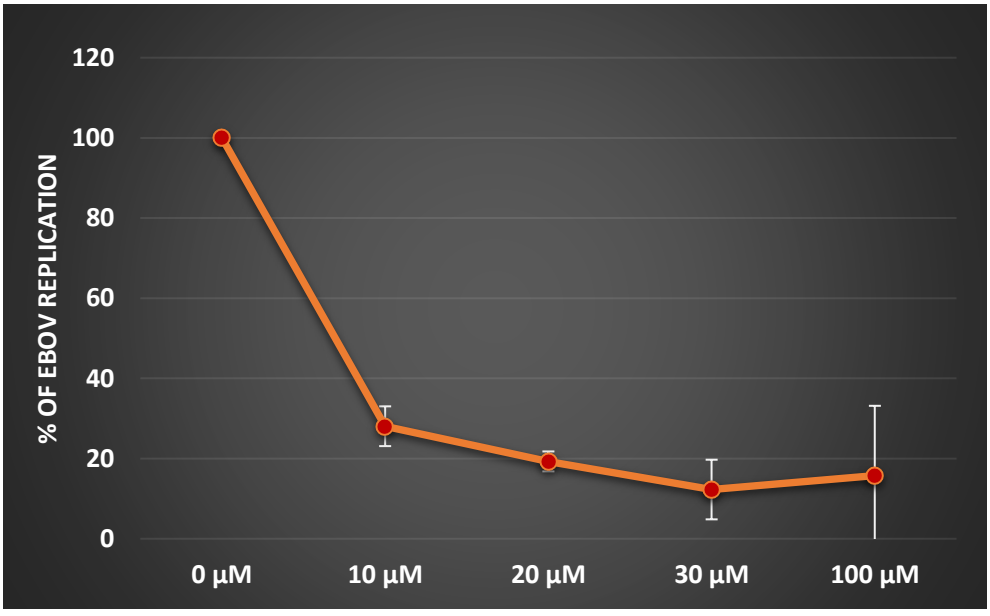

Fig. 49. Compound B evaluation of anti-Ebola virus infection. A549 cells were infected with roughly 0.005-0.05 FFU/cell of virus in the presence of the appropriate compound concentration and analyzed after 24 h. Data (mean ± SD,) are percentages of Ebola virus infected cells with respect to untreated cells, set as 100%.

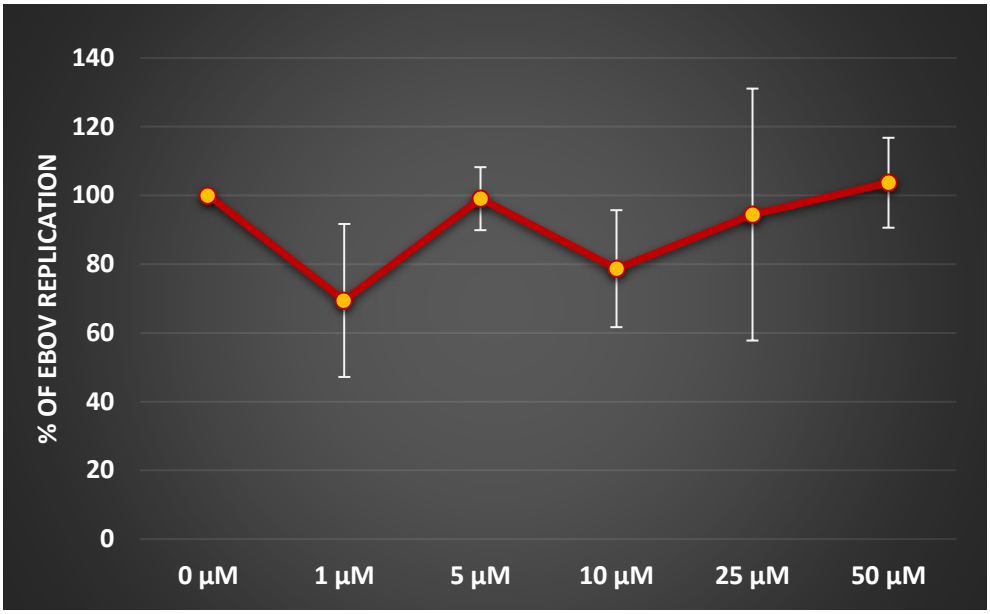

Fig. 50. Compound F evaluation of anti-Ebola virus infection. A549 cells were infected with roughly 0.005-0.05 FFU/cell of virus in the presence of the appropriate compound concentration and analyzed after 24 h. Data (mean ± SD,) are percentages of Ebola virus infected cells with respect to untreated cells, set as 100%.

Further, it is important to note that these results on EBOV replication assays are in accordance with drug concentrations that demonstrated to be significantly effective in the previous cellular inhibition assay, in which compounds A, B and F showed to be capable in subverting the EBOV VP35 inhibitory activity on the IFN production at 30, 30-10 and 3 µM respectively. Overall, these data suggest that the compounds we selected through the VS procedure are indeed able to inhibit EBOV replication and, by interfering with the inhibitory activity of VP35, play a key role in regulating this fundamental process for the viral life cycle.

Table 10. The effect of VS-selected compounds. The table illustrates the results directed to investigate the effects of the nine VS-selected compounds both on dsRNA-dependent RIG-I-mediated IFN-β production and its inhibition mediated by EBOV VP35. Furthermore, the table shows the effect of the selected compounds when tested on viral replication (in a BSL4 setting) and with the *in vitro* dsRNA-VP35 binding assay. Each data shows the results of three independent experiments.

Compound	[a] Effect on IFN-β induction	[b] Effect on VP35 inhibition	[c] Effect on viral replication	[d] IC_{50} (μM)
A	-	+	++	28.3 ± 0.9
B	-	+	+++	> 100
C	-	-	-	98.4
D	-	-	-	> 100 (57.7 %) [e]
E	-	-	-	> 300 (69.2 %) [e]
F	+	+	+	> 100 (79.5 %) [e]
G	-	-	-	> 100 (76.2 %) [e]
H	-	-	-	> 300 (62.0 %) [e]
I	+	+	-	> 100 (84.6 %) [e]
IFN-α			+++	
dsRNA 500 bp				36.9 ± 2.1 [f]

[a] Ability of the compound to increase the dsRNA-dependent RIG-I-mediated IFN-β induction; + or – indicate the ability of the compound to improve the IFN production in response to vRNA stimulation.

[b] Ability of the compound to subvert the dsRNA-dependent RIG-I-mediated IFN-β induction inhibition; + or – indicate the ability of the compound to improve the IFN production in response to EBOV VP35 inhibition.

[c] Compound effect on EBOV replication; + or – indicate the ability to inhibit viral replication: (-) less than 40% inhibition, (+) 40-60% inhibition, (++) 60-80% inhibition, (+++) more than 80% inhibition.

[d] Compound concentration (mean ± standard deviation) required to inhibit VP35 binding to dsRNA by 50%.

[e] Percentage of control binding of VP35 to dsRNA in the presence of 100 μM compound concentration.

[f] Concentration expressed in nM.

5.3 DISCUSSION

To discover a small molecule able to counteract the inhibitory strategies operated by EBOV through its VP35 protein on the innate antiviral response, reinforcing the host IFN response when under viral attack, represents a powerful approach directed against the virus. Further, since the EBOV VP35 ability of high efficient IFN production

inhibition the resides, among the others, in a powerful upstream prevention of dsRNA RIG-I recognition, we focused on the RBD/IID end-capping region of VP35, selecting small molecules able to interact with this specific area within the protein. For this purpose, we explored in our experimental systems the effects of nine synthetical compounds, outcoming from a VS selection process of the FDA approved drugs Database, as potential antiviral drugs directed to EBOV VP35.

In the system that evaluates the IFN induction increase, only two compounds among the nine (namely compounds F and I) showed the ability to potentiate the IFN-β induction. When compounds F and I were tested on VP35 inhibition, together with compounds A and B, showed to be able to overcome the effects of the viral protein on the RIG-I cascade. Only compounds A and B, among the nine selected compounds, showed a very significant effect in increasing IFN-β vRNA induced production in response to VP35 inhibition. Remarkably, they did not stimulate the innate antiviral response when tested in the absence of a vRNA stimulus (data not-shown), indicating that these compounds specifically function in a context of viral inhibition. This VP35 overwhelming activity, along with the fact that these four compounds act only under antiviral response induction, make these molecules very attractive for the further development of an antiviral drug.

Moreover, we tested their effects on viral replication. Out of the four, two compounds (compound A and B) confirmed the previous results obtained with the cellular inhibition assay, demonstrating to be strongly effective in inhibiting the replication at high percentages more than 70% and at low micromolar concentrations (at 100 μM and 10, 30 μM respectively). By contrast, compound I was unable to influence the viral replication. Further, even if it showed to slightly influence the viral replication at the concentration of 1 μM, compound F did not exhibit a clear antiviral effect, an aspect that needs to be further investigated.

Accordingly, these results on EBOV replication reflect with fidelity the range of concentrations that demonstrated to be significantly effective in the previous cellular

inhibition assay, in which compounds A, F and I showed to be effective in subverting the EBOV VP35 inhibitory activity on the IFN production. Therefore, this result suggests that the contrasting activity of the VS compounds towards EBOV VP35 could have a key role in blocking the replication process, also considering the pivotal role of the protein within this fundamental process for the viral life cycle.

Due to the novelty of this target and the importance of the results obtained we cannot show the structures and commercial names of the VS-selected compounds. In fact, up to now, these chemicals are the only ones acting with this mechanism and showing to inhibit VP35 at low concentrations. Indeed, further studies will need to be performed to: i. determine the specific target of the compounds that, presumably, is situated in one or more components belonging to RIG-I-mediated IFN signalling pathway, ii. understand if they directly interact with the VP35 protein thus interfering with its inhibitory activity, and if this interference is sufficient to induce an innate immune response that could be effective treatment for EVD, iii. define if the inhibition of the EBOV VP35 activity is sufficient to generate an abruption of the viral replication and if not, determine if other known intracellular pathways that regulate IFN responses could be involved in this inhibition of the viral replication.

6 EXPLOITING THE POTENTIAL OF MONOCLONAL ANTIBODIES DIRECTED TO EBOV VP35

6.1 Introduction

The use of antibodies to counteract EBOV

Among the different strategies that can be exploited to counteract the strong immune inhibitory activity of EBOV, an approach is represented by the development of an antibody-based therapy, possibly also linked to gene therapy approaches. Compared to vaccines, that require longer time to induce protection, antibody-based therapies can potentially offer protection immediately after EBOV exposure (Pettitt et al. 2013). However, it must be noted that their major drawbacks are a lack of availability and a significantly declining efficacy when given later in the course of experimental infection (Trad et al. 2017).

As previously mentioned, human survivors to EVD tend to mount an early, vigorous, and long standing neutralizing antibodies (NAbs) response (Shedlock et al. 2010). Moreover, since a single antibody may not be able to neutralize every single viral particle, a cocktail of antibodies is typically required. For this reason, NAbs have been exploited in monoclonal antibody (mAb) combinations and blood products. This is the case of ZMAb, MB-003, and in particular ZMapp, all of them antibody cocktails produced *in vitro* from convalescent blood that demonstrated, at least in animal models, a therapeutic potential for treating EVD (Audet et al. 2014; Davidson et al. 2015; Rivera and Messaoudi 2016).

It is worth to note that these NAbs preparations are in the form of mixtures of mAbs directed to bind the EBOV structural envelop glycoprotein GP, a common target of such therapeutic antibodies. Diversely, in the present study, with the aim to explore the possibility to counteract the functionality of the EBOV multifunctional protein VP35, that is a core protein in Ebola virus biology, specific mAbs directed to such protein were developed.

Development of single-chain variable fragment mAbs directed to EBOV VP35

Monoclonal antibodies can be designed that have customized affinity and specificity. Because antibodies can be designed in various forms, *in vivo* pharmacokinetic characteristics can be tailored to suit specific clinical applications.

A single-chain variable fragment (ScFv), asymmetrical and heterodimeric antibodies typically created to facilitate phage display, is a fusion protein made of the variable regions of the heavy (VH) and light chains (VL) of immunoglobulins (Fig. 51). Connected with a short linker peptide of 10 to about 25 amino acids, usually rich in glycine for flexibility, as well as serine or threonine for solubility and specificity, can either connect the N-terminus of the VH with the C-terminus of the VL, or vice versa. Usefully, this protein retains the specificity of the original immunoglobulin, despite removal of the constant regions and the introduction of the linker.

More in particular, the choice of the variable domain of an antibody, also referred to as the Fv region, resides in the fact that it is the most important region for binding to antigens. In fact, variable loops of β-strands, both on the VL and VH chains are responsible for binding to the antigen. These loops are referred to as the complementarity determining regions (CDRs).

In the present study, a series of antibody specifically directed to bind EBOV VP35, were isolated from an antibody phage display library in scFv format (Flego and Di Bonito data not published) created at the Istituto Superiore di Sanità.

6.2 RESULTS

As a first step, an antibody phage display strategy aimed to isolate specific human single chain fragment variable (scFv) directed towards the pathogenic EBOV VP35 was performed. To this aim, an antibody phage library, that consists of a large array (more than 10^8 antibody combinations) of scFv polypeptides displayed on the surface of M13 phage was used.

To successfully recover and isolate antigen-specific antibody phages, an aliquot of the antibody library containing 10^{12} cfu phage was used for the panning procedure. After 3 phage enrichment cycles (Table. 11), in which eluted phages were used to infect log phase TG1 *E. coli* bacteria and then concentrated by precipitation for the following rounds of selection, individual colonies were grown in 96 flat bottomed wells and induced with 50 μl 2 × YTA medium and 6 mM IPTG. Subsequently, recovered supernatants containing soluble-scFv derived from IPTG inducted colonies were tested for specificity through ELISA assay, and several of them proved to be specific for VP35 protein (Fig. 53). Finally, scFv antibodies were assayed for reactivity and DNA sequences of their encoding genes.

Table 11. Selection of synthetic in-house antibody phage library on EBOV VP35 recombinant protein. The table shows the phage enrichment during the selections. Phage input (I) and output (O) was determined by titration, determining phage colony forming units (cfu) of infected *E. coli* TG1 cells before and after each round of selection. Enrichment was calculated by ratio of outputs from each cycle and output from the first cycle.

[Ag]	*Panning cycle*	Input	Output	Ratio (O/I)	Enrichment
15 μg/ml	1	$5x10^{12}$	$2,7x10^{4}$	$6.2x10^{-9}$	1
15 μg/ml	2	$1x10^{12}$	$6,8x10^{6}$	$6,8x10^{6}$	$2.5x10^{2}$
15 μg/ml	3	$1x10^{12}$	$1.2x10^{7}$	$1.2x10^{7}$	$4.4x10^{2}$

The different scFvs were PCR amplified with opportune oligonucleotides and cloned in pTarget vector (Promega) for the expression in eukaryotic systems. Next, we proceeded testing the different scFv mAbs in pTarget, kindly provided by Dr. Paola Di Bonito and Michela Flego from the Istituto Superiore di Sanità (ISS) - Department of Infectious Diseases and Global Health Center, Rome (Italy).

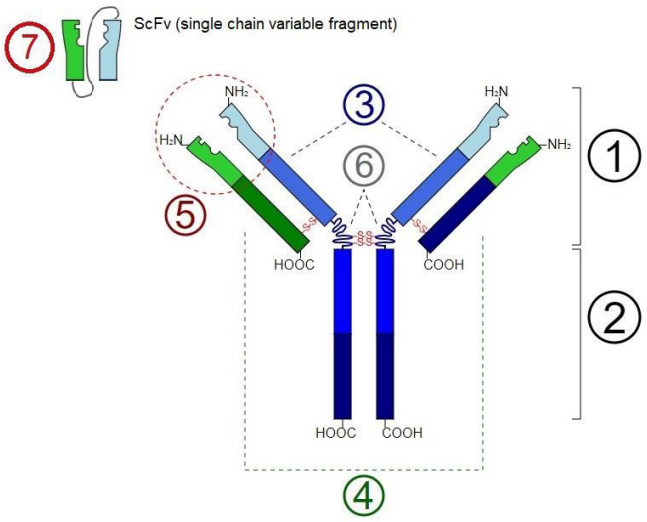

Fig. 51. Typical structure of an antibody. Schematic diagram of the basic unit of an immunoglobulin (antibody). Numbers indicate as follows: 1. Fragment, antigen-binding (Fab) region, 2. Fragment, crystallizable (Fc) region, 3. Heavy chain (blue) with one variable heavy (VH) domain (light blue) followed by a constant domain (CH1), a hinge region, and two more constant (CH2 and CH3) domains, 4. Light chain (green) with one variable light (VL) region (light green) and one constant (CL) domain, 5. Antigen binding site (paratope) 6. Hinge regions. 7. Region scFv (single chain variable fragment) with VH and VL regions connected through a linker peptide (grey).

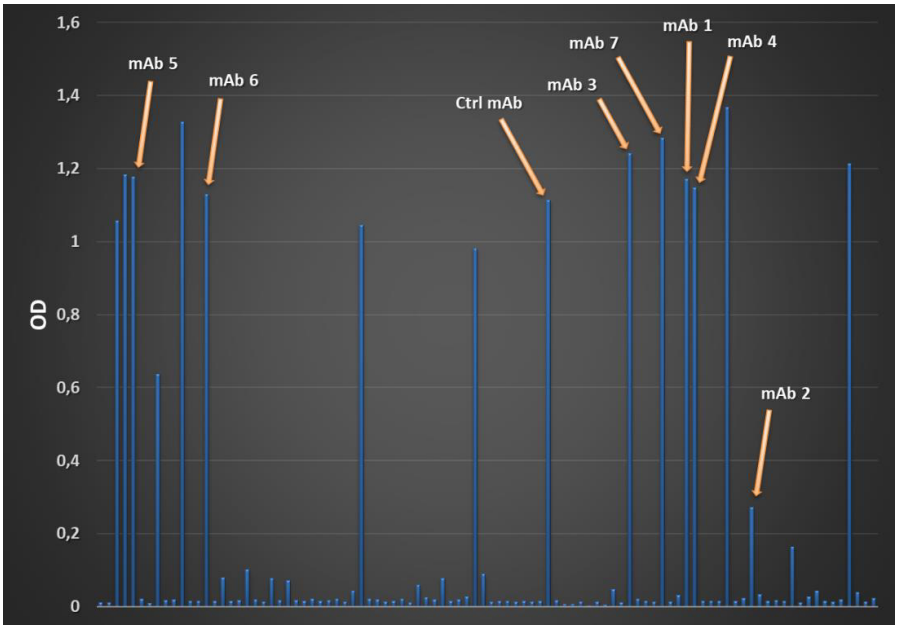

Fig. 53. Recombinant EBOV VP35 specific scFvs antibodies determined by ELISA. IPTG inducted bacterial supernatants of individual colonies from the third round of the in-house phage library selection on recombinant EBOV VP35 protein were tested in 96-well microtiter plates coated with the VP35 antigen. The cut-off value separating positive from negative samples was calculated as 3 standard deviation above the mean of the value obtained from irrelevant scFv anti Glucose Oxidase (0,079 OD).

In order to assay the provided scFv mAbs in their efficacy to counteract the dsRNA RIG-I-mediated IFN-β induction inhibition of EBOV VP35, we wanted first to ensure the stability of the experimental controls. To this aim, we first verified that the expression of the null scFv mAb (namely *Ctrl mAb*) had no influence in the IFN-β induction, both in absence and in presence of VP35 expression. To this aim, A549 cells were co-transfected with the expression plasmids pGL IFN-β luc and *Ctrl mAb*, both in presence and in absence of the expression vector pcDNA3-EBOV-VP35 (Fig. 54, blue bars).

Further, to exclude any interference in the co-transfection procedure, we also co-transfected the cells with the expression vector pGL IFN-β luc and a pcDNA3 empty vector, confirming no influence on transfection efficiency of the IFN-β controls (Fig. 54, black and grey bars). The result showed that the *Ctrl mAb* had no influence in IFN-β induction, in both cases of the presence or absence of VP35 expression, resulting in an expected IFN-β fold-induced signal.

Particularly, the emitted signal in the case of the contemporaneous expression of the vector pGL IFN-β luc and *Ctrl mAb* was comparable to the IFN-β controls (Fig. 54, grey, black and dark blue bars). Importantly, in the case of the simultaneous presence of EBOV VP35 and *Ctrl mAb*, the measured IFN-β signal was comparable to one of the VP35 control (Fig. 54, pink and light blue).

Next, we tested all the provided scFv mAbs in the dsRNA RIG-I-mediated luciferase reporter gene inhibition assay. Out of five scFv mAbs tested, one antibody showed a significant ability to subvert the inhibition of the IFN-β production generated by VP35, namely the scFv mAb 2, (p value = 0.0003). Contrarily, scFv mAbs 1, 3, 4, and 5 showed no ability to counteract the IFN-β induction inhibition mediated by EBOV VP35 in the cellular assay (Fig. 55).

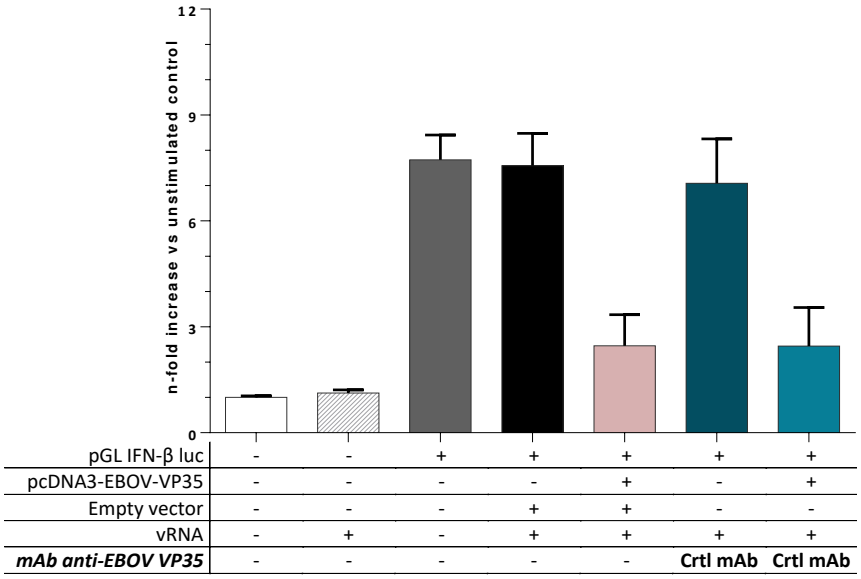

Fig. 54. Controls stability test in the luciferase assay. The histogram shows the effect of transfection procedures on the IFN-β induction. 24 hours post-transfection with pGL IFN-β luc, or co-transfection with empty vector or pcDNA3 EBOV wtVP35 expression vectors, cells were transfected with Ctrl mAb. The next day, cells were additionally transfected with IAV vRNA. The results from four independent experiments (triplicated samples) are shown in n-fold compared to unstimulated control (gray-lined bar).

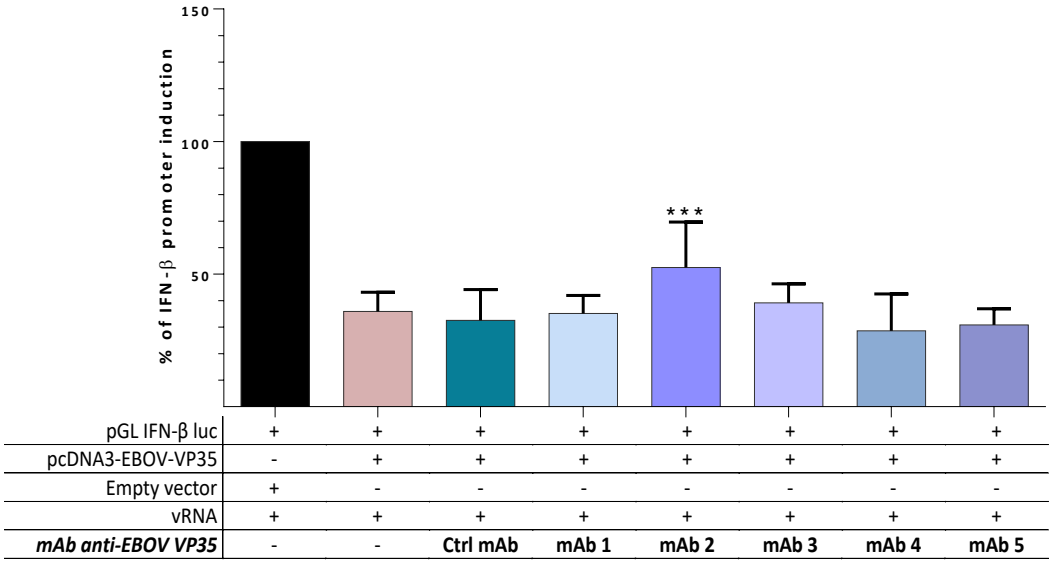

Fig. 55. ScFv monoclonal antibodies effect on IFN-β induction inhibition of VP35. 24 hours post co-transfection with pGL IFN-β luc and pcDNA3 EBOV wtVP35 expression vectors, cells were treated with different mAbs and additionally transfected with IAV vRNA. The results from three independent experiments, displayed as percentage of the IFN-β promoter induction, showed a significant effect for mAb 2 (*** p value < 0.001).

6.3 DISCUSSION

The strong impulse to find effective counter-measures against EVD caused by the most recent 2014-2016 epidemic, has led the academic and, in a broader vision, the international scientific community, to develop a series of defense strategies to counteract the virus.

To do this, various are possibilities that can be conducted to finally achieve this purpose, such as developing vaccine-, drug- and antibody-based therapies, all object, among other things, of the present thesis. Typically, the development of specific antibodies against EVD has been directed to the viral glycoprotein GP. Here we wanted to develop antibodies, in the form of scFv monoclonal antibodies, directed against another viral target which is one of the most important proteins of the Ebola virus biology, the VP35 protein.

Subsequent to a phage panning from an antibody phage library, a typical and powerful method for both studying the immune response as well as to rapidly select and evolve human antibodies for therapy, a study on the effects of series of scFv mAbs on the dsRNA RIG-I-mediated IFN-β induction inhibition of EBOV VP35 was conducted.

Here we showed that, out of five selected scFv antibodies tested, one was significantly active against the IFN-β induction inhibition of the RIG-I signaling cascade mediated by EBOV VP35. Therefore, this result suggests that the contrasting activity of the mAb towards EBOV VP35 could play a key role in blocking the immune response inhibition mediated by EBOV. Indeed, further studies need to be performed to: i. understand if the direct interaction mAb-VP35 protein is sufficient to interfere with the inhibitory activity of EBOV on the immune response; ii. define if the inhibition of VP35 activity is also capable to generate also an abruption of the viral replication; iii. verify if through gene therapy approaches it possible to envision the possibility of DCs expressing mAb against VP35 facilitating the elimination of the virus from EVD survivors.

7. CONCLUSIONS

The devastating EVD West African epidemic occurred among the years 2014-2016 stands as a landmark in EBOV history. The impressive numbers of this outbreak, more than 28000 cases and 10000 deaths, represented a strong push for scientific community to deepen the knowledge about the virus and its interaction with the host organism, in the fast, more complete and deepened way possible. For obvious reason, the study of such a pathogenic virus, especially during the first outbreaks, was limited by the remoteness of the areas involved and by the limitations of analytical and laboratory settings. However, the tools and analytical techniques available today led to a strong acceleration in the study of the virus and its biology, giving way to better understand its functional aspects, to know its schemes of attack and those of defence, to reveal the structure and function of viral proteins in the best possible way. Thanks to all these information, research strongly focused in searching effective anti-viral countermeasures, thus developing vaccines, new drugs and antibody-based therapies, aimed to better contrast the disease.

Without a doubt, the development of vaccines would seem to bear fruits, thanks to the recent development of the rVSV-ZEBOV (Henao-Restrepo et al. 2017). However, this type of approach can not be the only current possible solution for EVD threat, even considering the limitation of the long time needed to induce protection with a vaccine-based therapy. In this context, the development of effective antiviral drugs or antibody therapies represents alternative approaches of great importance. Antibody-based therapies can solve this problem, because they potentially offer protection immediately after EBOV exposure; however, their lack of availability and a declining efficacy when given later in the course of experimental infection limit their use (Pettitt et al. 2013, Trad et al. 2017). Further, an effective therapeutic have to be available in large quantities and could not only treat individual cases, but halt outbreaks.

Therefore, since to date supportive care remains the mainstay of treatment and no EBOV-specific therapy has been proven efficacious, nor has any therapy achieved

regulatory approval for use in humans, this thesis work focused on the development of interfering strategies to counteract the viral protein VP35, that stands as a key and validated viral drug target. In fact, The EBOV VP35 protein plays a central role in the inhibition of the host initial innate immune responses to EBOV infection, leading to the development of EVD. The interactions of VP35 with the RLR cascade components inhibit the IFNs production, preventing to generate a proper immune response.

For achieving this aim, we applied different approaches. A first approach was the search of molecules, both of synthetic and natural origin, capable to prime the IFN production and reinforce the innate immune system when under viral attack. By applying this strategy, we screened 76 plant extracts from the Italian, Sardinian, African, Indian and Chinese traditional medicines. Among the plants and relative compounds tested, we found some capable to boost the IFN-β induction and, importantly, active only in presence of a viral stimulation, with the latter being a property that represents a key aspect in drug development. In particular, the extracts from *Scutellaria baicalensis* (one of the 50 fundamental herbs in TCM), *Embelia ribes* (a well-known plant of the ATM) and its main constituent *Embelin*, together with an *Asphodelus microcarpus* leaves extracts, showed the ability to improve the IFN production in a dose-response manner. Significantly, when the same were tested in the inhibition assay, *S. baicalensis*, *Embelin* and *A. microcarpus* demonstrated to be strongly capable in counteracting the dsRNA IFN-β induction inhibition mediated by EBOV VP35.

The extract of *S. baicalensis* showed to be capable to modulate both the IFN-β production and the inhibition mediated by EBOV VP35. However, when we assayed its four main constituents (namely *baicalin*, *baicalein*, *wogonin*, *wogonoside*) they were not sufficiently potent to induce the same effect of the whole extract. This suggest that other constituents of the *S. baicalensis* extract could be involved in this effect, or that more than one of them need to be present to induce an antiviral effect, an aspect that will be further investigated.

Although further studies are needed to deeply characterize its molecular action, we found that *Embelin* significantly reverted the inhibitory effect of VP35 in the cellular inhibition assay. This result suggests that *embelin* could be a core molecule from which to start for further drug development of new and effective antiviral molecules for the treatment of EVD.

Likewise, we found that *A. microcarpus* leaves extract was capable to modulate the IFN-β production as well as the inhibition mediated by EBOV VP35. Even if the window of AE efficacy in subverting the VP35 inhibition of the IFN production was not completely overlapping with the dose-response IFN production, an aspect that will be further investigated in the next future, this potential antiviral activity, combined with the antimicrobial properties showed by the AE, makes this plant extract very attractive for the development of an antiviral drug.

Further, in order to identify small molecules able to inhibit EBOV VP35 blockade of the innate immune system activation, we utilized a novel *in vitro* fluorescent biochemical assay, with which it is possible to measure the binding dsRNA-VP35 and the relative inhibition when in presence of a molecule capable to interfere with this process, to screen the ability of plant extracts and derived compounds to inhibit the rVP35 binding to dsRNA. The selected active plant extracts and derived compounds were also tested in a cellular luciferase reporter gene assay to evaluate their ability to counteract the inhibitory activity of VP35 on the IFN response.

Interestingly, we identified the flavonol *myricetin* from the plant *L. morisianum* was able to inhibit rVP35 binding to dsRNA in biochemical assay but it was ineffective in the luciferase reporter gene assay. Conversely, we identified another flavonol compound, *quercetin*, from the plant *H. hircinum*, that was unable to inhibit rVP35 binding to dsRNA in biochemical assay, while it subverted VP35 inhibition of IFN production. Interestingly, we identified the compound *cynarin*, from the plant *O. illyricum*, that was active in both biochemical and cellular assays. This concordant result may suggest that *cynarin* has the ability to interact with the VP35 pocket, thus affecting VP35 interaction

with its cellular targets. Therefore, it would be interesting to verify if *cynarin* owns any ability to inhibit EBOV replication, with the perspective to develop *cynarin* derivatives having more potent anti-VP35 activity.

Collectively, these data provide a further proof on the importance of plants as a source of antiviral molecules. Plants are a natural and inexhaustible source of metabolites and molecules that we can look for to develop new and effective countermeasures against highly pathogenic viruses, such as Ebola.

One of the most popular strategies for EBOV therapeutics is to develop antivirals that directly target critical stages in the viral life cycle, such as binding and/or entry of the virus into host cells, viral replication, packaging, regulation of the immune system, or release of viral progeny from target cells. Bearing this in mind, we performed a VS procedure of an FDA approved drugs database with the aim to find small molecules capable di interact with a specific pocket within the EBOV VP35 protein, in particular with the end-capping domain of the VP35 RBD/IID. As a result of this screening process, we selected nine compounds and we tested them in both biochemical and cellular systems.

Among the VS-selected drugs, three compounds (namely compound A, compound B, compound F) were found able to significantly counteract the dsRNA RIG-I-mediated IFN-β inhibition regulated by EBOV VP35. Further, their effects on EBOV replication were investigated. Out of the three, the compounds A and B confirmed the previous results, demonstrating to be strongly effective in inhibiting the replication at high percentages more than 70% and at low micromolar concentrations, also reliably reflecting the range of concentrations that demonstrated to be significantly effective in the previous cellular inhibition assay, indicating that this contrasting activity of the VS compounds towards EBOV VP35 could have a key role in regulating the replication process of the virus.

Finally, the efficiency of a number of scFv antibodies, developed to directly interact with EBOV VP35, was also investigated. Here we found that two mAbs were

significantly capable to subvert the VP35 inhibition, and this result opens the field to further investigations aimed to understand if this blockade could be reflected also in an abruption of the viral replication, thus determining a viral clearance. Since no antibody-based therapy has been approved so far for EVD treatment in humans, with cocktails of monoclonal NAbs being used under emergency compassionate protocols, to reveal this aspect would be crucial in order to develop new effective antibody-based therapies.

In conclusion, we demonstrated that some natural extracts, as well as small molecules interacting with EBOV VP35, can subvert the IFN production inhibition mediated by this key viral protein, possibly inhibiting its interactions with cellular components within the RLR pathway. Furthermore, we discovered the potential of scFv monoclonal antibodies developed for specifically interacting with VP35. Lastly, we found some synthetic compounds that, through a specific and direct interaction with VP35, are able to positively subvert the IFN production blockade mediated by VP35 and, very importantly, to interfere with the replication of the virus, setting the basis for a further drug development.

AKNOWLEDGEMENTS

I would like to express all my appreciation and thanks to my principal supervisor, Professor Enzo Tramontano, for his guide and support during these years, for his precious advice and encouragement expressed in the days of this journey.

This research was performed thanks to the incomparable help and support of my colleagues and students of the lab, thus I have to say a big thank you to Dr. Francesca Esposito (aka "P.I."), Dr. Angela Corona, Dr. Nicole Grandi, Dr. Gian Luca Daino, to my cell-culture partner - PhD student Elisa Fanunza, the incomparable Alessia Caredda, PhD student Maria Paola Pisano, my master degree students Michela Falqui, Gianfranca Mastroni and Stefania Musinu.

I would like to thank also Professor Ali Mirazimi and his research group of the Karolinska Institute of Sweden, for the kind hospitality, support and help.

Furthermore, I would like to thank also all the professors, researcher, students that directly or indirectly gave their contribute to my research: Prof. Simona Distinto, Prof. Elias Maccioni, PhD Amalia di Petrillo, of the University of Cagliari, Dr. Paola Di Bonito and Michela Flego from the Istituto Superiore di Sanità (ISS) - Department of Infectious Diseases and Global Health Center, Rome (Italy).

Finally, I dedicate this work to the only person who have been close to me every single day of this journey, who has tolerated and supported me in these years, giving me strength and courage to move forward in the bad days. It has been tough, but I made it. Thank you love of my life.

Data presented in this Ph.D. thesis have been published in the following research articles:

Ngoutane Mfopa, Alvine, Angela Corona, Kodjo Eloh, Enzo Tramontano, **Aldo Frau**, Fabrice Fekam Boyom, Pierluigi Caboni, and Graziella Tocco. 2017. "Uvaria Angolensis as a Promising Source of Inhibitors of HIV-1 RT-Associated RNA-Dependent DNA Polymerase and RNase H Functions." Natural Product Research 6419 (May). Taylor & Francis: 1–8. doi:10.1080/14786419.2017.1332615.

Petrillo, Amalia Di, Antonella Fais, Francesca Pintus, Celestino Santos-Buelga, Ana M. González-Paramás, Vincenzo Piras, Germano Orrù, Antonello Mameli, Enzo Tramontano, and **Aldo Frau**. 2017. "Broad-Range Potential of Asphodelus Microcarpus Leaves Extract for Drug Development." BMC Microbiology 17 (1). BMC Microbiology: 159. doi:10.1186/s12866-017-1068-5.

Il presente lavoro di tesi è stato prodotto durante la frequenza del corso di dottorato in Scienze della Vita dell'Ambiente e del Farmaco dell'Università degli Studi di Cagliari, a.a. 2016/2017 - XXX ciclo, con il supporto di una borsa di studio finanziata con le risorse del P.O.R. SARDEGNA F.S.E. 2007-2013 - Obiettivo competitività regionale e occupazione, Asse IV Capitale umano, Linea di Attività l.3.1 "Finanziamento di corsi di dottorato finalizzati alla formazione di capitale umano altamente specializzato, in particolare per i settori dell'ICT, delle nanotecnologie e delle e biotecnologie, dell'energia e dello sviluppo sostenibile, dell'agroalimentare e dei materiali tradizionali".

This thesis work was produced during the PhD program in Life Sciences of the Environment and Medicine of the University of Cagliari, a.y. 2016/2017 - XXX cycle, with the support of a scholarship funded with the resources of P.O.R. SARDEGNA F.S.E. 2007-2013 - Regional competitiveness and employment objective, Axis IV Human capital, Line of activity l.3.1 "Financing of doctoral courses aimed at the formation of highly specialized human capital, in particular for the ICT, nanotechnology and biotechnology, energy and sustainable development, agri-food and traditional materials".

Aldo Frau gratefully acknowledges Sardinia Regional Government for the financial support of her PhD scholarship (P.O.R. Sardegna F.S.E. Operational Programme of the Autonomous Region of Sardinia, European Social Fund 2007-2013 - Axis IV Human Resources, Objective l.3, Line of Activity l.3.1.).

REGIONE AUTÒNOMA DE SARDIGNA
REGIONE AUTONOMA DELLA SARDEGNA

REFERENCES

Albariño, C. G. et al. 2013. "Genomic Analysis of Filoviruses Associated with Four Viral Hemorrhagic Fever Outbreaks in Uganda and the Democratic Republic of the Congo in 2012." *Virology* 442(2): 97–100.

Amarasinghe, Gaya K. et al. 2017. "Taxonomy of the Order Mononegavirales: Update 2017." *Archives of Virology*: 1–12.

Aniya, Y et al. 2002. "Free Radical Scavenging Action of the Medicinal Herb Limonium Wrightii from the Okinawa Islands." *Phytomedicine : international journal of phytotherapy and phytopharmacology* 9(3): 239–44.

Ansari, Aftab A. 2015. "Clinical Features and Pathobiology of Ebolavirus Infection." *Journal of Autoimmunity* 55(1): 1–9.

Ashburn, Ted T, and Karl B Thor. 2004. "Drug Repositioning: Identifying and Developing New Uses for Existing Drugs." *Nature reviews. Drug discovery* 3(8): 673–83.

Atanasov, Atanas G et al. 2015. "Discovery and Resupply of Pharmacologically Active Plant-Derived Natural Products: A Review." *Biotechnology advances* 33(8): 1582–1614.

Audet, Jonathan et al. 2014. "Molecular Characterization of the Monoclonal Antibodies Composing ZMAb: A Protective Cocktail Against Ebola Virus." *Scientific Reports* 4: 6881.

Bailey, Charles C, Guocai Zhong, I-Chueh Huang, and Michael Farzan. 2014. "IFITM-Family Proteins: The Cell's First Line of Antiviral Defense." *Annual review of virology* 1: 261–83.

Bale, S. et al. 2013. "Ebolavirus VP35 Coats the Backbone of Double-Stranded RNA for Interferon Antagonism." *Journal of Virology* 87(18): 10385–88.

Baltimore, D. 1971. "Expression of Animal Virus Genomes." *Bacteriological Reviews* 35(3): 235–41.

Banadyga, Logan et al. 2017. "Ebola Virus VP24 Interacts with NP to Facilitate Nucleocapsid Assembly and Genome Packaging." *Scientific Reports* 7(1): 7698.

Baron, R. C., J. B. McCormick, and O. A. Zubeir. 1983. "Ebola Virus Disease in Southern Sudan: Hospital Dissemination and Intrafamilial Spread." *Bulletin of the World Health Organization* 61(6): 997–1003.

Barrette, Roger W et al. 2009. "Discovery of Swine as a Host for the Reston Ebolavirus." *Source: Science, New Series* 325(5937): 204–6.

Baseler, Laura et al. 2017. "The Pathogenesis of Ebola Virus Disease." *Annual Review of Pathology: Mechanisms of Disease* 12(1): 387–418.

Basler, C F et al. 2000. "The Ebola Virus VP35 Protein Functions as a Type I IFN Antagonist." *Proceedings of the National Academy of Sciences of the United States of America* 97(22): 12289–94.

Basler, Christopher F et al. 2003. "The Ebola Virus VP35 Protein Inhibits Activation of Interferon Regulatory Factor 3." *Journal of virology* 77(14): 7945–56.

Basler, Christopher F. 2017. "Molecular Pathogenesis of Viral Hemorrhagic Fever." *Seminars in Immunopathology*: 1–11..

Basler, Christopher F. 2015. "Innate Immune Evasion by Filoviruses." *Virology* 479–480: 122–30.

Basler, Christopher F, and Gaya K Amarasinghe. 2009. "Evasion of Interferon Responses by Ebola and Marburg Viruses." *Journal of interferon & cytokine research : the official journal of the International Society for Interferon and Cytokine Research* 29(9): 511–20.

Bebell, Lisa M., Titilope Oduyebo, and Laura E. Riley. 2017. "Ebola Virus Disease and Pregnancy: A Review of the Current Knowledge of Ebola Virus Pathogenesis, Maternal, and Neonatal Outcomes." *Birth Defects Research* 109(5): 353–62.

Bedard, K. M. et al. 2012. "Isoflavone Agonists of IRF-3 Dependent Signaling Have Antiviral Activity against RNA Viruses." *Journal of Virology* 86(13): 7334–44.

Beniac, Daniel R. et al. 2012. "The Organisation of Ebola Virus Reveals a Capacity for

Extensive, Modular Polyploidy." *PLoS ONE* 7(1).

Bharaj, Preeti et al. 2017. "The Host E3-Ubiquitin Ligase TRIM6 Ubiquitinates the Ebola Virus VP35 Protein and Promotes Virus Replication." *Journal of Virology* (July): JVI.00833-17.

Bharat, Tanmay A M et al. 2012. "Structural Dissection of Ebola Virus and Its Assembly Determinants Using Cryo-Electron Tomography." *Proceedings of the National Academy of Sciences of the United States of America* 109(11): 4275–80.

Biedenkopf, Nadine et al. 2016. "RNA-Binding of Ebola Virus VP30 Is Essential for Activating Viral Transcription." *Journal of virology* 90(16): 7481–96.

Biek, Roman, Peter D. Walsh, Eric M. Leroy, and Leslie A. Real. 2006. "Recent Common Ancestry of Ebola Zaire Virus Found in a Bat Reservoir." *PLoS Pathogens* 2(10): 0885–86.

Bixler, Sandra L., Allen J. Duplantier, and Sina Bavari. 2017. "Discovering Drugs for the Treatment of Ebola Virus." *Current Treatment Options in Infectious Diseases*: 299–317.

Bower, Hilary et al. 2016. "Exposure-Specific and Age-Specific Attack Rates for Ebola Virus Disease in Ebola-Affected Households, Sierra Leone." *Emerging Infectious Diseases* 22(8): 1403–11.

Brass, Abraham L et al. 2009. "The IFITM Proteins Mediate Cellular Resistance to Influenza A H1N1 Virus, West Nile Virus, and Dengue Virus." *Cell* 139(7): 1243–54.

Bray, M, and T W Geisbert. 2005. "Ebola Virus: The Role of Macrophages and Dendritic Cells in the Pathogenesis of Ebola Hemorrhagic Fever." *International Journal of Biochemistry & Cell Biology* 37(8): 1560–66.

Bray, Mike, and Siddhartha Mahanty. 2003. "Ebola Hemorrhagic Fever and Septic Shock." *The Journal of infectious diseases* 188(11): 1613–17.

Bruni, A, M Ballero, and F Poli. 1997. "Quantitative Ethnopharmacological Study of the Campidano Valley and Urzulei District, Sardinia, Italy." *Journal of ethnopharmacology* 57(2): 97–124.

Vande Burgt, Nathan H., Rachel L. Kaletsky, and Paul Bates. 2015. "Requirements within the Ebola Viral Glycoprotein for Tetherin Antagonism." *Viruses* 7(10): 5587–5602.

Calzado, Marco A et al. 2005. "Inhibition of NF-κB Activation and Expression of Inflammatory Mediators by Polyacetylene Spiroketals from Plagius Flosculosus." *Biochimica et Biophysica Acta (BBA) - Gene Structure and Expression* 1729(2): 88–93.

Cannas, Valeria et al. 2015. "A Luciferase Reporter Gene Assay to Measure Ebola Virus Viral Protein 35-Associated Inhibition of Double-Stranded RNA-Stimulated, Retinoic Acid-Inducible Gene 1-Mediated Induction of Interferon β." *Journal of Infectious Diseases* 212: S277–81.

Cardenas, W. B. et al. 2006. "Ebola Virus VP35 Protein Binds Double-Stranded RNA and Inhibits Alpha/Beta Interferon Production Induced by RIG-I Signaling." *Journal of Virology* 80(11): 5168–78.

Cardile, Anthony P et al. 2016a. "Antiviral Therapeutics for the Treatment of Ebola Virus Infection." *Current Opinion in Pharmacology* 30: 138–43.

Cardile, Anthony P. et al. 2016b. "Antiviral Therapeutics for the Treatment of Ebola Virus Infection." *Current Opinion in Pharmacology* 30: 138–43. http://dx.doi.org/10.1016/j.coph.2016.08.016.

Carroll, S. A. et al. 2013. "Molecular Evolution of Viruses of the Family Filoviridae Based on 97 Whole-Genome Sequences." *Journal of Virology* 87(5): 2608–16.

Chang, Tsung Hsien et al. 2009. "Ebola Zaire Virus Blocks Type I Interferon Production by Exploiting the Host SUMO Modification Machinery." *PLoS Pathogens* 5(6).

Chen, Junchao et al. 2017. "The Characteristics of TCM Clinical Trials: A Systematic Review of ClinicalTrials.gov." *Evidence-based Complementary and Alternative Medicine* 2017.

Chen, Zhijian J., and Lijun J. Sun. 2009. "Nonproteolytic Functions of Ubiquitin in Cell Signaling." *Molecular Cell* 33(3): 275–86.

Chung, Jae Yoon, Jung-Mi Hah, and Art E Cho. 2009. "Correlation between Performance of QM/MM Docking and Simple Classification of Binding Sites." *Journal of chemical information and modeling* 49(10): 2382–87.

Clark, Danielle V. et al. 2015. "Long-Term Sequelae after Ebola Virus Disease in Bundibugyo, Uganda: A Retrospective Cohort Study." *The Lancet Infectious Diseases* 15(8): 905–12.

Cragg, Gordon M, and David J Newman. 2013. "Natural Products: A Continuing Source of Novel Drug Leads." *Biochimica et biophysica acta* 1830(6): 3670–95.

Van Damme, Nanette et al. 2008. "The Interferon-Induced Protein BST-2 Restricts HIV-1 Release and Is Downregulated from the Cell Surface by the Viral Vpu Protein." *Cell Host and Microbe* 3(4): 245–52.

Davidson, Edgar et al. 2015. "Mechanism of Binding to Ebola Virus Glycoprotein by the ZMapp, ZMAb, and MB-003 Cocktail Antibodies." *Journal of Virology* 89(21): 10982–92.

Dean, Natalie E, M Elizabeth Halloran, Yang Yang, and Ira M Longini. 2016. "Transmissibility and Pathogenicity of Ebola Virus: A Systematic Review and Meta-Analysis of Household Secondary Attack Rate and Asymptomatic Infection." *Clinical infectious diseases : an official publication of the Infectious Diseases Society of America* 62(10): 1277–86.

Deen, Gibrilla F. et al. 2015. "Ebola RNA Persistence in Semen of Ebola Virus Disease Survivors — Preliminary Report." *New England Journal of Medicine*: 151014140118009.

Deng, I. M., O. Duku, and A. L. Gillo. 1978. "Ebola Haemorrhagic Fever in Sudan, 1976. Report of a WHO/International Study Team." *Bulletin of the World Health Organization* 56(2): 247–70.

Derksen, Andrea et al. 2016. "Antiviral Activity of Hydroalcoholic Extract from Eupatorium Perfoliatum L. Against the Attachment of Influenza A Virus." *Journal of Ethnopharmacology* 188: 144–52.

Dornemann, Jenny et al. 2017. "First Newborn Baby to Receive Experimental Therapies Survives Ebola Virus Disease." *The Journal of infectious diseases* 215(2): 171–74.

Douglas, Janet L. et al. 2010. "The Great Escape: Viral Strategies to Counter BST-2/ Tetherin." *PLoS Pathogens* 6(5): 1–12.

Dutto, M. et al. 2016. "Ebola Virus and Arthropods: A Literature Review and Entomological Consideration on the Vector Role." *Bulletin de la Société de pathologie exotique* 109(4): 244–47.

Edwards, Megan R. et al. 2016. "Differential Regulation of Interferon Responses by Ebola and Marburg Virus VP35 Proteins." *Cell Reports* 14(7): 1632–40.

Esposito, Francesca et al. 2012. "New Anthraquinone Derivatives as Inhibitors of the HIV-1 Reverse Transcriptase-Associated Ribonuclease H Function." *Chemotherapy* 58(4): 299–307.

Esposito, Francesca et al. 2013. "Hypericum Hircinum L. Components as New Single-Molecule Inhibitors of Both HIV-1 Reverse Transcriptase-Associated DNA Polymerase and Ribonuclease H Activities." *Pathogens and Disease* 68(3): 116–24.

Fabozzi, Giulia, Christopher S Nabel, Michael a Dolan, and Nancy J Sullivan. 2011. "Ebolavirus Proteins Suppress the Effects of Small Interfering RNA by Direct Interaction with the Mammalian RNA Interference Pathway." *Journal of virology* 85(6): 2512–23.

Fairman-Williams, Margaret E, Ulf-Peter Guenther, and Eckhard Jankowsky. 2010. "SF1 and SF2 : Family Matters." 20(3): 313–24.

Fang, Jiansong et al. 2017. "In Silico Polypharmacology of Natural Products." *Briefings in Bioinformatics*: bbx045-bbx045. http://dx.doi.org/10.1093/bib/bbx045.

Feldmann, Heinz, and Thomas W. Geisbert. 2011. "Ebola Haemorrhagic Fever." *The*

Lancet 377(9768): 849–62.

Feng, Z., M. Cerveny, Z. Yan, and B. He. 2007. "The VP35 Protein of Ebola Virus Inhibits the Antiviral Effect Mediated by Double-Stranded RNA-Dependent Protein Kinase PKR." *Journal of Virology* 81(1): 182–92.

Fitzgerald, Katherine A. et al. 2003. "IKKε and TBK1 Are Essential Components of the IRF3 Signaling Pathway." *Nature Immunology* 4(5): 491–96.

Formisano, Carmen et al. 2017. "Anti-Inflammatory Sesquiterpene Lactones from Onopordum Illyricum L. (Asteraceae), an Italian Medicinal Plant." *Fitoterapia* 116: 61–65.

Francica, Joseph R et al. 2010. "Steric Shielding of Surface Epitopes and Impaired Immune Recognition Induced by the Ebola Virus Glycoprotein." 6(9).

Friesner, Richard A et al. 2006. "Extra Precision Glide: Docking and Scoring Incorporating a Model of Hydrophobic Enclosure for Protein-Ligand Complexes." *Journal of medicinal chemistry* 49(21): 6177–96.

Georges, a J et al. 1999. "Ebola Hemorrhagic Fever Outbreaks in Gabon, 1994-1997: Epidemiologic and Health Control Issues." *The Journal of infectious diseases* 179 Suppl: S65–75.

Gerlier, D., and D. S. Lyles. 2011. "Interplay between Innate Immunity and Negative-Strand RNA Viruses: Towards a Rational Model." *Microbiology and Molecular Biology Reviews* 75(3): 468–90.

Glisic, Sanja et al. 2015. "Improving Attrition Rates in Ebola Virus Drug Discovery." *Expert opinion on drug discovery* 10(9): 1025–32.

Gnirss, Kerstin et al. 2014. "Analysis of Determinants in Filovirus Glycoproteins Required for Tetherin Antagonism." *Viruses* 6(4): 1654–71.

Le Guenno, B. et al. 1995. "Isolation and Partial Characterisation of a New Strain of Ebola Virus." *The Lancet* 345(8960): 1271–74.

Gulland, Anne. 2017. "WHO Ready to Deploy Ebola Vaccine in Disease Outbreak." *Bmj* 2454(16): j2454.

Guo, Fang et al. 2012. "RO 90-7501 Enhances TLR3 and RLR Agonist Induced Antiviral Response." *PLOS ONE* 7(10): e42583.

Guvench, Olgun et al. 2002. "Application of the Frozen Atom Approximation to the GB/SA Continuum Model for Solvation Free Energy." *Journal of Computational Chemistry* 23(2): 214–21.

Haasnoot, Joost et al. 2007. "The Ebola Virus VP35 Protein Is a Suppressor of RNA Silencing." *PLoS Pathogens* 3(6): 0794–0803.

Haller, Otto, Georg Kochs, and Friedemann Weber. 2006. "The Interferon Response Circuit : Induction and Suppression by Pathogenic Viruses." 344: 119–30.

Hammonds, Jason, Jaang-Jiun Wang, Hong Yi, and Paul Spearman. 2010. "Immunoelectron Microscopic Evidence for Tetherin/BST2 as the Physical Bridge between HIV-1 Virions and the Plasma Membrane." *PLoS pathogens* 6(2): e1000749.

Hartman, A. L., B. H. Bird, et al. 2008. "Inhibition of IRF-3 Activation by VP35 Is Critical for the High Level of Virulence of Ebola Virus." *Journal of Virology* 82(6): 2699–2704.

Hartman, A. L., L. Ling, S. T. Nichol, and M. L. Hibberd. 2008. "Whole-Genome Expression Profiling Reveals That Inhibition of Host Innate Immune Response Pathways by Ebola Virus Can Be Reversed by a Single Amino Acid Change in the VP35 Protein." *Journal of Virology* 82(11): 5348–58.

Harvey, Robert et al. 2009. "GSK983: A Novel Compound with Broad-Spectrum Antiviral Activity." *Antiviral Research* 82(1): 1–11.

Hastie, Kathryn M, Shridhar Bale, Christopher R Kimberlin, and Erica Ollmann. 2013. "Hiding the Evidence:two Strategies for Innate Immune Evasion by Hemorrhagic Fever Viruses." *Current Opinion in Microbiology* 2(2): 151–56.

He, Felix et al. 2017. "Ebolavirus Protein VP24 Interferes with Innate Immune Responses by Inhibiting Interferon-λ1 Gene Expression." *Virology* 509(February): 23–34.

He, Jing et al. 2017. "Ebola Virus Delta Peptide Is a Viroporin." *Journal of Virology* (May): JVI.00438-17.

Henao-Restrepo, Ana Maria et al. 2015. "Efficacy and Effectiveness of an rVSV-Vectored Vaccine Expressing Ebola Surface Glycoprotein: Interim Results from the Guinea Ring Vaccination Cluster-Randomised Trial." *The Lancet* 386(9996): 857–66.

Henao-Restrepo, Ana Maria et al. 2017. "Efficacy and Effectiveness of an rVSV-Vectored Vaccine in Preventing Ebola Virus Disease: Final Results from the Guinea Ring Vaccination, Open-Label, Cluster-Randomised Trial (Ebola Ça Suffit!)." *The Lancet* 389(10068): 505–18.

Hlberger, Elke M et al. 1999. "Comparison of the Transcription and Replication Strategies of Marburg Virus and Ebola Virus by Using Artificial Replication Systems." *Journal of Virology* 73(3): 2333–42.

Honda, Kenya et al. 2005. "IRF-7 Is the Master Regulator of Type-I Interferon-Dependent Immune Responses." *Nature* 434(7034): 772–77.

Huang, I. Chueh et al. 2011. "Distinct Patterns of IFITM-Mediated Restriction of Filoviruses, SARS Coronavirus, and Influenza A Virus." *PLoS Pathogens* 7(1).

Huynh, Do Luong et al. 2017. "Anti-Tumor Activity of Wogonin, an Extract from Scutellaria Baicalensis, through Regulating Different Signaling Pathways." *Chinese Journal of Natural Medicines* 15(1): 15–40.

Iampietro, Mathieu et al. 2017. "Ebola Virus Glycoprotein Directly Triggers T Lymphocyte Death despite of the Lack of Infection." *PLOS Pathogens* 13(5): e1006397.

Ito, Hiroshi, Shinji Watanabe, and Ayato Takada. 2015. "Ebola Virus Glycoprotein : Proteolytic Processing , Acylation , Cell Tropism , and Detection of Neutralizing Antibodies." 75(3): 1576–80.

Ivashkiv, Lionel B., and Laura T. Donlin. 2015. "Regulation of Type I Interferon Responses." *Nature Reviews Immunology* 14(1): 36–49.

Iversen, Patrick L et al. 2012. "Discovery and Early Development of AVI-7537 and AVI-7288 for the Treatment of Ebola Virus and Marburg Virus Infections." *Viruses* 4(11): 2806–30.

Jacobs, Michael et al. 2016. "Late Ebola Virus Relapse Causing Meningoencephalitis: A Case Report." *Lancet (London, England)* 388(10043): 498–503.

Jeong, Eunshil, and Joo Young Lee. 2011. "Intrinsic and Extrinsic Regulation of Innate Immune Receptors." *Yonsei Medical Journal* 52(3): 379–92.

Jin, Huali et al. 2010. "The VP35 Protein of Ebola Virus Impairs Dendritic Cell Maturation Induced by Virus and Lipopolysaccharide." *Journal of General Virology* 91(2): 352–61.

Johansen, Lisa M et al. 2013. "FDA-Approved Selective Estrogen Receptor Modulators Inhibit Ebola Virus Infection." *Science translational medicine* 5(190): 190ra79.

Johansen, Lisa M et al. 2015. "A Screen of Approved Drugs and Molecular Probes Identifies Therapeutics with Anti-Ebola Virus Activity." *Science translational medicine* 7(290): 290ra89.

Johnson, Reed F RF et al. 2006. "Effect of Ebola Virus Proteins GP, NP and VP35 on VP40 VLP Morphology." *Virology journal* 3(1): 31.

Jones, Lyn H. 2015. "Medicinal Chemistry." *Future Medicinal Chemistry* 7(16): 2131–41.

Judson, Seth, Joseph Prescott, and Vincent Munster. 2015. "Understanding Ebola Virus Transmission." *Viruses* 7(2): 511–21.

Kaletsky, Rachel L, Joseph R Francica, Caroline Agrawal-Gamse, and Paul Bates. 2009. "Tetherin-Mediated Restriction of Filovirus Budding Is Antagonized by the Ebola Glycoprotein." *Proceedings of the National Academy of Sciences of the United States of America* 106(8): 2886–91.

Kallstrom, George et al. 2005. "Analysis of Ebola Virus and VLP Release Using an Immunocapture Assay." *Journal of Virological Methods* 127(1): 1–9.

Kanadaswami, Chithan et al. 2005. "The

Antitumor Activities of Flavonoids." *In Vivo* 19(5): 895–910.

Kato, Hiroki et al. 2008. "Length-Dependent Recognition of Double- Stranded Ribonucleic Acids by Retinoic Acid – Inducible Gene-I and Melanoma Diff Erentiation – Associated Gene 5." 205(7): 1601–10.

Khalafallah, Mahmoud Tawfik, Omar Ali Aboshady, Shaban Ahmed Moawed, and Menna Said Ramadan. 2017. "Ebola Virus Disease : Essential Clinical Knowledge." : 96–102.

Khan, Ali S et al. 1995. "The Reemergence of Ebola Hemorrhagic Fever, Democratic Republic of the Congo, 1995." *The Journal of Infectious Diseases* 179(Suppl: S76-86.

Khiar, Samira et al. 2017. "Identification of a Small Molecule That Primes the Type I Interferon Response to Cytosolic DNA." *Scientific Reports* 7(1): 2561.

Kimberlin, C. R. et al. 2010. "Ebolavirus VP35 Uses a Bimodal Strategy to Bind dsRNA for Innate Immune Suppression." *Proceedings of the National Academy of Sciences* 107(1): 314–19.

Kirchdoerfer, Robert N., Crystal L. Moyer, Dafna M. Abelson, and Erica Ollmann Saphire. 2016. "The Ebola Virus VP30-NP Interaction Is a Regulator of Viral RNA Synthesis." *PLoS Pathogens* 12(10): 1–22.

Kondratowicz, A. S. et al. 2011. "T-Cell Immunoglobulin and Mucin Domain 1 (TIM-1) Is a Receptor for Zaire Ebolavirus and Lake Victoria Marburgvirus." *Proceedings of the National Academy of Sciences* 108(20): 8426–31.

Kühl, A., and S. Pöhlmann. 2012. "How Ebola Virus Counters the Interferon System." *Zoonoses and Public Health* 59(SUPPL.2): 116–31.

Kuhl, Annika et al. 2011. "The Ebola Virus Glycoprotein and HIV-1 Vpu Employ Different Strategies to Counteract the Antiviral Factor Tetherin." *The Journal of infectious diseases* 204 Suppl: S850-60.

Kuhn, Jens H et al. 2010. "Proposal for a Revised Taxonomy of the Family Filoviridae: Classification, Names of Taxa and Viruses, and Virus Abbreviations." *Archives of Virology* 155(12): 2083–2103.

Kumar, Shashank, and Abhay K Pandey. 2013. "Chemistry and Biological Activities of Flavonoids: An Overview." *TheScientificWorldJournal* 2013: 162750.

Kupzig, Sabine et al. 2003. "Bst-2/HM1.24 Is a Raft-Associated Apical Membrane Protein with an Unusual Topology." *Traffic (Copenhagen, Denmark)* 4(10): 694–709.

de La Vega, Marc-Antoine, Gary Wong, Gary P. Kobinger, and Xiangguo Qiu. 2015. "The Multiple Roles of sGP in Ebola Pathogenesis." *Viral Immunology* 28(1): 3–9.

de La Vega, Marc Antoine, Derek Stein, and Gary P. Kobinger. 2015. "Ebolavirus Evolution: Past and Present." *PLoS Pathogens* 11(11): 1–10.

Langer, Thierry, and Camille-Georges Wermuth. 2012. "Selective Optimization of Side Activities (SOSA): A Promising Way for Drug Discovery." In *Polypharmacology in Drug Discovery*, John Wiley & Sons, Inc., 227–43.

Lee, Jeffrey E, Torrey Pines Road, and La Jolla. 2010. "Ebolavirus Glycoprotein Structure and Mechanism of Entry." *North* 4(6): 621–35.

Leelananda, Sumudu P., and Steffen Lindert. 2016. "Computational Methods in Drug Discovery." *Beilstein Journal of Organic Chemistry* 12: 2694–2718.

Leirs, H et al. 1999. "Search for the Ebola Virus Reservoir in Kikwit, Democratic Republic of the Congo: Reflections on a Vertebrate Collection." *The Journal of infectious diseases* 179 Suppl(Suppl 1): S155–63.

Leroy, Eric M et al. 2009. "Human Ebola Outbreak Resulting from Direct Exposure to Fruit Bats in Luebo, Democratic Republic of Congo, 2007." *Vector borne and zoonotic diseases (Larchmont, N.Y.)* 9(6): 723–28.

Leung, Daisy W, Nathaniel D Ginder, D Bruce Fulton, et al. 2009. "Structure of the Ebola VP35 Interferon Inhibitory Domain." *Proceedings of the National Academy of Sciences of the United States of America*

106(2): 411–16.

Leung, Daisy W., Nathaniel D. Ginder, Jay C. Nix, et al. 2009. "Expression, Purification, Crystallization and Preliminary X-Ray Studies of the Ebola VP35 Interferon Inhibitory Domain." *Acta Crystallographica Section F: Structural Biology and Crystallization Communications* 65(2): 163–65.

Leung, Daisy W., Dominika Borek, et al. 2010. "Crystallization and Preliminary X-Ray Analysis of Ebola VP35 Interferon Inhibitory Domain Mutant Proteins." *Acta Crystallographica Section F: Structural Biology and Crystallization Communications* 66(6): 689–92.

Leung, Daisy W., Kathleen C. Prins, Christopher F. Basler, and Gaya K. Amarasinghe. 2010. "*Ebolavirus* VP35 Is a Multifunctional Virulence Factor." *Virulence* 1(6): 526–31.

Licata, Jillian M, and et al. 2004. "Contribution of Ebola Virus Glycoprotein , Nucleoprotein , and VP24 to Budding of VP40 Virus-Like Particles." *Society* 78(14): 7344–51.

Lier, Clemens, Stephan Becker, and Nadine Biedenkopf. 2017. "Dynamic Phosphorylation of Ebola Virus VP30 in NP-Induced Inclusion Bodies." *Virology* 512(September): 39–47.

Lucas-Hourani, Marianne et al. 2013. "Inhibition of Pyrimidine Biosynthesis Pathway Suppresses Viral Growth through Innate Immunity." *PLoS Pathogens* 9(10).

Luo, Dahai et al. 2011. "Structural Insights into RNA Recognition by RIG-I." *Cell* 147(2): 409–22.

Luthra, P et al. 2015. "Ebola Virus VP35 Interaction with Dynein Light Chain 8 Regulates Viral RNA Synthesis." *J Virol* 89(9): 5148–53.

Luthra, Priya et al. 2013. "Mutual Antagonism between the Ebola Virus VP35 Protein and the RIG-I Activator PACT Determines Infection Outcome." *Cell Host and Microbe* 14(1).

Ma, Daphne Y., and Mehul S. Suthar. 2015. "Mechanisms of Innate Immune Evasion in Re-Emerging RNA Viruses." *Current Opinion in Virology* 12: 26–37.

MacNeil, Adam et al. 2011. "Filovirus Outbreak Detection and Surveillance: Lessons from Bundibugyo." *Journal of Infectious Diseases* 204(SUPPL. 3): 761–67.

Madrid, Peter B et al. 2013. "A Systematic Screen of FDA-Approved Drugs for Inhibitors of Biological Threat Agents." *PloS one* 8(4): e60579.

Maganga, Gaël D. et al. 2014. "Ebola Virus Disease in the Democratic Republic of Congo." *New England Journal of Medicine* 371(22): 2083–91.

Martínez-Gil, Luis et al. 2012. "Identification of Small Molecules with Type I Interferon Inducing Properties by High-Throughput Screening." *PLOS ONE* 7(11): e49049.

Martinez, Osvaldo, Charalampos Valmas, and Christopher F Basler. 2007. "Ebola Virus-like Particle-Induced Activation of NF-κB and Erk Signaling in Human Dendritic Cells Requires the Glycoprotein Mucin Domain." *Virology* 364(2): 342–54.

Martins, Karen A, Peter B Jahrling, Sina Bavari, and Jens H Kuhn. 2016. "Ebola Virus Disease Candidate Vaccines under Evaluation in Clinical Trials." *Expert review of vaccines* 15(9): 1101–12.

Mate, Suzanne E. et al. 2015. "Molecular Evidence of Sexual Transmission of Ebola Virus." *New England Journal of Medicine* 373(25): 2448–54.

Mateo, M. et al. 2010. "Ebolavirus VP24 Binding to Karyopherins Is Required for Inhibition of Interferon Signaling." *Journal of Virology* 84(2): 1169–75.

McMullan, Laura K et al. 2016. "The Lipid Moiety of Brincidofovir Is Required for in Vitro Antiviral Activity against Ebola Virus." *Antiviral Research* 125(Supplement C): 71–78.

Medini, F et al. 2011. "Effects of Physiological Stage and Solvent on Polyphenol Composition, Antioxidant and Antimicrobial Activities of Limonium Densiflorum." *Journal of Medicinal Plant Research* 5(31): 6719–30.

Mirza, Muhammad Usman, and Nazia Ikram. 2016. "Integrated Computational Approach for Virtual Hit Identification against Ebola Viral Proteins VP35 and VP40." *International Journal of Molecular Sciences* 17(11).

Misasi, John, and Nancy J. Sullivan. 2014. "Camouflage and Misdirection: The Full-on Assault of Ebola Virus Disease." *Cell* 159(3): 477–86.

Mohammadi, Dara. 2014. "First Trials for Ebola Treatments Announced." *The Lancet* 384(9957): 1833.

Moller, P., N. Pariente, H.-D. Klenk, and S. Becker. 2005. "Homo-Oligomerization of Marburgvirus VP35 Is Essential for Its Function in Replication and Transcription." *Journal of Virology* 79(23): 14876–86.

Morris, Garrett M et al. 1998. "Automated Docking Using a Lamarckian Genetic Algorithm and an Empirical Binding Free Energy Function." *Journal of Computational Chemistry* 19(14): 1639–62.

Morris, Garrett M et al. 2009. "AutoDock4 and AutoDockTools4: Automated Docking with Selective Receptor Flexibility." *Journal of computational chemistry* 30(16): 2785–91.

Morvan, Jacques M. et al. 1999. "Identification of Ebola Virus Sequences Present as RNA or DNA in Organs of Terrestrial Small Mammals of the Central African Republic." *Microbes and Infection* 1(14): 1193–1201.

Mühlberger, Elke. 2013. "NIH Public Access." 2(2): 205–15.

Muhlberger, Elke, Beate L Tfering, Hans-Dieter Klenk, and Stephan Becker. 1998. "Three of the Four Nucleocapsid Proteins of Marburg Virus, NP, VP35, and L, Are Sufficient To Mediate Replication and Transcription of Marburg Virus-Specific Monocistronic Minigenomes." *Journal of Virology* 72(11): 8756–64.

Mukherjee, Pulok K. et al. 2017. "Development of Ayurveda – Tradition to Trend." *Journal of Ethnopharmacology* 197: 10–24.

Murray, Ana P, and Silvana Rodriguez. 2004. "Antioxidant Metabolites from." *Seven*: 5–8.

Negredo, Ana et al. 2011. "Discovery of an Ebolavirus-like Filovirus in Europe." *PLoS Pathogens* 7(10): 1–8.

Neil, Stuart J. D., Trinity Zang, and Paul D. Bieniasz. 2008. "Tetherin Inhibits Retrovirus Release and Is Antagonized by HIV-1 Vpu." *Nature* 451(7177): 425–30.

Nielsen, Carrie F et al. 2015. "Improving Burial Practices and Cemetery Management during an Ebola Virus Disease Epidemic - Sierra Leone, 2014." *MMWR. Morbidity and mortality weekly report* 64(1): 20–27.

Ning, Yun Jia, Fei Deng, Zhihong Hu, and Hualin Wang. 2017. "The Roles of Ebolavirus Glycoproteins in Viral Pathogenesis." *Virologica Sinica* 32(1): 3–15.

Noda, Takeshi et al. 2006. "Assembly and Budding of Ebolavirus." *PLoS Pathogens* 2(9): 0864–72.

Olival, Kevin J., and David T S Hayman. 2014. "Filoviruses in Bats: Current Knowledge and Future Directions." *Viruses* 6(4): 1759–88.

Olszanecki, R, and G Gawlik. 2014. "Pharmacotherapy of Ebola Hemorrhagic Fever: A Brief Review of Current Status and Future Perspectives." *Folia Med Cracov* 54(3): 67–77.

Oudshoorn, Diede, Gijs A. Versteeg, and Marjolein Kikkert. 2012. "Regulation of the Innate Immune System by Ubiquitin and Ubiquitin-like Modifiers." *Cytokine and Growth Factor Reviews* 23(6): 273–82..

Panne, Daniel, Tom Maniatis, and Stephen C. Harrison. 2007. "An Atomic Model of the Interferon-?? Enhanceosome." *Cell* 129(6): 1111–23.

Park, Nahee, Hyoung Seok Baek, and Young-Jin Chun. 2015. "Embelin-Induced Apoptosis of Human Prostate Cancer Cells Is Mediated through Modulation of Akt and β-Catenin Signaling" ed. Seok-Geun Lee. *PLoS ONE* 10(8): e0134760.

Patel, Dhara A et al. 2012. "High Throughput Screening for Small Molecule Enhancers of the Interferon Signaling Pathway to Drive Next-Generation Antiviral Drug

Discovery." *PLOS ONE*.

Pattabhi, Sowmya et al. 2016. "Targeting Innate Immunity for Antiviral Therapy through Small Molecule Agonists of the RLR Pathway." *Journal of Virology* 90(5): 2372–87.

Paweska, Janusz T. et al. 2016. "Experimental Inoculation of Egyptian Fruit Bats (Rousettus Aegyptiacus) with Ebola Virus." *Viruses* 8(2): 1–11.

Peana, A T, M D Moretti, and C Juliano. 1999. "Chemical Composition and Antimicrobial Action of the Essential Oils of Salvia Desoleana and S. Sclarea." *Planta medica* 65(8): 752–54.

Petrecca, K et al. 2012. "UDCA Slows down Intestinal Cell Proliferation by Inducing High and Sustained ERK Phosphorylation." *International Journal of Cancer* 29(5): 1–11.

Di Petrillo, Amalia et al. 2017. "Broad-Range Potential of Asphodelus Microcarpus Leaves Extract for Drug Development." *BMC Microbiology* 17(1): 159.

Pettitt, James et al. 2013. "Therapeutic Intervention of Ebola Virus Infection in Rhesus Macaques with the MB-003 Monoclonal Antibody Cocktail." *Science Translational Medicine* 5(199): 199ra113 LP-199ra113.

Picazo, Edwige, and Fabrizio Giordanetto. 2015. "Small Molecule Inhibitors of Ebola Virus Infection." *Drug discovery today* 20(2): 277–86.

Pigott, David M. et al. 2014. "Mapping the Zoonotic Niche of Ebola Virus Disease in Africa." *eLife* 3(December 2013): e04395.

Pihan, Emilie, Lionel Colliandre, Jean-Francois Guichou, and Dominique Douguet. 2012. "E-Drug3D: 3D Structure Collections Dedicated to Drug Repurposing and Fragment-Based Drug Design." *Bioinformatics (Oxford, England)* 28(11): 1540–41.

Pintus, Francesca et al. 2017. "New Insights into Highly Potent Tyrosinase Inhibitors Based on 3-Heteroarylcoumarins: Anti-Melanogenesis and Antioxidant Activities, and Computational Molecular Modeling Studies." *Bioorganic & Medicinal Chemistry* 25(5): 1687–95..

Pintus, Francesca, Delia Spanò, Angela Corona, and Rosaria Medda. 2015. "Antityrosinase Activity of Euphorbia Characias Extracts" ed. Vijai Kumar Gupta. *PeerJ* 3: e1305.

Pourrut, Xavier et al. 2005. "The Natural History of Ebola Virus in Africa." *Microbes and Infection* 7(7–8): 1005–14.

Prabhu, Kirti S. et al. 2017. "Targeting of X-Linked Inhibitor of Apoptosis Protein and PI3-kinase/AKT Signaling by Embelin Suppresses Growth of Leukemic Cells." *PLoS ONE* 12(7): 1–17.

Prins, K. C. et al. 2010. "Mutations Abrogating VP35 Interaction with Double-Stranded RNA Render Ebola Virus Avirulent in Guinea Pigs." *Journal of Virology* 84(6): 3004–15.

Prins, Kathleen C, Washington B Cárdenas, and Christopher F Basler. 2009. "Ebola Virus Protein VP35 Impairs the Function of Interferon Regulatory Factor-Activating Kinases IKKepsilon and TBK-1." *Journal of virology* 83(7): 3069–77.

Rajsbaum, Ricardo et al. 2014. "Unanchored K48-Linked Polyubiquitin Synthesized by the E3-Ubiquitin Ligase TRIM6 Stimulates the Interferon-IKKε Kinase-Mediated Antiviral Response." *Immunity* 40(6): 880–95.

Rajsbaum, Ricardo, and Adolfo García-Sastre. 2013. "Viral Evasion Mechanisms of Early Antiviral Responses Involving Regulation of Ubiquitin Pathways." *Trends in Microbiology* 21(8): 421–29.

Reid, St. P. et al. 2006. "Ebola Virus VP24 Binds Karyopherin 1 and Blocks STAT1 Nuclear Accumulation." *Journal of Virology* 80(11): 5156–67.

Reid, St Patrick, Washington B Cardenas, and Christopher F Basler. 2005. "Homo-Oligomerization Facilitates the Interferon-Antagonist Activity of the Ebolavirus VP35 Protein." *Virology* 341(2): 179–89.

Rivera, Andrea, and Ilhem Messaoudi. 2016. "Molecular Mechanisms of Ebola Pathogenesis." *J. Leukoc. Biol* 3(100): 889–904.

Rizk, Maryan G, Christopher F Basler, and John Guatelli. 2017. "Cooperation of the Ebola Virus Proteins VP40 and GP1,2 with BST2 To Activate NF-kappaB Independently of Virus-Like Particle Trapping." *Journal of virology* 91(22).

Rodriguez, L. L. et al. 1999. "Persistence and Genetic Stability of Ebola Virus during the Outbreak in Kikwit, Democratic Republic of the Congo, 1995." *The Journal of Infectious Diseases* 179(s1): S170–76.

Roels, T H et al. 1999. "Ebola Hemorrhagic Fever, Kikwit, Democratic Republic of the Congo, 1995: Risk Factors for Patients without a Reported Exposure." *The Journal of infectious diseases* 179 Suppl: S92-7.

Rosa, Antonella et al. 2017. "Chemical Composition of Lycium Europaeum Fruit Oil Obtained by Supercritical CO2 Extraction and Evaluation of Its Antioxidant Activity, Cytotoxicity and Cell Absorption." *Food chemistry* 230: 82–90.

Rosenstierne, Maiken Worsøe et al. 2016. "Rapid Bedside Inactivation of Ebola Virus for Safe Nucleic Acid Tests." *Journal of Clinical Microbiology* 54(10): 2521–29.

Salata, Cristiano et al. 2015. "Amiodarone and Metabolite MDEA Inhibit Ebola Virus Infection by Interfering with the Viral Entry Process." *Pathogens and Disease* 73(5): 1–9.

Sanchez, a et al. 1998. "Biochemical Analysis of the Secreted and Virion Glycoproteins of Ebola Virus." *Journal of virology* 72(8): 6442–47.

Schafer, Georgia, and Catherine H Kaschula. 2014. "The Immunomodulation and Anti-Inflammatory Effects of Garlic Organosulfur Compounds in Cancer Chemoprevention." *Anti-cancer agents in medicinal chemistry* 14(2): 233–40.

Schumann, M., T. Gantke, and E. Muhlberger. 2009. "Ebola Virus VP35 Antagonizes PKR Activity through Its C-Terminal Interferon Inhibitory Domain." *Journal of Virology* 83(17): 8993–97.

Seelinger, Günter, Irmgard Merfort, and Christoph M. Schempp. 2008. "Anti-Oxidant, Anti-Inflammatory and Anti-Allergic Activities of Luteolin." *Planta Medica* 74(14): 1667–77.

Sekimoto, T et al. 1997. "Extracellular Signal-Dependent Nuclear Import of Stat1 Is Mediated by Nuclear Pore-Targeting Complex Formation with NPI-1, but Not Rch1." *The EMBO journal* 16(23): 7067–77.

Seth, Rashu B., Lijun Sun, Chee Kwee Ea, and Zhijian J. Chen. 2005. "Identification and Characterization of MAVS, a Mitochondrial Antiviral Signaling Protein That Activates NF-κB and IRF3." *Cell* 122(5): 669–82.

Shabman, Reed S. et al. 2011. "DRBP76 Associates with Ebola Virus VP35 and Suppresses Viral Polymerase Function." *Journal of Infectious Diseases* 204(SUPPL. 3): 911–18.

Shah, Priyank et al. 2016. "Embelin Inhibits Proliferation, Induces Apoptosis and Alters Gene Expression Profiles in Breast Cancer Cells." *Pharmacological reports : PR* 68(3): 638–44.

Sharma, S B, and Richa Gupta. 2015. "Drug Development from Natural Resource: A Systematic Approach." *Mini reviews in medicinal chemistry* 15(1): 52–57.

Shedlock, Devon J et al. 2010. "Antibody-Mediated Neutralization of Ebola Virus Can Occur by Two Distinct Mechanisms." *Virology* 401(2): 228–35.

Sissoko, Daouda et al. 2016. "Experimental Treatment with Favipiravir for Ebola Virus Disease (the JIKI Trial): A Historically Controlled, Single-Arm Proof-of-Concept Trial in Guinea." *PLOS Medicine* 13(3): e1001967.

Swanepoel, Robert et al. 1996. "Experimental Inoculation of Plants and Animals with Ebola Virus." *Emerging Infectious Diseases* 2(4): 321–25.

Taylor, Derek J, Katharina Dittmar, Matthew J Ballinger, and Jeremy A Bruenn. 2011. "Evolutionary Maintenance of Filovirus-like Genes in Bat Genomes." *BMC Evolutionary Biology* 11(1): 336.

Taylor, Raymond et al. 2017. "BCX4430 – A Broad-Spectrum Antiviral

Adenosine Nucleoside Analog under Development for the Treatment of Ebola Virus Disease." *Journal of Infection and Public Health* 9(3): 220–26.

Topal, Meryem et al. 2016. "Antioxidant, Antiradical, and Anticholinergic Properties of Cynarin Purified from the Illyrian Thistle (Onopordum Illyricum L.)." *Journal of enzyme inhibition and medicinal chemistry* 31(2): 266–75.

Trad, M. A. et al. 2017. "Ebola Virus Disease: An Update on Current Prevention and Management Strategies." *Journal of Clinical Virology* 86: 5–13.

Uyeki, T M et al. 2016. "Clinical Management of Ebola Virus Disease in the United States and Europe." *N Engl J Med* 374(7): 636–46.

Vandegraaff, N et al. 2001. "Specific Inhibition of Human Immunodeficiency Virus Type 1 (HIV-1) Integration in Cell Culture: Putative Inhibitors of HIV-1 Integrase." *Antimicrobial agents and chemotherapy* 45(9): 2510–16.

Versteeg, Gijs A., and Adolfo García-Sastre. 2010. "Viral Tricks to Grid-Lock the Type I Interferon System." *Current Opinion in Microbiology* 13(4): 508–16.

Wahyuni, Tutik Sri et al. 2013. "Antiviral Activities of Indonesian Medicinal Plants in the East Java Region against Hepatitis C Virus." *Virology Journal* 10(1): 1. Virology Journal.

Wang, Han et al. 2016. "Ebola Viral Glycoprotein Bound to Its Endosomal Receptor Niemann-Pick C1." *Cell* 164(1–2): 258–68.

Wang, Lingyan, Shitao Li, and Martin E. Dorf. 2012. "NEMO Binds Ubiquitinated TANK-Binding Kinase 1 (TBK1) to Regulate Innate Immune Responses to RNA Viruses." *PLoS ONE* 7(9).

Warren, Travis K et al. 2014. "Protection against Filovirus Diseases by a Novel Broad-Spectrum Nucleoside Analogue BCX4430." *Nature* 508: 402.

Warren, Travis K et al. 2016. "Therapeutic Efficacy of the Small Molecule GS-5734 against Ebola Virus in Rhesus Monkeys." *Nature* 531: 381.

Weidmann, Manfred et al. 2011. "Quantitative Analysis of Particles, Genomes and Infectious Particles in Supernatants of Haemorrhagic Fever Virus Cell Cultures." *Virology Journal* 8(1): 81..

Wermuth, Camille G. 2006. "Selective Optimization of Side Activities: The SOSA Approach." *Drug discovery today* 11(3–4): 160–64.

WHO. 1978. "Ebola Haemorrhagic Fever in Zaire , 1976." *Bull WHO* 56(October 1976): 271–93.

WHO. 2009. "Ebola Reston in Pigs and Humans, Philippines." *Weekly Epidemiological Record* 84(7): 49–50.

Wolber, Gerhard, and Thierry Langer. 2005. "LigandScout: 3-D Pharmacophores Derived from Protein-Bound Ligands and Their Use as Virtual Screening Filters." *Journal of chemical information and modeling* 45(1): 160–69.

World Health Organization. 2016. "Ebola Virus Disease." *Situation Report* (JUNE): 1–2.

Wrensch, Florian et al. 2015. "Interferon-Induced Transmembrane Protein-Mediated Inhibition of Host Cell Entry of Ebolaviruses." *Journal of Infectious Diseases* 212(Suppl 2): S210–18.

Xia, Ning et al. 2014. "Artichoke, Cynarin and Cyanidin Downregulate the Expression of Inducible Nitric Oxide Synthase in Human Coronary Smooth Muscle Cells." *Molecules (Basel, Switzerland)* 19(3): 3654–68.

Xu, Lijia et al. 2015. "From the Traditional Chinese Medicine Plant Schisandra Chinensis New Scaffolds Effective on HIV-1 Reverse Transcriptase Resistant to Non-Nucleoside Inhibitors." *Journal of Microbiology* 53(4): 288–93.

Xu, Wei et al. 2017. "Ebola Virus VP30 and Nucleoprotein Interactions Modulate Viral RNA Synthesis." *Nature Communications* 8: 15576.

Yasuda, Jiro. 2012. "Ebolavirus Replication and tetherin/BST-2." *Frontiers in Microbiology* 3(APR): 1–5.

Yen, Benjamin, Lubbertus C F Mulder, Osvaldo Martinez, and Christopher F Basler. 2014.

"Molecular Basis for Ebolavirus VP35 Suppression of Human Dendritic Cell Maturation." *Journal of virology* 88(21): 12500–510.

Yoneyama, Mitsutoshi et al. 2004. "The RNA Helicase RIG-I Has an Essential Function in Double-Stranded RNA-Induced Innate Antiviral Responses." 5: 730.

Zachowski, A. 1993. "Phospholipids in Animal Eukaryotic Membranes: Transverse Asymmetry and Movement." *Biochemical Journal* 294(1): 1–14.

Zinzula, Luca et al. 2009. "Purification and Functional Characterization of the Full Length Recombinant Ebola Virus VP35 Protein Expressed in E. Coli." *Protein Expression and Purification* 66(1): 113–19.

Zinzula, Luca, Francesca Esposito, Daniela Pala, and Enzo Tramontano. 2012. "DsRNA Binding Characterization of Full Length Recombinant Wild Type and Mutants Zaire Ebolavirus VP35." *Antiviral Research* 93(3): 354–63.

Zinzula, Luca, and Enzo Tramontano. 2013. "Strategies of Highly Pathogenic RNA Viruses to Block dsRNA Detection by RIG-I-like Receptors: Hide, Mask, Hit." *Antiviral Research* 100(3): 615–35.